

**TOWARDS A LOW TEMPERATURE SYNTHESIS OF GRAPHENE
WITH SMALL ORGANIC MOLECULE PRECURSORS**

A Dissertation
Presented to
The Academic Faculty

by

Juan Manuel Vargas Morales

In Partial Fulfillment
of the Requirements for the Degree
Doctor of Philosophy in the
School of Chemistry and Biochemistry

Georgia Institute of Technology
December 2013

COPYRIGHT 2013 BY JUAN MANUEL VARGAS MORALES

**TOWARDS A LOW TEMPERATURE SYNTHESIS OF GRAPHENE
WITH SMALL ORGANIC MOLECULE PRECURSORS**

Approved by:

Dr. Laren M. Tolbert, Advisor
School of Chemistry and Biochemistry
Georgia Institute of Technology

Dr. Clifford L. Henderson
School of Chemical and Biomolecular
Engineering
Georgia Institute of Technology

Dr. David M. Collard
School of Chemistry and Biochemistry
Georgia Institute of Technology

Dr. Jean-Luc Brédas
School of Chemistry and Biochemistry
Georgia Institute of Technology

Dr. Ronald R. Chance
School of Chemical and Biomolecular
Engineering
Georgia Institute of Technology

Dr. Mohan Srinivasarao
School of Material Science and
Engineering
Georgia Institute of Technology

Date Approved: August 23, 2013

To My Family

ACKNOWLEDGEMENTS

I want to thank the many people that directly or indirectly made this dissertation possible. First I would like to thank my advisor Dr. Laren M. Tolbert for giving me the opportunity to be a part of his research group. His guidance and encouragement throughout the years has made this dissertation come to fruition. The freedom he provided while conducting research and his valuable opinions and insights allowed me to expand my ideas to move in the right direction. I would also like to extend my gratitude to Dr. Clifford L. Henderson for all his unlimited help and support during the years that took to finish this dissertation.

I also want to thank research scientists Dr. Janusz Kowalik and Dr. Kyril Solntsev, and all the members of the Tolbert group as well as Jose Baltazar for their friendship and invaluable discussions during my years at Georgia Tech.

Additionally, I would like to thank my friends Jeremy Crouch, and Cesar Omar Flores Garcia for their friendship and all their help that they have provided to me and my family.

It goes without saying that this dissertation could not have been possible without the support of my family. Although far away, I want to thank my father Manuel Vargas Torres and mother Claudia Delfina Morales Amaya, my brothers Narciso Vargas Morales and Alejandro de Jesus Vargas Morales and my sister Wendy Lizbeth Vargas Morales for all their moral support and long talks over the phone.

Finally, I would like to offer my most special thanks and gratitude to my wife Jennifer Ann Vargas who has provided me with all the support that only a wife can provide during all my years of study. I would also like to thank her for all those long hours she spent sitting by me while writing this dissertation. She has been at my side in every step of the way and continues to do so without hesitation.

TABLE OF CONTENTS

	Page
ACKNOWLEDGEMENTS	iv
LIST OF TABLES	viii
LIST OF FIGURES	ix
LIST OF SYMBOLS AND ABBREVIATIONS	xii
SUMMARY	xiii
<u>CHAPTER</u>	
1 INTRODUCTION	1
1.1 Introduction to Graphene	1
1.2 Applications of Graphene	2
1.3 Graphene Synthetic Methods	2
1.3.1 Mechanical Exfoliation of Graphene	4
1.3.2 Epitaxial Growth from Silicon Carbide (SiC)	4
1.3.3 Reduction of Graphene Oxide	6
1.3.4 Liquid Exfoliation of Graphite	7
1.3.5 Chemical Vapor Deposition (CVD) on Metal Substrates	9
1.3.6 Total Organic Synthesis	10
1.3.7 Unzipping of Carbon Nanotubes (CNTs)	11
1.4 Characterization	12
1.5 Structure of Thesis	13
1.6 References	15
2 Synthesis of Anthracene Derivatives	22
2.1 Introduction	22

2.2	Experimental Protocol	22
2.3	Results	32
2.4	Conclusions	34
2.5	References	35
3	Synthesis of Polycyclic Aromatic Hydrocarbons	36
3.1	Introduction	36
3.2	Experimental Protocol	37
3.3	Results	41
3.3.1	UV Spectral Characteristics of PAHs	45
3.4	Conclusions	48
3.5	References	49
4	Synthesis of Graphene by Chemical Vapor Deposition on Copper	51
4.1	Introduction	51
4.2	Experimental Protocol	54
4.3	Results	57
4.3.1	APCVD	57
4.3.2	CVD	60
4.4	Conclusions	67
4.5	References	68
5	Synthesis of Graphene Nanoribbons (GNRs) by Encapsulation in Single-Walled Aluminosilicate Nanotubes	72
5.1	Introduction	72
5.2	Experimental Protocol	74
5.3	Results	75
5.4	Conclusions	78
5.5	References	79

6	Summary and Recommendations for Future Work	82
6.1	Synthesis and Study of the Properties and Chemistry of Dibenzo[<i>bc,kl</i>]coronene	83
6.2	Synthesis of Graphene at Low Temperatures by CVD on Copper	83
6.3	Synthesis of GNRs Encapsulated in Aluminosilicate Nanotubes	84
6.4	References	84
	APPENDIX A: Characterization of Synthesized Compounds	86
	VITA	124

LIST OF TABLES

	Page
Table 1.1: Comparison of common methods for the isolation or synthesis of graphene.	3
Table 2.1: Percentage yield of synthesized anthracene derivatives	33
Table 4.1: Single layer graphene grown on copper foil at different pressures and from different carbon sources.	64
Table 4.2: Results from experiments of graphene growth on copper foil at 600 °C at different pressures and from different carbon sources.	66

LIST OF FIGURES

	Page
Figure 1.1: Graphene as the building block for other carbon allotropes.	1
Figure 1.2: Mechanical exfoliation of HOPG using Scotch tape [®] to isolate graphene.	4
Figure 1.3: Epitaxial Graphene.	5
Figure 1.4: Lerf-Klinowski model of graphene oxide.	6
Figure 1.5: Schematic illustration of the graphene exfoliation process.	8
Figure 1.6: A transparent ultralarge-area graphene film transferred on a 35-inch PET sheet.	10
Figure 1.7: Bottom-up fabrication of atomically precise GNRs.	11
Figure 1.8: Comparison of Raman spectra at 514 nm for bulk graphite and graphene.	12
Figure 1.9: High-frequency first- and second-order microRaman spectra of <i>n</i> GL films supported on a SiO ₂ :Si substrate and HOPG.	13
Figure 2.1: Synthetic scheme for the synthesis of anthracene derivatives.	24
Figure 2.2: Synthetic scheme for the synthesis of 9,10-bis(2,6bis(bromomethyl)phenyl)anthracene (5) from 9,10-bis(2,6-dimethylphenyl)anthracene (4a).	27
Figure 2.3: Synthetic scheme for the synthesis of 1,4,5,8-tetramethylantracene-9,10-dione (11).	30
Figure 2.4: Anthracene derivatives, 1,4,5,8-tetramethyl-9,10-diphenyl-9,10-dihydroanthracene-9,10-diol (14) and 1,4,5,8-tetramethyl-9,10-diphenylanthracene (15).	34
Figure 3.1: Two possible Kekulé structures for dibenzo[<i>bc,kl</i>]coronene.	37
Figure 3.2: Synthetic scheme for the synthesis of dibenzo[<i>cd,lm</i>]perylene (18) from perinaphthenone (17).	38
Figure 3.3: Synthetic scheme for the synthesis of 1,12-dimethylnaphtho[1,2,3,4- <i>rst</i>]pentaphene (19) from 1,4-dimethyl-9,10-di- <i>o</i> -tolylanthracene (13).	39

Figure 3.4: Synthetic scheme for the synthesis of dibenzo[<i>bc,kl</i>]coronene (16) from 1,4-dimethyl-9,10-di- <i>o</i> -tolylanthracene (13).	41
Figure 3.5: Synthesis of dibenzo[<i>bc,kl</i>]coronene (16).	42
Figure 3.6: Reactivity of anthracene derivatives.	43
Figure 3.7: UV-vis spectrum of 1-dodecyl-1 <i>H</i> -pyrrole-2,5-dione (20), 1,4-dimethyl-9,10-di- <i>o</i> -tolylanthracene (13), and Diels-Alder adduct (21) an/or (22).	44
Figure 3.8: UV-vis spectrum of 1,4-dimethyl-9,10-di- <i>o</i> -tolylanthracene (13) and dibenzo[<i>bc,kl</i>]coronene (16). Fluorescence obtained at 510 nm.	46
Figure 3.9: UV-vis spectrum of dibenzo[<i>bc,kl</i>]coronene (16) in 1-methylnaphthalene.	46
Figure 3.10: Decomposition of (16) in air and light.	47
Figure 3.11: Long thin needles of (16).	48
Figure 4.1: Schematic of the CVD setup for graphene growth.	56
Figure 4.2: Raman spectrum of graphene from benzene on copper foil.	59
Figure 4.3: Raman spectrum of graphene from toluene on copper foil.	59
Figure 4.4: SEM image of graphene on copper foil by APCVD.	60
Figure 4.5: Molecular structures of Poly(methyl methacrylate) (24), coronene (25) and perylene (26)..	61
Figure 4.6: Controllable growth of pristine PMMA-derived graphene films.	62
Figure 4.7: Raman spectrum of graphene grown from PMMA (24) at 1000 °C.	63
Figure 4.8: Raman spectrum of graphene grown from 1,4-dimethyl-9,10-di- <i>o</i> -tolylanthracene (13) at 1000 °C.	63
Figure 4.9: Anthracene derivatives.	65
Figure 5.1: Aluminosilicate nanotubes	74
Figure 5.2: Raman spectrum of aluminosilicate nanotubes.	76
Figure 5.3: Raman spectrum of perylene (26).	76
Figure 5.4: Raman spectrum of a graphene nanoribbon (GNR) from perylene (26).	77

Figure 5.5: Typical micro-Raman spectra in the 100-1800 cm^{-1} frequency range of PPN films. 77

Figure 5.6: Polyperinaphthalene, the narrowest possible armchair nanoribbon. 78

LIST OF SYMBOLS AND ABBREVIATIONS

λ	Wavelength
nm	Nanometer
UV-Vis	Ultraviolet-Visible
IR	Infrared
TGA	Thermogravimetric Analysis
CVD	Chemical Vapor Deposition
IR	Infrared
MHz	Mega Hertz
Me	Methyl
Et	Ethyl

SUMMARY

Graphene, a 2D honeycomb lattice of sp^2 hybridized carbons, has attracted the attention of the scientific community not only for its interesting theoretical properties but also for its myriad of possible applications. The discovery of graphene led to the Nobel Prize in physics for 2010 to be awarded to Andrei Geim and Konstantin Novoselov.

Since its discovery, many methods have been developed for the synthesis of this material. Two of those methods stand out for the growth of high quality and large area graphene sheets, namely, epitaxial growth from silicon carbide (SiC) and chemical vapor deposition (CVD). As it stands today, both methods make use of high concentrations of hydrogen (10-20%) in N_2 or Ar, high temperatures, and a vacuum system. Epitaxial growth from SiC in addition requires very expensive single crystal SiC wafers. In the case of CVD, organic molecules are used as the carbon source to grow graphene on a metal substrate. Although graphene has been grown on many metal substrates, the experiments highlighted here make use of copper as the metal substrate of choice since it offers the advantage of availability, low price, and, most importantly, because this substrate is self-limiting in other words, it mostly grows single layer graphene. Because the CVD method provides with a choice as for the carbon source to use, the following question arises: can a molecule, either commercially available or synthesized, be used as a carbon source that would allow for the synthesis of graphene under low temperatures, low concentrations of hydrogen and at atmospheric pressure?

This dissertation focuses on the synthesis of graphene at lower temperatures by using carbon sources with characteristics that might make this possible. It also focuses on

the use of forming gas (3% H₂ and 97% N₂ or Ar) in order to make the overall process a lot safer and cost effective. This dissertation contains two chapters on the synthesis of organic molecules of interest, and observations about their reactivity are included.

CVD experiments were performed at atmospheric pressure, and under vacuum. In both instances forming gas was used as the annealing and carrier gas. Results from CVD at atmospheric pressure (CVDAP), using organic solvents as carbon sources, show that at 1000 °C, low quality graphene was obtained. On the other hand, CVD experiments using a vacuum in the range of 25 mTorr to 1 Torr successfully produced good quality graphene. For graphene growth under vacuum conditions, commercially available and synthesized compounds were used. Attempts at growing graphene at 600 °C from the same carbon sources only formed amorphous carbon. These results point to the fact that good quality graphene can basically be grown from any carbonaceous material as long as the growth temperature is 1000 °C and the system is under vacuum.

In addition to the synthesis of graphene at low temperatures, there is a great amount of interest on the synthesis of graphene nanoribbons (GNR's) and, as with graphene, several approaches to their synthesis have been developed. One such method is the synthesis of GNRs encapsulated in carbon nanotubes. Experiments were conducted in which aluminosilicate nanotubes were used. These nanotubes provided for an easier interpretation of the Raman spectrum since the signals from the nanotubes do not interfere with those of the GNR's as in the case when carbon nanotubes are used. The use of aluminosilicate nanotubes also allowed for the successful synthesis of GNR's at temperatures as low as 200 °C when perylene was used as the carbon source.

CHAPTER 1

INTRODUCTION

1.1 Introduction to Graphene

Graphene, a 2D carbon allotrope of sp^2 hybridized carbon atoms arranged in a honeycomb crystal lattice, has recently attracted the interest of many researchers in the fields of physics, chemistry, biology, etc, due to its interesting electronic, optical, mechanical and thermal properties.¹⁻¹⁴ Figure 1.1 shows graphene as the building block for all other sp^2 hybridized carbon allotropes. When wrapped in a ball, it forms the 0D Buckminsterfullerene or fullerene. If rolled, it produces 1D carbon nanotubes and when stacked in a 3D manner, it forms 3D graphite.⁵

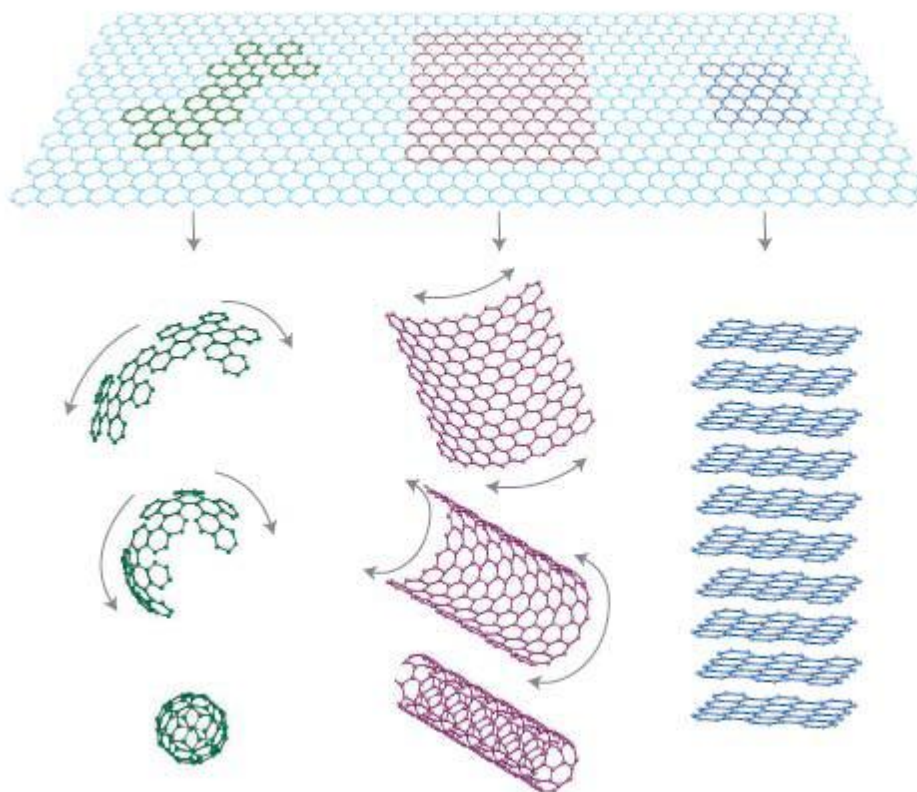


Figure 1.1. Graphene as the building block for other carbon allotropes.⁵

It is an interesting historical fact that before the interest of graphene as a “nanomaterial”, the scientific community attention was directed at the fullerenes (discovered by Kroto *et al* in 1985)¹⁵ and carbon nanotubes (discovered by Iijima in 1991).¹⁶

As early as 1947 Wallace explored the electronic properties of graphene as a starting point to understand the more complex graphite¹ and possibly, the first synthesis of this material was performed by Boehm in 1962 using the graphene oxide reduction method.¹⁷

The existence of graphene as a free-standing film was dismissed for some time by Landau¹⁸ first and then by Mermin¹⁹ as not being thermodynamically stable. In 2004, Andrei Geim and Konstantin Novoselov at the University of Manchester isolated high quality graphene by the mechanical exfoliation method.³ Experiments on this material, which verified the many predicted exotic behaviors of the charge carriers in graphene, were recognized with the Physics Nobel Prize in 2010.²⁰

1.2 Applications of Graphene

Due to the electronic, thermal, optical, and mechanical properties of this material,¹⁻¹⁴ many possible applications have been envisioned and are being pursued. Graphene and graphene-based materials might find applications in organic electronics,²¹ transparent flexible electrodes,^{22,23} energy storage,²⁴ sensors,²⁵ printable electronics,²¹ and in mechanical parts as graphene-polymer composites.²⁶⁻²⁸

1.3 Graphene Synthetic Methods

Since the discovery of graphene, research groups have developed several methods to synthesize or isolate graphene. The most common methods include, mechanical

exfoliation, also referred as micromechanical cleavage or the Scotch tape[®] method, epitaxial growth from silicon carbide, reduction of graphene oxide, liquid exfoliation and chemical vapor deposition (CVD) on metal substrates. Each of these methods has its advantages and disadvantages (**Table 1.1**) but so far none has accomplished the goal of synthesizing high quality graphene in an industrial large scale, reproducible manner, and at a low cost.

Table 1.1. Comparison of common methods for the isolation or synthesis of graphene.

Method	Advantage	Disadvantage
Mechanical Exfoliation	High Quality Flakes	High Cost Small Scale Production Non Scalable
Epitaxial Growth from Silicon Carbide (SiC)	High Quality Large Graphene Sheets	High Cost Low Yield High Temperature Low Vacuum Non transferable
Reduction of Graphene Oxide (GO)	High Scalability Low Cost	Low Purity High Defect Density Poor Electrical Properties
Liquid Exfoliation	Moderate Quality High Scalability Low Cost	Low Yield Poor Electrical Properties
Chemical Vapor Deposition (CVD)	High Quality Large Graphene Sheets Moderate Scalability Transferable	High Cost High Temperature Vacuum

1.3.1 Mechanical Exfoliation of Graphene

The mechanical exfoliation of graphene method was developed by Andrei Geim and Konstantin Novoselov.^{3,6} This method uses Scotch tape[®] to peel off graphene from commercially available highly oriented pyrolytic graphite (HOPG). The nature of this method provides a very easy and convenient way to isolate high quality (high mobility and low defect) single layer (or a few layers) of graphene with flakes as large as $100\ \mu\text{m}^2$. On the other hand, this method suffers from being tedious, not scalable, and with low yields. Figure 1.2 shows an example of this method.²⁹

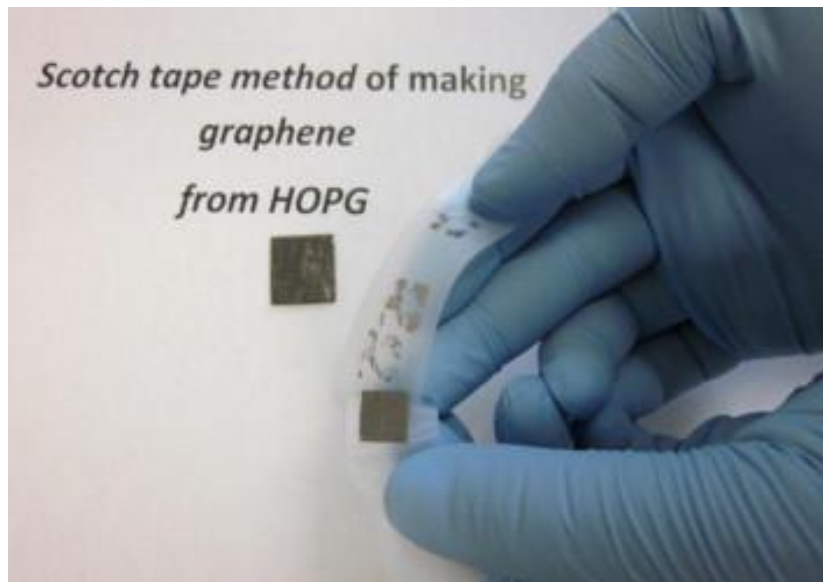


Figure 1.2. Mechanical exfoliation of HOPG using Scotch tape[®] to isolate graphene.²⁹

1.3.2 Epitaxial Growth from Silicon Carbide (SiC)

The epitaxial growth from SiC method was developed by Professor Walter A. de Heer and Claire Berger at Georgia Institute of Technology in 2006. In this novel method, graphene is grown from a single crystal of silicon carbide (4H or 6H-)³⁰⁻³³ at temperatures of approximately $1300\ \text{°C}$. At this temperature the less tightly bound silicon atoms are removed from the surface by sublimation leaving behind the carbon atoms for

graphitization.^{32,47} Experiments have shown that the quality of the graphene obtained is dependent on the face of the silicon carbide crystal exposed^{31,33}. In the case of a Si-terminated (0001) surface, the process is slow which allows for the control of the number of graphene layers. On the other hand, when the C-terminated (000 $\bar{1}$) surface is used, the graphitization process is very fast producing multi-layer graphene.³⁵ Figure 1.3 shows the distance between the graphene layers produced from this method. As it can be seen from the figure, the first graphene layer is tightly bound to the SiC substrate. According to X-ray diffraction measurements, the distance between the first graphene layer and the SiC substrate is 0.20 nm for a Si-terminated surface and 0.17 nm for a C-terminated surface.³³ When compared to the distance between graphene sheets in crystalline graphite (0.34 nm), these distances are much smaller, which points to a tightly bound first graphene layer, or buffer layer. Above this layer the distance between sheets becomes 38 to, 39 nm, a distance about 20% larger than that found in crystalline graphite, which would point to less tightly bound graphene sheets (**Figure 1.3**).^{33,36}

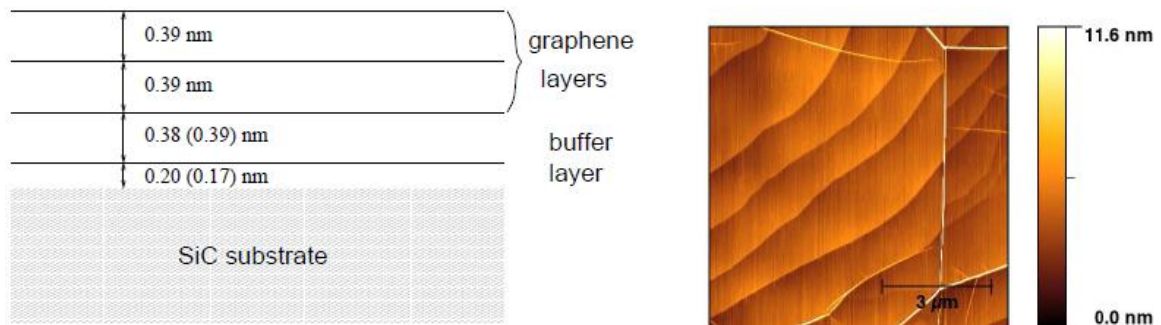


Figure 1.3. Epitaxial Graphene. (a) Schematic view of epitaxial graphene. On top of the SiC substrate the graphitic layer consists of a buffer layer, which is tightly bound to the substrate, at a distance of 0.2 (0.17) nm for a C-terminated SiC. The graphene layers are formed on top of this layer at a distance of 0.38 (0.39) nm and equally spaced by 0.39 nm afterwards. (b) AFM image of epitaxial graphene on C-terminated SiC substrate. The steps are those of the SiC substrate. The 5-10 graphene layers lie on the substrate. The white lines on the image are folds on the graphene layers.³⁶

At the time of development, this method produced the largest, continuous, wafer scale, graphene films observed, the quality of which was comparable to that obtained by mechanically exfoliated graphene. Although this method seems promising, it suffers from high cost, the need for high temperatures, ultra high vacuum (UHV), and the lack of transferability of the resulting graphene.

1.3.3 Reduction of Graphene Oxide (GO)

The reduction of GO method has also attracted the interest of many research groups due to the stable dispersions that graphene oxide forms in water³⁷. These stable dispersions, allow for the separation of the oxidized flakes which upon reduction with hydrazine³⁸ or thermal reduction³⁹ can form graphene. The most common method for the synthesis of GO was developed in 1958 by Hummer and Offeman.⁴⁰ In this method, a strong oxidizing solution of sodium nitrate, potassium permanganate, and concentrated sulfuric acid was used to oxidize graphite resulting in the formation of hydroxyl and epoxide groups on sp^3 hybridized carbons in the basal plane, and carboxylic, and carbonyl groups on sp^2 hybridized carbons on the sheet edges.^{41,42} Figure 1.4 shows a sheet of graphene oxide according to the Lerf-Klinowski model.^{43,44}

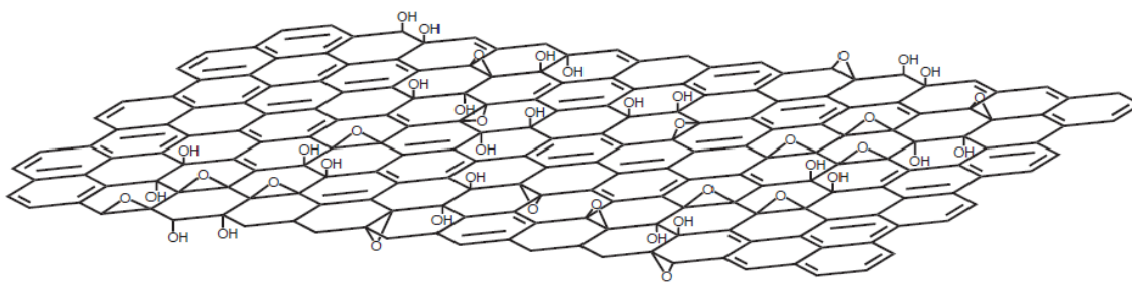


Figure 1.4. Lerf-Klinowski model of graphene oxide.^{43,44}

Although this model is widely used, it does not explain the acidity of GO in aqueous solution. A new dynamic method has been proposed by Tour *et al*, in which GO behaves as a dynamic system, changing functional groups as it interacts with water to give rise to the observed acidity.⁴⁵

A new method for the synthesis of GO has also been developed by the Tour group in which a solution of sulfuric and phosphoric acid is used in conjunction with potassium permanganate. This method eliminates the use of sodium nitrate, preventing in this way the release of toxic fumes produced in Hummer's synthesis while increasing the yield.⁴⁶

One of the main drawbacks from this method is that the defects formed during the process of oxidation render reduced graphene oxide (rGO) with only a fraction of its electronic mobility, thermal conductivity and strength as compare to that of pristine graphene.⁴⁷

1.3.4 Liquid Exfoliation of Graphite

The liquid exfoliation of graphite method, also known as solution based graphene exfoliation, relies in the sonication of graphite flakes in organic solvents with surface energies similar to that of graphene. This technique was first demonstrated by the Coleman group in 2008 when they were able to exfoliate and disperse graphite to form graphene dispersions with concentrations of up to ~0.01 mg/mL in *N*-methylpyrrolidone. This is possible because the energy required to exfoliate graphene is balanced by graphene-solvent interactions.⁴⁸ Surfactants, such as sodium cholate, have been shown to help prevent colloidal aggregation of graphene when working with aqueous dispersions (**Figure 1.5**).⁴⁹

Intercalation of graphite with alkaline⁵⁰ or interhalogen compounds⁵¹ to form graphite intercalation compounds (GICs) has also been explored in liquid exfoliation. These GICs can be prepared directly by exfoliation and dispersion via sonication.⁵⁰ or by

thermal expansion at high temperatures to form expanded graphite (EG) once the intercalating agents have been removed through volatilization.⁵² Once obtained, the EG is further exfoliated in solution through sonication.⁵¹ Exfoliation of graphite by supercritical fluids (SCF),⁵³ and CO₂⁵⁴ has also been reported.

The advantage of this technique relies on the low cost of the starting materials and the ease of the procedure. However, re-aggregation of graphene in solution, the yield of single layer graphene, the dispersion concentration and the lack of a continuous graphene layer are some of the mayor drawbacks associated with this technique.⁵⁵

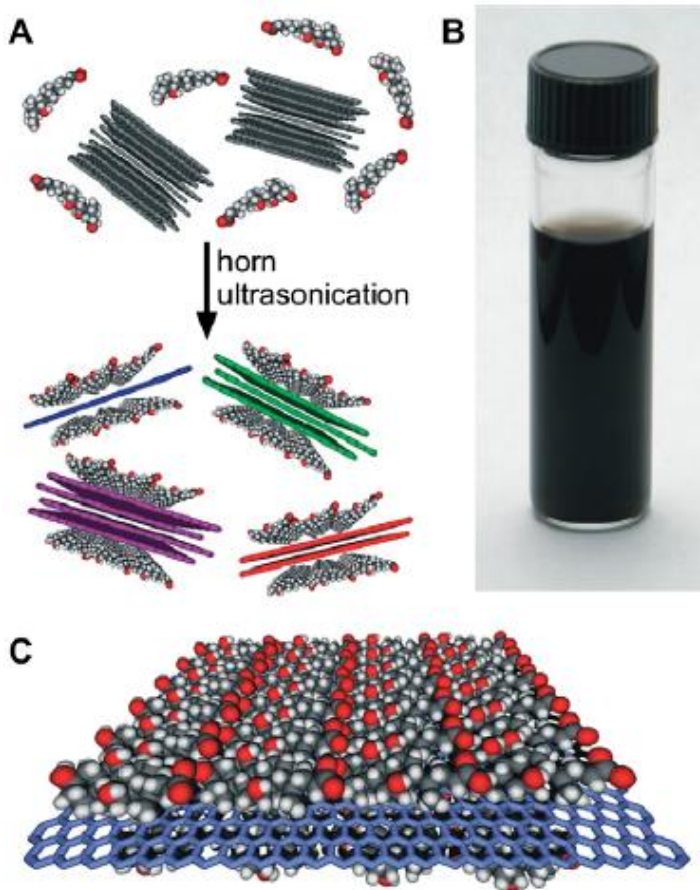


Figure 1.5 (A) Schematic illustration of the graphene exfoliation process. Graphite flakes are combined with sodium cholate (SC) in aqueous solution. Horn-ultrasonication exfoliates few-layer graphene flakes that are encapsulated by SC micelles. (B) Photograph of 90 μgmL^{-1} graphene dispersion in SC 6 weeks after it was prepared. (C) Schematic illustrating an ordered SC monolayer on graphene.⁴⁹

1.3.5 Chemical Vapor Deposition (CVD) in Metal Substrates

The CVD method seems to be the most promising technique for large scale production of single layer graphene. The synthesis of graphene on metal substrates by CVD was first reported in 2006 by Somani and coworkers.⁵⁶ In their work, camphor was evaporated into a chamber containing a nickel substrate held at 700-850 °C. This experiment demonstrated that graphene could be synthesized by a CVD process similar to that used for the synthesis of carbon nanotubes. As described above, the method for graphene growth by CVD relies on the evaporation and subsequent graphitization of an organic molecule on a metallic substrate. Although graphitic material had been grown on metal single crystals in early CVD studies,⁵⁷⁻⁵⁹ and a large number of surface science studies of graphene on different transition metals exist,^{60,61} this study opened a new route for the synthesis of graphene by CVD.

Although graphene has been grown successfully on many metals, a great interest in copper substrate has developed over the years since it was shown that single or bilayer graphene can be grown using this metal.⁶²⁻⁶⁴ The low carbon solubility (<0.001 atomic %) of copper at even high temperatures accounts for the self-terminating graphene monolayer growth.

Many carbon sources have been used to grow high quality graphene on copper foil but methane⁴⁷ continues to be the carbon source of choice. This growth takes place under high to moderate vacuum and at temperatures in the range of 1000-1035 °C with hydrogen as the reducing gas.⁶³ There are also some examples in the literature where graphene has been synthesized at lower temperatures.⁶⁵⁻⁶⁷ Once graphene has been grown, the layer can be transferred to other substrates by chemical etching of the metal substrate.

In a paper by Bae *et al*, a roll-to-roll production of graphene films was reported.⁶⁸ The graphene films exhibited a sheet resistance of 30 Ω/\square , a 90 % optical transparency, and a relative high mobility of 5100 $\text{cm}^2\text{V}^{-1}\text{s}^{-1}$ (**Figure 1.6**). This work emphasizes the

utility of the CVD method to synthesize large area, high quality graphene. Research in CVD continues in order to develop better and more efficient ways to synthesize high quality graphene in an industrial scale and at a low cost.

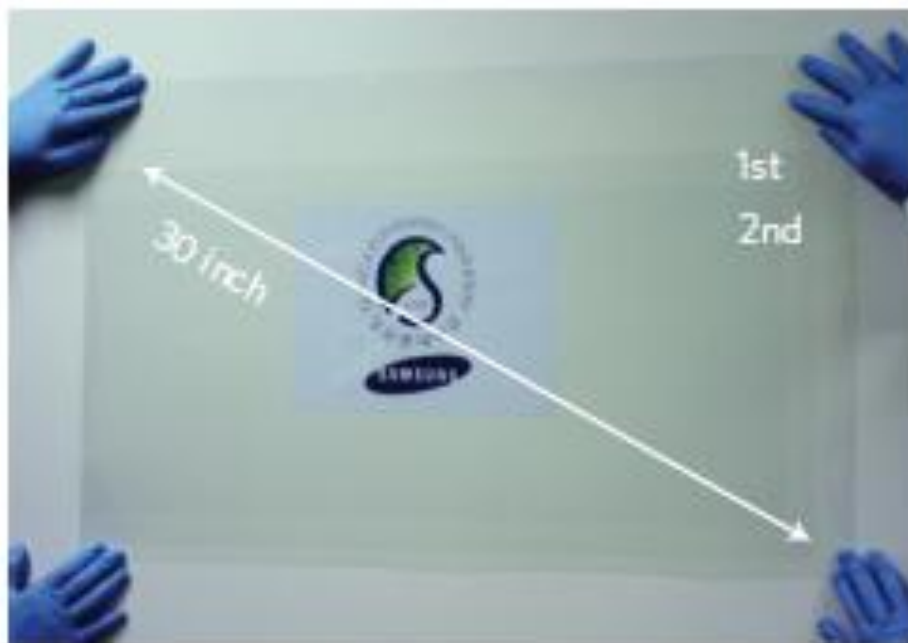


Figure 1.6. A transparent ultralarge-area graphene film transferred on a 35-inch PET sheet.⁶⁸

1.3.6 Total Organic Synthesis

The total organic synthesis of graphene is not a new concept. It was developed decades ago with the synthesis of graphene-like polycyclic aromatic hydrocarbons (PAHs) and recently has caught much attention as a bottom-up approach for the synthesis of graphene. Although there are many synthetic routes to PAHs,⁶⁹ the important work developed by Mullen's group has allowed for the synthesis of graphene nanoribbons (GNRs).^{70,71} As an example, Figure 1.7 shows one of the synthetic approaches developed by the Mullen's group for this purpose.

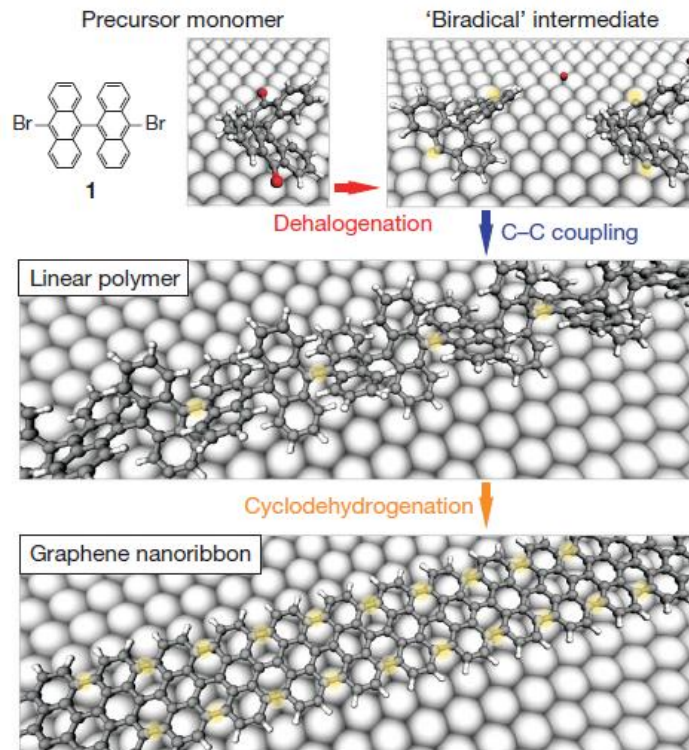


Figure 1.7. Bottom-up fabrication of atomically precise GNRs. Basic steps for surface-supported GNR synthesis, illustrated with a ball-and-stick model of the example of 10,10'-dibromo-9,9'-bianthryl monomers (1). Grey, carbon; white, hydrogen; red, halogens; underlying surface atoms shown by large spheres. Top, dehalogenation during adsorption of the di-halogen functionalized precursor monomers. Middle, formation of linear polymers by covalent interlinking of the dehalogenated intermediates. Bottom, formation of fully aromatic GNRs by cyclodehydrogenation.⁷¹

1.3.7 Unzipping of Carbon Nanotubes (CNTs)

Because graphene is a zero-gap material, the introduction of a band gap is of much interest. It is one of the goals of researchers pursuing graphene for applications in the semiconductor industry. A way to introduce a band gap is by constraining the domain of graphene in one direction with the subsequent formation of GNRs.^{31,32} Since carbon nanotubes (CNTs) are graphene sheets rolled up to form a one dimension cylinder, then by unzipping the CNT, a GNR can be formed. Dai *et al* developed a method to unzip

CNTs in a controlled manner by using an Ar plasma etching method.⁷² Many other examples are described in the literature for the unzipping of CNTs.⁷³⁻⁷⁵

1.4 Characterization

Several methods have been developed over the years for the characterization of a single layer or multiple layers of graphene. This methods include, optical imaging,⁷⁶⁻⁷⁸ fluorescence quenching,⁷⁹ atomic force microscopy (AFM),^{80,81} transmission electron microscopy (TEM),^{82,83} and Raman spectroscopy.⁸⁴⁻⁸⁷

Raman spectroscopy allows for the rapid identification of carbon allotropes. The Raman spectrum of these allotropes consist mostly of D, G, and 2D peaks around 1360 cm^{-1} , 1580 cm^{-1} , and 2700 cm^{-1} respectively (**Figure 1.8**).⁸⁵ The D peak originates from breathing modes of sp^2 carbon atoms in rings, the G peak is due to the bond stretching of sp^2 carbon atoms in the rings⁸⁸⁻⁹⁰ and the 2D peak is the second order of the D Peak.⁹¹ Besides identification of graphene, this technique also offers a way to determine the number of layers that make up the graphene sample (**Figure 1.9**).⁸⁷

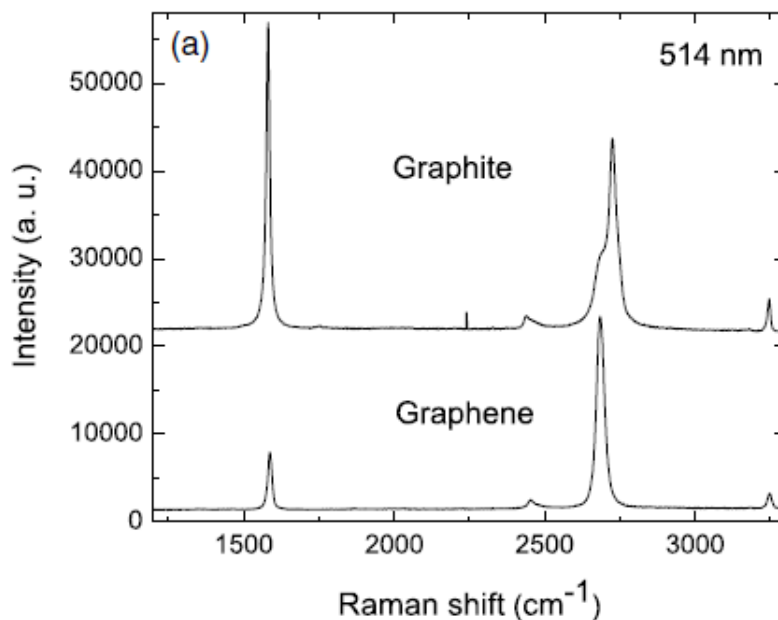


Figure 1.8. Comparison of Raman spectra at 514 nm for bulk graphite and graphene. They are scaled to have similar height of the 2D peak at $\sim 2700 \text{ cm}^{-1}$.⁸⁵

The ease of identification of carbon allotropes, coupled with the non-destructive nature of the technique, makes Raman spectroscopy the method of choice for the characterization and quality determination of graphene.

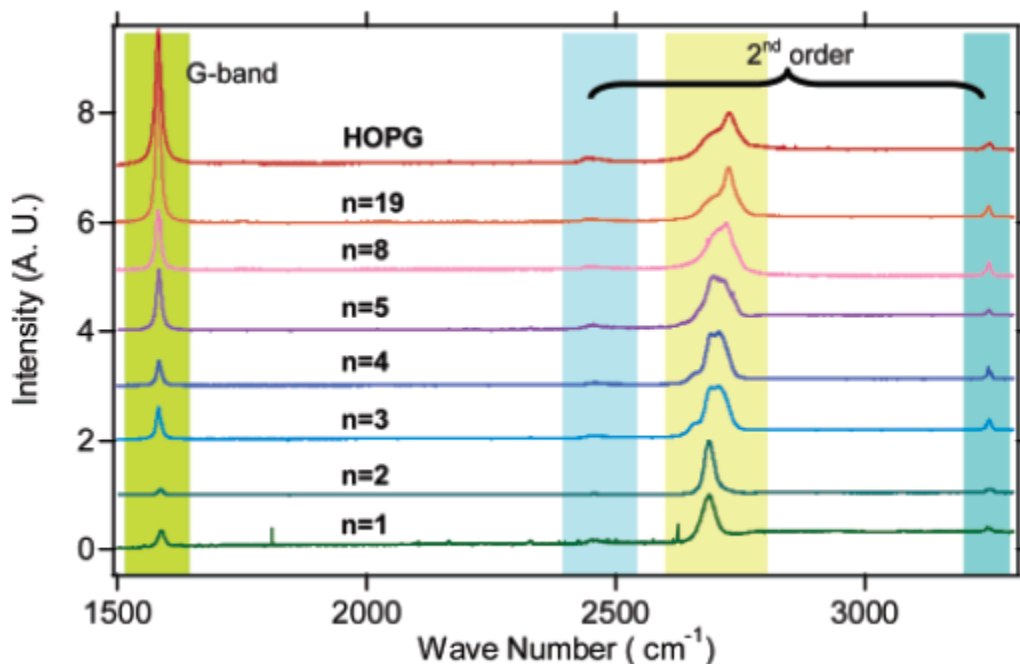


Figure 1.9. High-frequency first- and second-order microRaman spectra of n GL films supported on a $\text{SiO}_2:\text{Si}$ substrate and HOPG. The data were collected using 514.5 nm radiation under ambient conditions. The spectra are scaled to produce an approximate match in intensity for the $\sim 2700 \text{ cm}^{-1}$ band. Note: (1) the shape and frequency of this second-order band is sensitive to the number of layers n , and (2) the relative intensity of the second-order band at 2700 cm^{-1} is larger than that of the first order-allowed G-band for $n < 5$.⁸⁷

1.5 Structure of Thesis

This thesis is divided into two main areas intertwined with one another. The main focus of this project is the growth of high quality graphene by Chemical Vapor Deposition (CVD) at relative low temperatures and moderate vacuum. This work focuses on the synthesis of novel compounds to be used as organic precursors for the synthesis of graphene. The reasoning behind the synthesis and use of these compounds will be

explained in the introductions of the respective chapters. Copper foil will be used as the metal substrate throughout all the experiments performed by CVD. The choice of this metal is simple: its low cost, and the good quality of the graphene grown on this substrate make it an ideal candidate for this type of experiments. The use of the safer forming gas as the carrier gas (3% H₂ and 97% N₂ or Ar) plays an important role in this work since it moves away from the conventional use of dangerous concentrations of hydrogen for graphene growth. Chapter 1 is a brief introduction to graphene. It also summarizes the synthetic methods currently in use for its production. This chapter also provides a glimpse at Raman spectroscopy as a characterization technique. Chapter 2 focuses on the synthesis and characterization of several anthracene derivatives and their use as novel molecular precursors for the synthesis of graphene on copper by CVD. Chapter 3 deals with the synthesis and characterization of dibenzo[*bc,kl*]coronene and dibenzo[*cd,lm*]perylene and their use as molecular precursors for the synthesis of graphene. Chapter 4 presents results obtained from our experiments aimed at synthesizing graphene at relatively low temperatures using compounds synthesized in our laboratory as the carbon sources, as well as commercially available compounds. Chapter 5 moves in a different direction since it provides results for experiments performed in our laboratories using a different but promising approach to the synthesis of GNRs at relatively low temperatures. This chapter focuses in the use of aluminosilicate nanotubes as one-dimensional reactors for the synthesis of GNRs from commercially available or synthesized compounds. These experiments show that GNRs can be synthesized at temperatures as low as 200 °C, thereby opening the door to the synthesis of these materials at low temperatures. Chapter 6 concludes this work with a brief summary and discussion of possible research directions.

1.6 References

- [1] Wallace, P. R. *Phys. Rev.* **1947**, *71*, 622-634.
- [2] McClure, J. W. *Phys. Rev.* **1957**, *108*, 612-618
- [3] Novoselov, K.S.; Geim, A.K.; Morozov, S. V.; Jiang, D.; Zhang, Y.; Dubonos, S. V.; Grigorieva, I. V.; Firsov, A. A. *Science* **2004**, *306*, 666–669.
- [4] Novoselov, K. S.; Geim, A. K.; Morozov, S. V.; Jiang, D.; Katsnelson, M. I.; Grigorieva, I. V.; Dubonos, S. V.; Firsov, A. A. *Nature* **2005**, *438*, 197–200.
- [5] Geim, A. K.; Novoselov, K. S. *Nat. Mater.* **2007**, *6*, 183–191.
- [6] Geim, A. K.; MacDonald, A. H. *Phys. Today* **2007**, *60*, 35.
- [7] Zhu, Y.W.;Murali, S.; Cai, W. W.; Li, X. S.; Suk, J.W.; Potts, J. R.; Ruoff, R. S. *Adv. Mater.* **2010**, *22*, 3906–3924.
- [8] Dreyer, D. R.; Ruoff, R. S.; Bielawski, C. W. *Angew. Chem., Int. Ed.* **2010**, *49*, 9336–9344.
- [9] Zhang, Y. B.; Tan, Y. W.; Stormer, H. L.; Kim, P. *Nature* **2005**, *438*, 201–204.
- [10] Schwierz, F. *Nat. Nanotechnol.* **2010**, *5*, 487–496.
- [11] Berger, C.; Song, Z. M.; Li, X. B.; Wu, X. S.; Brown, N.; Naud, C.; Mayou, D.; Li, T. B.; Hass, J.; Marchenkov, A. N.; et al. *Science* **2006**, *312*, 1191–1196.
- [12] Balandin, A. A.; Ghosh, S.; Bao, W.; Calizo, I.; Teweldebrhan, D.; Miao, F.; Lau, C. N. *Nano Lett.* **2008**, *8*, 902
- [13] Stoller, M. D.; Park, S.; Zhu, Y.; An, J.; Ruoff, R. S. *Nano Lett.* **2008**, *8*, 3498.
- [14] Lee, C.; Wei, X.; Kysar, J. W.; Hone, J. *Science* **2008**, *321*, 385

- [15] H.W. Kroto, J.R. Heath, S.C. O'Brien, R.F. Curl, R.E. Smalley, *Nature* **1985**, 318, 162–163.
- [16] Iijima, S. *Nature* **1991**, 354, 56–58.
- [17] H.P. Boehm, A. Clauss, G.O. Fischer, U. Hoffmann, *Z. Naturforsch.* **1962**, B 17, 150–153.
- [18] L.D. Landau, *Phys. Z. Sowjetunion* **1937**, 11, 26.
- [19] Mermin, N. D. *Phys. Rev.* **1968**, 176, 250–254.
- [20] RSAS, Graphene. *Scientific Background on the Nobel Prize in Physics 2010* **2010**.
- [21] Wu, J.; Agrawal, M.; Becerril, H. A.; Bao, Z.; Liu, Z.; Chen, Y.; Peumans, P. *ACS Nano* **2010**, 4, 43-48.
- [22] Bae, S.; Kim, H.; Lee, Y.; Xu, X.; Park, J-S.; Zheng, Y. Balakrishnan, J.; Lei, T.; Kim, H. R.; Song, Y. I.; Kim, Y-J.; Kim, K. S.; Özyilmaz, B.; Ahn, J-H.; Hong, B. H.; Iijima, S. *Nat Nanotechnol.* **2010**, 5. 574-578.
- [23] Bauld, R.; Sharifi, F.; Fanchini, G.; *Int. J. Mod. Phys. B* **2012**, 1242004.
- [24] Stoller, M. D.; Park, S.; Zhu, Y.; An, J.; Ruoff, R. S. *Nano Lett.* **2008**, 8, 3498.
- [25] Wang, S.; Ang, P. k.; Wang, Z.; Tang, A. L. L. *Nano. Lett.* **2010**, 10, 92-98.
- [26] Kim H, Macosko C.W. *Macromol.* **2008**, 41, 3317.
- [27] Kim H, Macosko C. W. *Polym.* **2009**, 50, 3797.
- [28] Kim H, Miura Y, Macosko C. W. *Chem. Mater.* **2010**, 22, 3441.
- [29] Singh, V.; Joung, D.; Zhai, L.; Das, S.; Khondaker, S. I.; Seal, S. *Prog. Mater. Sci.* **2011**, 56, 1178–1271.

- [30] Berger, C.; Song, Z.; Li, X.; Wu, X.; Brown, N.; Naud, C.; Mayou, D.; Li, T.; Hass, J.; Marchenkov, A. N.; Conrad, E. H.; First, P. N. de Heer, W. A. *Science* **2006**, *312*, 1191.
- [31] Faugeras, C.; Nerrière, A.; Potemski, M.; Mahmood, A.; Dujardin, E.; Berger, C.; de Heer, W. A. *Appl. Phys. Lett.* **2008**, *92*, 011914.
- [32] Berger, C. Song, Z.; Li, T.; Li, X.; Ogbazghi, A. Y.; Feng, R.; Dai, Z.; Marchenkov, A. N.; Conrad, E. H.; First, P. N.; de Heer, W. A. *J. Phys. Chem. B* **2004**, *108*, 19912-19916.
- [33] Varchon, F.; Feng, R.; Hass, J.; Li, X.; Nguyen, B. N.; Naud, C.; Mallet, P.; Veuillen, J.-Y.; Berger, C.; Conrad, E. H.; Magaud, L. *Phys. Rev. Lett.* **2007**, *99*, 126805.
- [34] Forbeaux, I.; Themlin, J. M.; Debever, J.M. *Phys. Rev.B* **1998**, *58*, 16396.
- [35] Riedl, C.; Coletti, C.; Starke, U. *J. Phys. D: Appl. Phys.* **2010**, *43*, 374009.
- [36] Hass, J.; de Heer, W. A.; Conrad, E. H. *J. Phys.: Condens. Matter* **2008**, *20*, 323202.
- [37] Some, S.; Kim, Y.; Hwang, E.; Yoo, H.; Lee, H. *Chem. Commun.* **2012**, *48*, 7732-7734.
- [38] Tung, V. C.; Allen, M. J.; Yang, Y.; Kaner, R. B. *Nat Nanotechnol.* **2009**, *4*, 25-29.
- [39] Gao, X.; Jang, J.; Nagase, S. *J. of Phys. Chem. C* **2010**, *114*, 832 – 842.
- [40] Hummer, W.; Offeman, R. *J. Am. Chem. Soc.* **1958**, *80*, 1339.
- [41] Cai, W.; Piner, R. D.; Stademann, F. J. Park, S. Shaibat, M. A. Ishii, Y.; Velamakanni, A.; An, S. J.; Stoller, M.; An, J.; Chen, D.; *Science* **2008**, *321*, 1815.
- [42] Gao, W.; Alemany, L. B.; Ci, L.; Ajayan, P. M. *Nat. Chem.* **2009**, *1*, 403.
- [43] He, H.; Klinowski, J.; Forster, M.; Lerf, A. *Chem. Phys. Lett.* **1998**, *287*, 53–56.

- [44] Lerf, A.; He, H.; Forster, M.; Klinowski, J. *Phys. Chem. B* **1998**, *102*, 4477.
- [45] Dimiev, A. M.; Alemany, L. B.; Tour, J. M. *ACS Nano* **2013**, *7*, 576-578.
- [46] Marcano, D.; Kosynkin, D. V.; Berlin, J. M.; Siniskii, A.; Sun, Z.; Slesarev, A.; Alemany, L. B.; Luand, W.; Tour, J. M. *ACS Nano* **2010**, *4*, 8.
- [47] Park, S.; Ruoff, R. S. *Nat. Nanotechnol.* **2009**, *4*, 217-224.
- [48] Hernandez, Y.; Nicolosi, V.; Lotya, M.; Blighe, F. M.; Sun, Z.; De, S.; McGovern, I. T.; Holland, B.; Byrne, M.; Gun'Ko, Y. K.; Boland, J. J.; Niraj, P.; Duesberg, G.; Krishnamurthy, S.; Goodhue, R.; Hutchison, J.; Scardac, V.; Ferrari, A.; Coleman, J. *Nat. Nanotechnol.* **2008**, *3*, 563-568.
- [49] Green A. A. Hersam, M. C. *Nano. Lett.* **2009**, *9*, 4031.
- [50] Park, K. H.; Kim, B. H.; Song, S. H.; Kwon, J.; Kong, B. S.; Kang, K.; Jeon, S. *Nano Lett* **2012**, *12*, 2871-2876.
- [51] Lin, S.; Shih, C.-J.; Strano, M. S.; Blankschtein, D. *J. Am. Chem. Soc.* **2011**, *133*, 12810-12823.
- [52] Nikitin, Y. A.; Pyatkovskii, M. L. *Powder Metall. Met. Ceram.* **1997**, *36*, 41-45.
- [53] Rangappa, D.; Sone, K, Wang, M.; Gautam, U. K.; Goldberg, D.; Itoh, H.; Ichihara, M.; Honma, I. *Chemistry - Chem. Eur. J.* **2010**, *16*, 6488-6494
- [54] Pu, N.-W.; Wang, C.-A.; Sung, Y.; Liu, Y.-M.; Ger, M.-D.; *Mater. Lett.* **2009**, *63*, 1987-1989.
- [55] Coleman, J. N. *Acc. Chem. Res.* **2013**, *46*, 14-22.
- [56] Somani, P. R., Somani, S. P., Umeno M. *Chem Phys Lett* **2006**, *430*, 56.
- [57] May, J. W. *Surf. Sci* **1969**, *17*, 267.

- [58] Shelton, J.C, Patil, H. R.; Blakely, J. M. *Surf Sci*, **1974**; *43*, 493.
- [59] Eizenberg, M.; Blakely, J. M. *Surf. Sci.* **1979**, *82*, 228.
- [60] Oshima, C.; Nagashima, A. *J. Phys.: Condens. Matter*. **1997**, *9*, 1.
- [61] Gall, N. R.; Rut'kov, E. V.; Tontegode, A. Y. *Internat. J. Modern Phys. B* **1997**, *11*, 1865.
- [62] Bao, W.; Miao, W. F.; Chen, Z.; Zhang, H.; Jang, W.; Dames, C.; Lau, C. N. *Nat. Nanotechnol.* **2009**, *4*, 562–566.
- [63] Li, X.; Cai, W.; An, J.; Kim, S.; Nah, J.; Yang, D.; Piner, R.; Velamakanni, A.; Jung, I.; Tutuc, E.; Banerjee, S. K. Sanjay, K.; Colombo, L.; Ruoff, R. S. *Science* **2009**, *324*, 1312–1314.
- [64] Kim, K. S.; Zhao, Y.; Jang, H.; Lee, S. Y. Kim, J. M.; Kim, K. S.; Ahn, J. H.; Kim, P.; Choi, J. Y.; Hong, B. H. *Nature* **2009**, *457*, 706.
- [65] Wan, X; Chen, K.; Liu, D.; Chen, J.; Miao, Q.; Xu, J. *Chem. Mater.* **2012**, *24*, 3906–3915.
- [66] Li, Z.; Wu, P.; Wang, C.; Fan, X.; Zhang, W.; Zhai, X.; Zeng, C.; Li, Z.; Yang, J.; Hou, J. *ACS Nano* **2011**, *4*, 3385–3390.
- [67] Zhang, B.; Lee, W. H. Piner, R.; Kholmanov, I. Wu, Y.; Li, H.; Ji, H.; Ruoff, R. S. *ACS Nano*, **2012**, *6*, 2471–2476.
- [68] Bae, S.; Kim, H.; Lee, Y.; Xu, X.; Park, J.-S.; Zheng, Y. Balakrishnan, J.; Lei, T.; Kim, H. R.; Song, Y. II.; Kim, Y.-J.; Kim, K. S.; Özyilmaz, B.; Ahn, J.-H.; Hong, B. H.; Lijima, S. *Nat. Nanotechnol.* **2010**, *5*, 574.
- [69] Wu, J.; Pisula, W.; Mullen K. *Chem. Rev.* **2007**, *107*, 718.
- [70] Yang, X.; Dou, X.; Rouhanipour, A.; Zhi, L.; Rader, H. J.; Mullen, K. *J. Am. Chem. Soc.* **2008**, *130*, 4216.

- [71] Cai, J.; Ruffieux, P.; Jaafar, R.; Bieri, M.; Braun, T.; Blankenburg, S.; Mouth, M.; Sietsonen, A. P.; Saleh, M.; Feng, X.; Müllen, K.; Fasel, R. *Nature* **2010**, *466*, 470.
- [72] Jiao, L.; Zhang, L.; Wang, X.; Diankov, G.; Dai, H. *Nature* **2009**, *458*, 877.
- [73] Kosynkin, D. V.; Higginbotham, A. L.; Sinitskii, A.; Lomeda, J. R.; Dimiev, A.; Price, B. K.; Tour, J. M. *Nature* **2009**, *458*, 872.
- [74] Bai, J. W.; Cheng, R.; Xiu, F. X.; Liao, L.; Wang, M. S.; Shailos, A.; Wang, K. L.; Huang, Y.; Duan, X. F. *Nat. Nanotechnol.* **2010**, *5*, 655.
- [75] Jiao, L. J.; L., Y.; Wang, X. R.; Diankov, G.; Wang, H. L.; Dai, H. J. *Nat. Nanotechnol.* **2010**, *5*, 321.
- [76] Jung, I.; Pelton M.; Piner, P.; Dikin, D. A.; Stankovich, S.; Watcharotone S.; Hauser, M.; Ruoff, R. S. *Nano Lett.* **2007**, *7*, 3569.
- [77] Ni, Z. H.; Wang, H. M.; Kasim, J.; Fan, H. M.; Yu, T.; Wu, Y. H.; Feng, Y. P.; Shen, Z. X. *Nano Lett.* **2007**, *7*, 2758.
- [78] Lambacher, A.; Fromherz, P. *Appl. Phys. A – Mater. Sci. Process.* **1996**, *63*, 207.
- [79] Kim, J.; Cote, L. J.; Kim, F.; Huang, J. *J. Am. Chem. Soc.* **2009**, *132*, 260.
- [80] Paredes, J. I.; Villar-Rodil, S.; Solis-Fernandez, P. Martinez-Alonso, A. Tascon, J. M. D. *Langmuir* **2009**, *25*, 5957.
- [81] Lee, C.; Wei, X.; Kysar, J. W.; Hone, J. *Science* **2008**, *321*, 385.
- [82] Meyer, J. C.; Kisielowski, C.; Erni, R.; Rossell, M. D.; Crommie, M. F. Zettl, A. *Nano Lett* **2008**, *8*, 3582.
- [83] Gass, M. H.; Bangert, U.; Bleloch, A. L.; Wang, P.; Nair, R. R. Geim, A. K.; *Nature Nanotechnol.* **2008**, *3*, 676.
- [84] Park, J. S.; Reina, A.; Saito, R.; Kong, J.; Dresselhaus, G.; Dresselhaus, M. S.; *Carbon* **2009**, *47*, 1303.

- [85] Ferrari, A. C.; Meyer, J. C.; Scardaci, V.; Casiraghi, C.; Lazzeri, M.; Mauri, F.; Piscanec, S.; Jiang, D.; Novoselov, K. S.; Roth, S.; Geim, A. K. *Phys. Rev. Lett.* **2006**, *97*, 187401.
- [86] Calizo, I.; Balandin, A. A.; Bao, W.; Miao, F.; Lau, C. N. *Nano. Lett.* **2007**, *7*, 2645.
- [87] Gupta, A.; Chen, G.; Joshi, P.; Tadigadapa, S.; Eklund, P. C. *Nano Lett.* **2006**, *6*, 2667-2673.
- [88] Tuinstra, F.; Koenig, J.L. *J. Chem. Phys.* **1970**, *53*, 1126.
- [89] Ferrari, A. C.; Robertson, J. *Phys. Rev. B* **2000**, *61*, 14095.
- [90] Castiglioni, C.; Negri, F.; Rigolio, M.; Zerbi, G. *J. Chem. Phys.* **2001**, *115*, 3769.
- [91] Ferrari, A. C.; Meyer, J. C.; Scardaci, V.; Casiraghi, C.; Lazzeri, M.; Mauri, F.; Piscanec, S.; Jiang, D.; Novoselov, K. S.; Roth, S.; Geim, A. K. *Phys. Rev. Lett.* **2006**, *97*, 187401.

CHAPTER 2

SYNTHESIS OF ANTHRACENE DERIVATIVES

2.1 Introduction

The search continues to find ways to synthesize high quality single layer graphene at low temperatures, with an emphasis in the development of reproducible methods that can be performed on an industrial scale. This goal has motivated the Tolbert and Henderson groups to work in collaboration to find ways to achieve this objective. This project emphasizes the synthesis and use of molecules as carbon sources. This chapter is devoted to the synthesis of anthracene derivatives to be used as carbon sources for the synthesis of graphene by CVD at low temperatures.

Our interest in these derivatives is two-fold. First, these molecules will be used as carbon sources for the synthesis of graphene. Our second interest in these molecules derives from their use as precursors for the synthesis of dibenzo[*bc,kl*]coronene.^{4,5} All synthesized compounds were characterized by ¹H-NMR, ¹³C-NMR, MS and IR among other techniques.

2.2 Experimental Protocol

General Experimental

All organic solvents and reagents to synthesize the anthracene derivatives were used as received from commercial sources without further purification unless otherwise noted. Melting points were measured on an Electrothermal melting point apparatus and

are uncorrected. NMR spectra were determined with a Varian Mercury Vx 300 spectrometer operating at 300 MHz for ^1H and at 75 MHz for ^{13}C , in deuterated solvents, as indicated in the text. Chemical shifts were referenced to TMS or the residual proton peak of the solvent. Low-resolution MS spectra (EI 70 eV) were measured on a Micromass AutoSpec spectrometer. UV-vis spectra were recorded with a Cary 5000 UV-Vis-NIR absorbance spectrometer instrument. TLC analyses were performed on Analtech Uniplate Silica Gel, GF plates. Column chromatography was performed using Sorbent Technologies 40-63 μM standard grade silica gel.

9,10-Bis(2,6-dimethylphenyl)-9,10-dihydroanthracene-9,10-diol (3a, Figure 2.1)

The synthesis of 9,10-bis(2,6-dimethylphenyl)-9,10-dihydroanthracene-9,10-diol (**3a**) was carried out with small modifications from the literature.¹ THF was distilled over sodium and benzophenone. A solution of 1-bromo-2,6-dimethylbenzene (9.09 g, 48.1 mmol) in dry THF (200 mL) was stirred under Ar and cooled at $-78\text{ }^\circ\text{C}$ in a dry ice/acetone bath. *n*-Butyllithium (25 mL, 40 mmol) was added dropwise. The solution was stirred for 3 hours at $-78\text{ }^\circ\text{C}$. Anthracene-9,10-dione (1.62 g, 7.76 mmol) was added to the pale yellow solution, and the mixture was allowed to gradually warm to r.t. with stirring under Ar. To the reaction mixture, saturated aqueous solution of NH_4Cl (200 mL) was added. The mixture was concentrated in a rotary evaporator to remove some of the THF. The product was extracted with CH_2Cl_2 (3 x 100 mL) and the organic layer was washed with water (200 mL) and dried over anhydrous MgSO_4 . The solvent was removed in a rotary evaporator until a small volume remained at which point hexane (250 mL) was added, resulting in the formation of a colorless precipitate. The desired 9,10-bis(2,6-dimethylphenyl)-9,10-dihydroanthracene-9,10-diol (**3a**) was isolated by vacuum filtration as a colorless solid (2.29 g, 5.45 mmol, 70.3 %), m.p. $326\text{--}328\text{ }^\circ\text{C}$. IR (powder): 3557 cm^{-1} (OH), 3052 cm^{-1} ($\text{sp}^2\text{ C-H}$), 2963 cm^{-1} ($\text{sp}^3\text{ C-H}$), 1471 cm^{-1} (C=C), 1158 cm^{-1} (C-O). 764

cm⁻¹ (C-H). ¹H-NMR (300 MHz, CDCl₃): δ 2.23 (s, 2H), 2.36 (bs, 12H), 7.02 (bd, 4H, *J* = 6 Hz), 7.14 (t, 2H, *J* = 7.5 Hz), 7.19-7.28 (m, 8H). ¹³C NMR (75 MHz, CDCl₃): δ 25.24, 78.85, 127.40, 127.75, 129.20, 131.35, 137.62, 140.14, 143.23. EI-MS *m/z*: 403 [M⁺ - OH], 386 [M⁺ - 2(OH)].

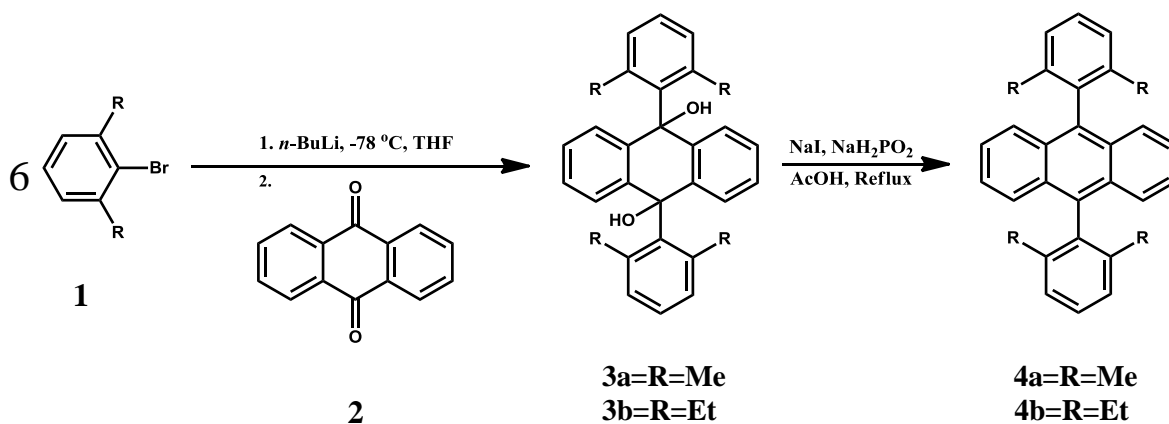


Figure 2.1. Synthetic scheme for the synthesis of anthracene derivatives.

9,10-Bis(2,6-dimethylphenyl)anthracene (**4a**, Figure 2.1)

The synthesis of 9,10-bis(2,6-dimethylphenyl)anthracene (**4a**) was carried out with small modifications from the literature.¹ A suspension of 9,10-bis(2,6-dimethylphenyl)-9,10-dihydroanthracene-9,10-diol (2.28 g, 5.43 mmol), sodium iodide (5.43 g, 36.2 mmol) and sodium hypophosphite (5.23 g, 49.3 mmol) in glacial acetic acid (150 mL) was heated at reflux for 3 hrs. After cooling, the mixture was filtered and the product was washed with cold water (200 mL) and cold methanol (50 mL). After drying under reduced pressure, 9,10-bis(2,6-dimethylphenyl)anthracene (**4a**) was obtained as a colorless solid (1.96 g, 5.08 mmol, 93.6 %), m.p. 290-292 °C. IR (powder): 3053 cm⁻¹ (sp² C-H), 2961 cm⁻¹ (sp³ C-H), 1467 cm⁻¹ (C=C), 769 cm⁻¹ (C-H). ¹H-NMR (300 MHz, CDCl₃): δ 1.80 (s, 12H), 7.26-7.39 (m, 10H), 7.46-7.52 (m, 4H). ¹³C NMR (75 MHz,

CDCl₃): δ 20.27, 125.63, 126.46, 127.65, 129.63, 135.42, 138.04, 138.09. EI-MS m/z: 386.2 [M⁺]. UV-Vis λ_{max} (nm): 394, 373, 354, 337.

9,10-Bis(2,6-diethylphenyl)-9,10-dihydroanthracene-9,10-diol (3b, Figure 2.1)

The synthesis of 9,10-bis(2,6-diethylphenyl)-9,10-dihydroanthracene-9,10-diol (**3b**) was carried out with small modifications from the literature.¹ THF was distilled over sodium and benzophenone. A solution of 1-bromo-2,6-diethylbenzene (2.45 g, 10.8 mmol) in dry THF (75 mL) was stirred under Ar and cooled at -78 °C in a dry ice/acetone bath. *n*-Butyllithium (6.5 mL, 10 mmol) was added dropwise. The solution was stirred for 5.5 hours at -78 °C. Anthracene-9,10-dione (574 mg, 2.75 mmol) was added to the yellow solution, and the mixture was allowed to gradually warm to r.t. with stirring under Ar. To the reaction mixture, 10% HCl in small increments until the reaction mixture turned acidic. The mixture was concentrated in a rotary evaporator to remove some of the THF. The product was extracted with CH₂Cl₂ (3 x 30 mL) and the organic layer was washed with water (100 mL) and dried over anhydrous CaCl₂. The solvent was removed in a rotary evaporator until a small volume remained at which point hexane (100 mL) was added, resulting in the formation of a light yellow precipitate. The desired 9,10-bis(2,6-diethylphenyl)-9,10-dihydroanthracene-9,10-diol (**3b**) was isolated by vacuum filtration as a light yellow solid (115 mg, 0.241 mmol, 8.8 %). ¹H-NMR (300 MHz, CDCl₃): δ 0.403-3.44 (bm, 22H), 7.10-7.28 (bm, 14H). ¹³C NMR (75 MHz, CDCl₃): δ 78.93, 127.72, 128.51, 128.95, 140.52, 142.21. EI-MS m/z: 459 [M⁺ - OH].

9,10-Bis(2,6-diethylphenyl)anthracene (4b, Figure 2.1)

The synthesis of 9,10-bis(2,6-diethylphenyl)anthracene (**4b**) was carried out with small modifications from the literature.¹ A suspension of 9,10-bis(2,6-diethylphenyl)-9,10-dihydroanthracene-9,10-diol (17.1 mg, 34.8 μ mol), sodium iodide (35.7 mg, 0.238

mmol) and sodium hypophosphite (33.3 mg, 0.298 mmol) in glacial acetic acid (2 mL) was heated at reflux for 1.5 hrs. After cooling, the mixture was filtered and the product was washed with cold water and cold methanol. After drying under reduced pressure, 9,10-bis(2,6-diethylphenyl)anthracene (**4b**) was obtained as a yellow solid (8.7 mg, 20 μ mol, 56 %), $^1\text{H-NMR}$ (300 MHz, CDCl_3): δ 0.759 (t, 12H, $J = 7.5$ Hz), 2.04 (q, 12H, $J = 7.5$ Hz), 7.18-7.22 (m, 5H), 7.29 (d, 4H $J = 7.5$ Hz), 7.40-7.46 (m, 5H). $^{13}\text{C NMR}$ (75 MHz, CDCl_3): δ 14.97, 26.78, 125.33, 125.88, 126.97, 128.27, 130.31, 135.02, 137.04, 143.77.

9,10-Bis(2,6-bis(bromomethyl)phenyl)anthracene (5, Figure 2.2)

A suspension of 9,10-bis(2,6-dimethylphenyl)anthracene (1.90 g, 4.92 mmol), N-bromosuccinimide (NBS) (3.5 g, 20 mmol) and benzoyl peroxide (BPO) (few grains) in carbon tetrachloride (100 mL) was heated at reflux overnight. After cooling, the mixture was filtered to remove the succinimide and the yellow solution was concentrated in a rotary evaporator. The resulting solid was washed with small volumes of cold methylene chloride and cold acetone to afford 9,10-bis(2,6-bis(bromomethyl)phenyl)anthracene (**5**) as a colorless solid (1.12 g, 1.60 mmol, 32.5 %), m.p. decomposes at 160 $^\circ\text{C}$. IR (powder): 3020 cm^{-1} (sp^2 C-H), 2970 cm^{-1} (sp^3 C-H), 1430 cm^{-1} (C=C), 1210 cm^{-1} ($\text{CH}_2\text{-Br}$), 769 cm^{-1} (C-H). $^1\text{H-NMR}$ (300 MHz, CDCl_3): δ 4.02 (s, 8H), 7.32-7.38 (m, 4H), 7.43-7.49 (m, 4H), 7.56-7.64 (m, 2H), 7.71 (s, 2H), 7.71-7.73 (m, 4H). $^{13}\text{C NMR}$ (75 MHz, CDCl_3): δ 31.41, 126.36, 126.83, 129.65, 130.28, 131.33, 132.11, 138.04, 138.17. EI-MS m/z : 701.8 [M^+]. UV-Vis λ_{max} (nm): 397, 376, 357, 340.

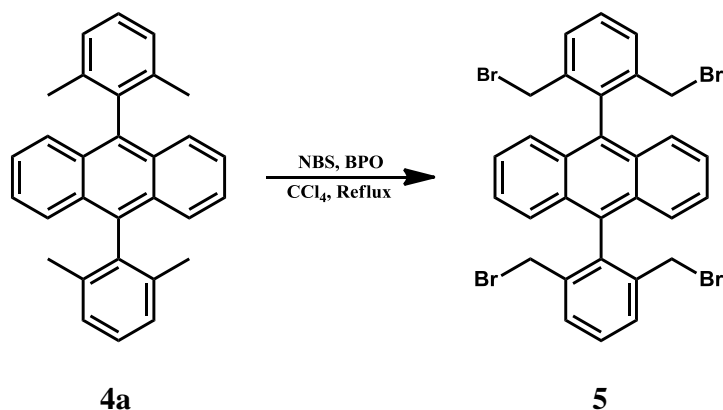


Figure 2.2. Synthetic scheme for the synthesis of 9,10-bis(2,6bis(bromomethyl) phenyl) anthracene (**5**) from 9,10-bis(2,6-dimethylphenyl)anthracene (**4a**).

4,7-Dimethyl-3a,4,7,7a-tetrahydro-4,7-epoxyisobenzofuran-1,3-dione (**8**, Figure 2.3)

The synthesis of 4,7-dimethyl-3a,4,7,7a-tetrahydro-4,7-epoxyisobenzofuran-1,3-dione (**8**) was carried out according to the literature.⁶ To a suspension of maleic anhydride (11.5 g, 116 mmol) in anhydrous diethyl ether (8 mL), 2,5-dimethylfuran (11.1 mg, 116 mmol) was added under Ar and the mixture was stirred overnight. The reaction mixture was filtered to afford 4,7-dimethyl-3a,4,7,7a-tetrahydro-4,7-epoxyisobenzofuran-1,3-dione (**8**) as a colorless solid (14.6 g, 75.2 mmol, 64.8%), m.p. 62-66 °C. IR (powder): 3056 cm⁻¹ (sp² C-H), 2983 cm⁻¹ (sp³ C-H), 1778 (C=O), 1592 cm⁻¹ (C=C), 1080 cm⁻¹ (C-O-C). ¹H-NMR (300 MHz, CDCl₃): δ 1.74 (s, 6H), 3.14 (s, 2H), 6.33 (s, 2H). ¹³C NMR (75 MHz, CDCl₃): δ 15.77, 54.19, 89.01, 141.31, 168.70.

4,7-Dimethylisobenzofuran-1,3-dione (**9**, Figure 2.3)

The synthesis of 4,7-dimethylisobenzofuran-1,3-dione (**9**) was carried out with a small modification from the literature.⁶ To concentrated sulfuric acid (170 mL) cooled at -6 °C, 4,7-dimethyl-3a,4,7,7a-tetrahydro-4,7-epoxyisobenzofuran-1,3-dione (**8**) (14.6 g, 75.0 mmol) was added in small portions with vigorous stirring. Once all the starting

material had been added, the reaction mixture was kept at -6 °C until the color became orange. At this point the temperature was allowed to rise slowly to 10 °C. The reaction mixture was poured slowly onto crushed ice (800 g). The resulting colorless solid was washed with cold water. The solid was dissolved in 10% aqueous NaOH (150 mL). Glacial acetic acid (25 mL) was added to the solution. The mixture was filtered to remove insoluble material and the resulting solution was acidified with 36% HCl (15 mL). The resulting precipitate was collected and washed with water until neutral. The precipitate was dissolved in CHCl₃ and dried over anhydrous MgSO₄. Filtration and concentration afforded 4,7-dimethylisobenzofuran-1,3-dione (**9**) as a light yellow solid (9.67 g, 54.9 mmol, 73.2%), m.p. 140-142 °C. IR (powder): 3040 cm⁻¹ (sp² C-H), 2914 cm⁻¹ (sp³ C-H), 1758 (C=O), 751 cm⁻¹ (C-H). ¹H-NMR (300 MHz, CDCl₃): δ 2.65 (s, 6H), 7.48 (s, 2H). ¹³C NMR (75 MHz, CDCl₃): δ 17.60, 128.70, 137.97, 138.0, 163.48. EI-MS m/z: 176.0 [M+].

Pseudo form of 2-(2,5-dimethylbenzoyl)-3,6-dimethylbenzoic acid. (10, Figure 2.3)

The synthesis of the *pseudo* form of 2-(2,5-dimethylbenzoyl)-3,6-dimethylbenzoic acid (**10**) was carried out with small modifications from the literature.⁶ A solution of 4,7-dimethylisobenzofuran-1,3-dione (**9**) (585 mg, 3.32 mmol) in *p*-xylene (5 mL) was cooled to 0 °C with vigorous stirring under Ar. Anhydrous AlCl₃ (2.22 g, 16.4 mmol) was added to the solid reaction mixture. The mixture was allowed to warm to r.t. and was stirred at 65 °C overnight. The reaction mixture was poured into ice water (10 mL) and acidified to pH<1. The mixture was extracted with benzene (4x10 mL). The organic solution was extracted with 5% aqueous NaOH (5x8 mL) and the NaOH extracts were treated with activated charcoal and filtered through celite 521. The aqueous solution was acidified with 36% HCl. The precipitate was collected by filtration and washed with water to afford the *pseudo* form of 2-(2,5-dimethylbenzoyl)-3,6-dimethylbenzoic acid (**10**) as a colorless solid (815 mg, 2.89 mmol, 87.0%), m.p. 140-142 °C. IR (powder):

3283 cm^{-1} (OH), 3018 cm^{-1} (sp^2 C-H), 2970 cm^{-1} (sp^3 C-H), 1722 (C=O). $^1\text{H-NMR}$ (300 MHz, CDCl_3): δ 2.08 (s, 6H), 2.29 (s, 3H), 2.57 (s, 3H) 4.01 (br. s, 1H), 6.90-7.37 (m, 5H). $^{13}\text{C NMR}$ (75 MHz, CDCl_3): δ 17.12, 17.21, 17.50, 20.28, 20.36, 20.48, 20.91, 21.22, 21.30, 126.38, 129.25, 130.42, 132.09, 132.12 132.51, 132.72, 132.80, 132.87, 133.39, 134.01, 135.27, 136.93, 136.96. EI-MS m/z : 282.1 $[\text{M}^+]$.

1,4,5,8-Tetramethylantraquinone. (11, Figure 2.3)

The synthesis of of 1,4,5,8-tetramethylantraquinone (**11**) was carried out according to the literature.⁶ The *pseudo* form of 2-(2,5-dimethylbenzoyl)-3,6-dimethyl benzoic acid (**10**) (661 mg, 2.34 mmol) and concentrated sulfuric acid (5.0 mL) was heated to 100 $^\circ\text{C}$ with stirring for 1.5 hrs. The resulting brown-red solution was poured into ice and the mixture filtered. The purple solid was extracted with hot benzene (> 60 $^\circ\text{C}$). The organic solution was washed with saturated Na_2CO_3 and dried over anhydrous MgSO_4 . Filtration and concentration afforded 1,4,5,8-tetramethylantraquinone (**11**) as yellow flaky solid (233 mg, 0.882 mmol, 37.7%), m.p. 220-221 $^\circ\text{C}$. IR (powder): 3018 cm^{-1} (sp^2 C-H), 2923 cm^{-1} (sp^3 C-H), 1664 (C=O). $^1\text{H-NMR}$ (300 MHz, CDCl_3): δ 2.59 (s, 12H), 7.24 (s, 4H). $^{13}\text{C NMR}$ (75 MHz, CDCl_3): δ 22.03, 134.56, 135.91, 137.16, 190.25. ESI-MS m/z : 264.1 $[\text{M}^+]$.

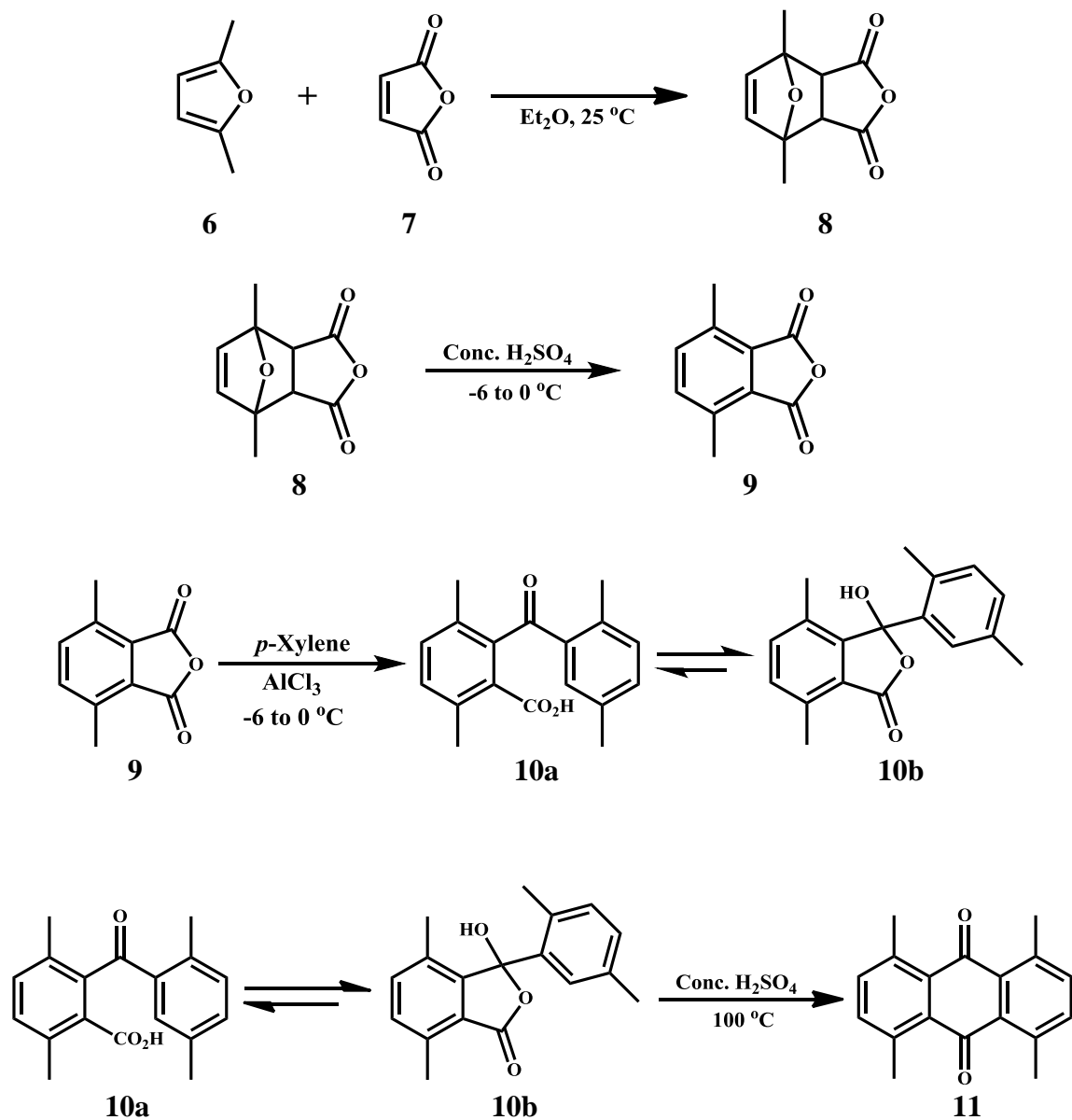


Figure 2.3 Synthetic scheme for the synthesis of 1,4,5,8-tetramethylantracene-9,10-dione (**11**).

1,4-Dimethyl-9,10-di-*o*-tolyl-9,10-dihydroanthracene-9,10-diol (**12**, Table 1)

The synthesis of 1,4-dimethyl-9,10-di-*o*-tolyl-9,10-dihydroanthracene-9,10-diol (**12**) was carried out with small modifications from the literature.¹ THF was distilled over sodium and benzophenone. A solution of 1-bromo-2-methylbenzene (2.10 g, 12.2 mmol)

in dry THF (75 mL) was stirred under Ar and cooled at $-78\text{ }^{\circ}\text{C}$ in a dry ice/acetone bath. *n*-Butyllithium (7.4 mL, 12 mmol) was added dropwise. The solution was stirred for 5 hours at $-78\text{ }^{\circ}\text{C}$. 1,4-dimethylantracene-9,10-dione (709 mg, 3.00 mmol) was added to the solution, and the mixture was allowed to gradually warm to r.t. with stirring under Ar. To the reaction mixture, saturated aqueous solution of NH_4Cl (60 mL) was added. The mixture was concentrated in a rotary evaporator to remove some of the THF. The product was extracted with CH_2Cl_2 (2 x 50 mL) and the organic layer was washed with water (100 mL) and dried over anhydrous MgSO_4 . The solvent was removed in a rotary evaporator until a small volume remained at which point hexane (100 mL) was added, resulting in the formation of a colorless precipitate. The desired 1,4-dimethyl-9,10-di-*o*-tolyl-9,10-dihydroanthracene-9,10-diol (**12**) was isolated by vacuum filtration as a light yellow solid (982 mg, 2.34 mmol, 77.9 %), m.p.228-231 $^{\circ}\text{C}$. IR (powder): 3593 cm^{-1} (OH), 3062 cm^{-1} ($\text{sp}^2\text{ C-H}$), 2945 cm^{-1} ($\text{sp}^3\text{ C-H}$), 1455 cm^{-1} (C=C), 1160 cm^{-1} (C-O). 747 cm^{-1} (C-H). $^1\text{H-NMR}$ (300 MHz, CDCl_3): δ 1.72 (bs, 6H), 2.00 (s, 6H), 2.65 (s, 2H), 6.91 (bd, 2H, $J = 7.2\text{ Hz}$), 6.96 (s, 2H), 7.10-7.24 (m, 6H), 7.34 (bt, 2H, $J = 7.2\text{ Hz}$), 8.36 (bs, 2H). $^{13}\text{C NMR}$ (75 MHz, CDCl_3): δ 21.94, 22.97, 125.35, 127.22, 127.25, 127.92, 128.25, 128.29, 128.48, 132.02, 133.38, 134.15, 135.49, 135.50, 146.05. EI-MS m/z : 420.

1,4-Dimethyl-9,10-di-*o*-tolylanthracene (13, Table 1)

The synthesis of 1,4-dimethyl-9,10-di-*o*-tolylanthracene (**13**) was carried out with small modifications from the literature.¹ A suspension of 1,4-dimethyl-9,10-di-*o*-tolyl-9,10-dihydroanthracene-9,10-diol (420.6 mg, 1.00 mmol), sodium iodide (1.00 g, 6.68 mmol) and sodium hypophosphite (1.06 g, 9.50 mmol) in glacial acetic acid (25 mL) was heated at reflux overnight. After cooling, the mixture was filtered and the product was washed with cold water (50 mL) and cold methanol. After drying under reduced pressure, 1,4-dimethyl-9,10-di-*o*-tolylanthracene (**13**) was obtained as a yellow solid (354 mg,

0.916 mmol, 91.6 %), m.p.164-165 °C. IR (powder): 3049 cm⁻¹ (sp² C-H), 2957 cm⁻¹ (sp³ C-H), 1460 cm⁻¹ (C=C), 747 cm⁻¹ (C-H). ¹H-NMR (300 MHz, CDCl₃): δ 1.94 (s, 6H), 1.97 (s, 6H), 7.02 (s, 2H), 7.21-7.43 (m, 12H). ¹³C NMR (75 MHz, CDCl₃): δ 20.61, 25.75, 125.32, 125.53, 126.78, 127.87, 128.97, 129.71, 130.23, 131.11, 132.06, 134.56, 136.83, 138.20, 142.82. EI-MS m/z: 386.

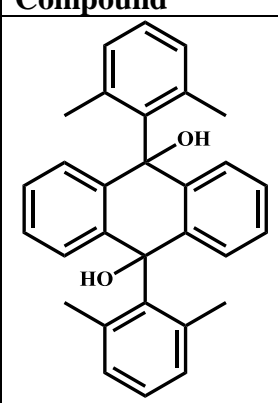
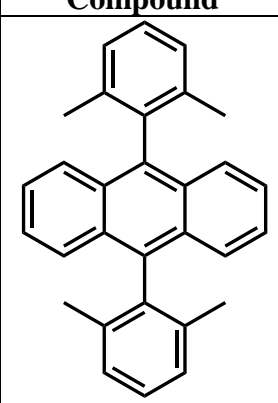
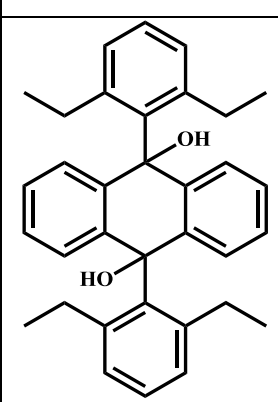
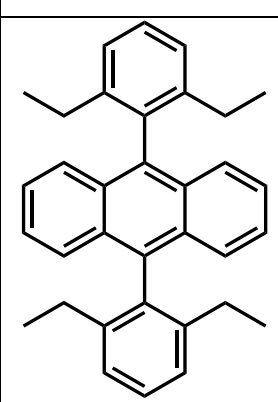
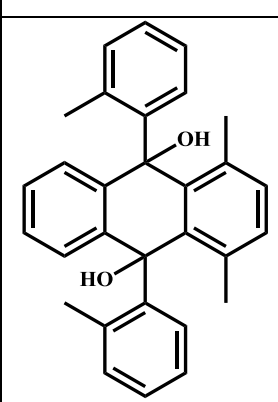
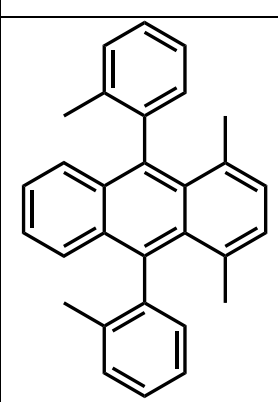
2.3 Results

The synthesis of anthracene derivatives and diol precursors is shown to be a straightforward synthesis when the alkyl substituents are methyl groups. In the case of the diethyl substituted compounds the synthesis gave only a low yield of the diol precursor (**Table 2.1**) This low percent yield could be due to the steric hindrance caused by the ethyl groups as the (2,6-diethylphenyl)lithium molecule attacks the anthraquinone during the formation of the diol anthracene. It should be mentioned that the formation of the reduced, i.e. aromatized, molecules proceeded in with good yield regardless if a methyl or ethyl group was the substituent (**Table 2.1**).

The synthesis of the bromomethyl anthracene derivative opens the door for the possibility to synthesize anthracene derivatives with other functionalities.

Finally, 1,4,5,8-tetramethylantracene-9,10-dione (**11**) was synthesized through a series of synthetic steps (**Figure 2.3**) in order to synthesize 1,4,5,8-tetramethyl-9,10-diphenyl-9,10-dihydroanthracene-9,10-diol (**14**, **Figure 2.4**) and 1,4,5,8-tetramethyl-9,10-diphenyl anthracene (**15**, **Figure 2.4**). The synthesis of 1,4,5,8-tetramethyl-9,10-diphenyl-9,10-dihydroanthracene-9,10-diol (**14**) following the procedure used for the previous anthracene derivatives resulted in a mixture of products with a small yield of the desired product. Several attempts to synthesize 1,4,5,8-tetramethyl-9,10-diphenylantracene (**15**) failed to provide the desired product.

Table 2.1. Percentage yield of synthesized anthracene derivatives.

Compound	%Yield	Compound	%Yield
 3a	70	 4a	93
 3b	8.8	 4b	56
 12	78	 13	92

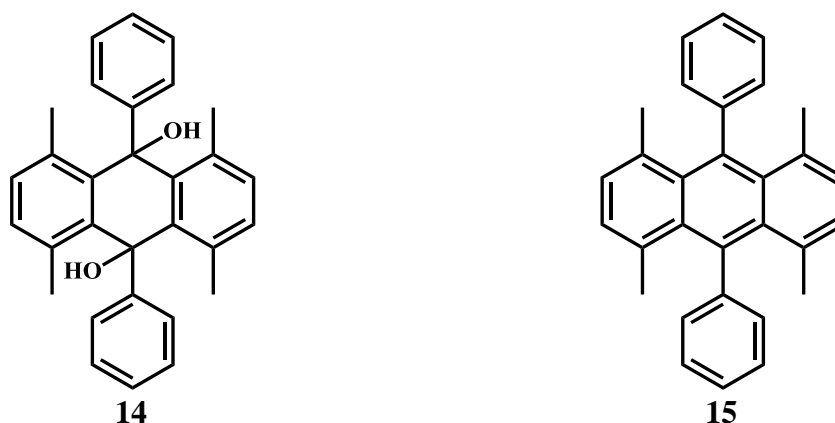


Figure 2.4. Anthracene derivatives, 1,4,5,8-tetramethyl-9,10-diphenyl-9,10-dihydroanthracene-9,10-diol (**14**) and 1,4,5,8-tetramethyl-9,10-diphenyl anthracene (**15**).

2.4 Conclusions

In conclusion, the synthesis of bis-alkylphenylanthracene derivatives proves to be a straightforward synthesis that can be easily accomplished as long as the substituent on the phenyl rings is a methyl group. The attempts at synthesizing 1,4,5,8-tetramethyl-9,10-diphenyl-9,10-dihydroanthracene-9,10-diol and 1,4,5,8-tetramethyl-9,10-diphenyl anthracene failed to produce the desired products. Attempts to synthesize 9,10-bis(2,6-diethylphenyl)-9,10-dihydroanthracene-9,10-diol show the steric effects of the alkyl groups on the phenyl rings at the 2,6 position on the course of the reaction. These results also show that once the diol is formed, reduction of the molecule to form the 9,10-bis(2,6-dimethylphenyl)anthracene derivative proceeds with good percentage yields. Finally, functionalization of the methyl group in the case of 9,10-bis(2,6-bis(bromomethyl)phenyl)anthracene might open the door to the synthesis of other anthracene derivatives.

The remainder of this dissertation details the applications of these compounds for the synthesis of graphene by the CVD method.

2.5 References

- [1] Kaur, I.; and Miller, G. P. *New J. Chem.* **2008**, *32*, 459–463
- [2] Wolak, M. A.; Jang, B.-B. Palilis, L. C.; and Kafafi, Z.; *J. Phys. Chem. B* **2004**, *108*, 5492-5499
- [3] Grein, K.; Kirste, B.; Kurreck, H. *Chem. Ber.* **1981**, *114*, 254-266.
- [4] Clar, E. Fell, G. S.; Ironside, C. T.; Balsillie, A. *Tetrahedron*, **1960**, *10*, 26-36.
- [5] Scholl, R.; Meyer, K. *Ber. Desch. Chem. Ges.* **1932**, *65*, 902.
- [6] Chan, T.-L.; Poon, C.-D.; Wong, H. N.; Hua, J.; Wang, L. L. *Tetrahedron* **1986**, *42*, 655-661.

CHAPTER 3

SYNTHESIS OF POLYCYCLIC AROMATIC HYDROCARBONS

3.1 Introduction

As with the previous chapter, this chapter focuses on the synthesis of molecules that can be used as carbon sources for the CVD synthesis of graphene at low temperature.

According to experimental¹ and theoretical² studies, five-membered rings are formed in isolated clusters from carbon monomers during the initial stage of the CVD process. These pentagons, when formed, diminish the quality of the graphene produced. A way to avoid the formation of these defects is by using polycyclic aromatic hydrocarbons (PAHs) with six-membered rings as the carbon source.³ Reports in the literature have shown that good quality graphene can be grown from materials such as coronene, pentacene and rubrene at temperatures as low as 550 °C in the case of coronene.³ These results suggest that the choice of the PAH is important in order to produce good quality graphene at low temperatures. Many other PAHs that can be used in attempts to synthesize graphene at low temperatures are commercially available. As an extension of the previous chapter, this chapter describes mainly the synthesis of dibenzo[*bc,kl*]coronene. Our interest in this molecule derives from the reasons described above and from its possible high reactivity. One of the 20 possible Kekulé structures⁴ shows this molecule to have some tetra-radical character (**Figure 3.1**). This radical character points to its possible high reactivity and can be used, in principle, to our advantage in the synthesis of graphene at low temperatures. This chapter focuses on the synthesis and reactivity of this molecule, although the synthesis of other PAHs will also be discussed.

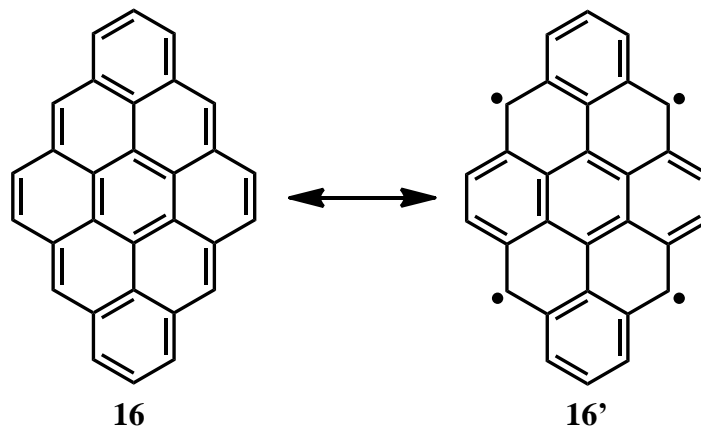


Figure 3.1 Two possible Kekulé structures for dibenzo[*bc,kl*]coronene.

3.2 Experimental Protocol

General Experimental

All organic solvents and reagents to synthesize the PAHs were used as received from commercial sources without further purification. THF was distilled over sodium and benzophenone. Melting points were measured on an Electrothermal melting point apparatus and are uncorrected. $^1\text{H-NMR}$ spectra were determined with a Varian Mercury Vx 300 spectrometer operating at 300 MHz for $^1\text{H-NMR}$, in deuterated solvents, as indicated in the text. Chemical shifts were referenced to TMS or the residual peak of the solvent. Low-resolution MS spectra (EI 70 eV) were measured on a Micromass AutoSpec spectrometer. UV-vis spectra were recorded with a Cary 5000 UV-Vis-NIR absorbance spectrometer. Reactions in glass ampoules were performed in a Lindberg Blue M Tube tube furnace. TLC analyses were performed on Analtech Uniplate Silica Gel, GF plates. Column chromatography was performed using Sorbent Technologies 40-63 μM standard grade silica gel.

Dibenzo[*cd,lm*]perylene (**18**, Figure 3.2)

The synthesis of dibenzo[*cd,lm*]perylene was carried out with small modifications from the literature.⁵ To a boiling solution of perinaphthenone (500 mg, 2.69 mmol) in dry benzene (15 mL), phosphorus pentasulfide (1.23 g, 5.55 mmol) was added. The reaction mixture was heated at reflux overnight. The reaction mixture was cooled and filtered and the residue was extracted with chloroform in a Soxhlet apparatus. Concentration afforded a brown solid. The solid was dissolved in dry THF and passed through a silica gel plug. Concentration afforded dibenzo[*cd,lm*]perylene as a brown powder (180 mg, 0.552 mmol, 20.5%), m.p. 371-376 °C. ¹H-NMR (300 MHz, CDCl₃): δ 8.12 (t, 2H, *J* = 7.8 Hz), 8.36 (d, 4H, *J* = 7.8 Hz), 8.41 (d, 4H, *J* = 9.3 Hz) 9.26 (d, 4H, *J* = 9.3 Hz). EI-MS *m/z*: 326.1 [M⁺]. UV-Vis λ_{max}(nm): 465, 439, 414, 390, 369, 325, 311.

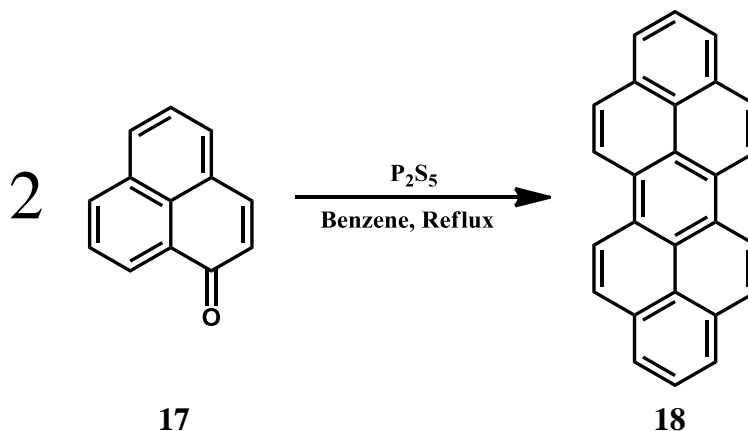


Figure 3.2 Synthetic scheme for the synthesis of dibenzo[*cd,lm*]perylene (**18**) from perinaphthenone (**17**).

1,12-Dimethylnaphtho[1,2,3,4-*rst*]pentaphene (**19**, Figure 3.3)

A solution of 1,4-dimethyl-9,10-di-*o*-tolylanthracene (**13**) (50.0 mg, 0.129 mmol) in chloroform or methylene chloride (4 mL) was added to 30% Pd/C (150 mg). The reaction mixture was concentrated in a rotary evaporator and transferred to a glass

ampoule. Dry ice (≈ 150 mg) was added. The glass ampoule was placed under vacuum for 2 minutes at r.t. and then cooled in liquid nitrogen. After 2 minutes of cooling, the system was sealed under vacuum and allowed to warm to room temperature gradually. The ampoule was heated to 200 °C at a ramp of 60 °C/min in a Lindberg furnace for 1 hr, allowed to cool to r.t., the ampoule was broken and the solids were extracted with chloroform. Concentration afforded the crude product as a brown solid. Purification by column chromatography (hexane: CH_2Cl_2 , 7:3) afforded an oily green residue, identified as 1,12-dimethylnaphtho[1,2,3,4-*rst*]pentaphene (**19**) (0.6 mg, 1.6 μmol , 1.2%). $^1\text{H-NMR}$ (300 MHz, CDCl_3): δ 2.70 (s, 6H), 7.46-7.50 (m, 2H), 7.59-7.62 (m, 2H), 7.70 (t, 2H, $J = 7.2$ Hz) 7.78 (s, 2H), 8.01-8.04 (m, 2H), 8.10 (d, 2H, $J = 7.8$ Hz), 8.36 (s, 2H). EI-MS m/z : 380.0 $[\text{M}^+]$. UV-Vis λ_{max} (nm): 577, 548, 409, 387, 366, 349.

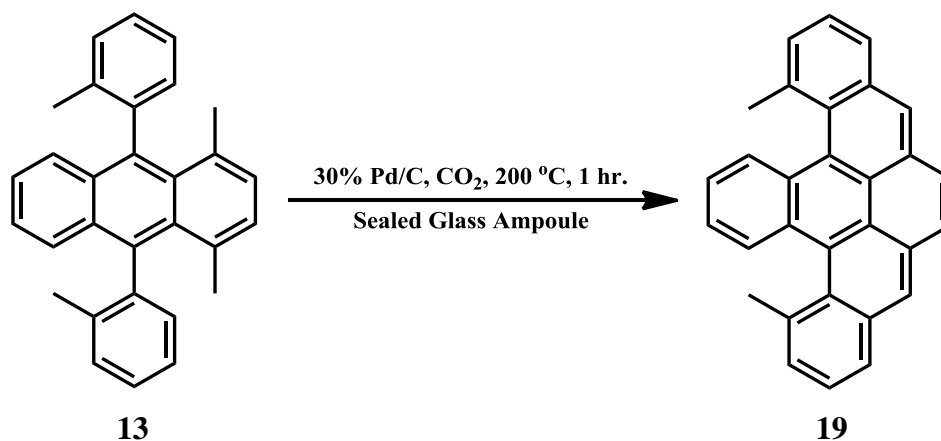


Figure 3.3 Synthetic scheme for the synthesis of 1,12-dimethylnaphtho[1,2,3,4-*rst*]pentaphene (**19**) from 1,4-dimethyl-9,10-di-o-tolylanthracene (**13**).

Dibenzo[*bc,kl*]coronene, glass ampoule approach (**16**, Figure 3.4)

The synthesis of dibenzo[*bc,kl*]coronene was carried out with modifications from the literature.⁶ A solution of 1,4-dimethyl-9,10-di-o-tolylanthracene (**13**) (50.0 mg, 0.129

mmol) in chloroform or methylene chloride (4 mL) was added to 30% Pd/C (150 mg). The mixture was concentrated in a rotary evaporator and transferred to a glass ampoule. Dry ice (\approx 150 mg) was added. The glass ampoule was placed under vacuum for 2 minutes at r.t. and then cooled in liquid nitrogen. After 2 minutes of cooling, the system was sealed under vacuum and allowed to warm to room temperature gradually. The ampoule was heated to 400 °C at a ramp of 60 °C/min in a Lindberg furnace. Once the temperature reached 400 °C, the reaction mixture was allowed to cool to r.t. The product was continuously extracted with dry THF (200 mL) in a Soxhlet apparatus for 48 hr. Concentration afforded dibenzo[*bc,kl*]coronene (**16**) as purple powder (15.3 mg, 0.0408 mmol, 31.7%). EI-MS *m/z*: 374.1 [M⁺]. UV–Vis λ_{max} (nm): 510, 477, 451, 356, 339.

Dibenzo[*bc,kl*]coronene glass reaction tube approach (16**, Figure 3.4)**

The synthesis of dibenzo[*bc,kl*]coronene (**16**) was carried out with modifications from the literature. A solution of 1,4-dimethyl-9,10-di-*o*-tolylanthracene (**13**) (15.0 mg, 0.0387 mmol) in chloroform or methylene chloride (4 mL) was added to 30% Pd/C (45 mg). The mixture was concentrated in a rotary evaporator and transferred to a glass reaction tube. Dry ice was added (\approx 150 mg). The reaction tube was closed with a glass stopper wrapped in aluminum foil. The reaction mixture was heated to 400 °C at a ramp of 60 °C/min in a Lindbergh furnace for 5 min, allowed to cool to r.t., and continuously extracted with dry THF (100 mL) in a Soxhlet apparatus for 48 hr. Concentration afforded dibenzo[*bc,kl*]coronene (**16**) as purple powder (4.07 mg, 10.9 μ mol, 28.1%). EI-MS *m/z*: 374.1 [M⁺]. UV–Vis λ_{max} (nm): 510, 477, 451, 356, 339.

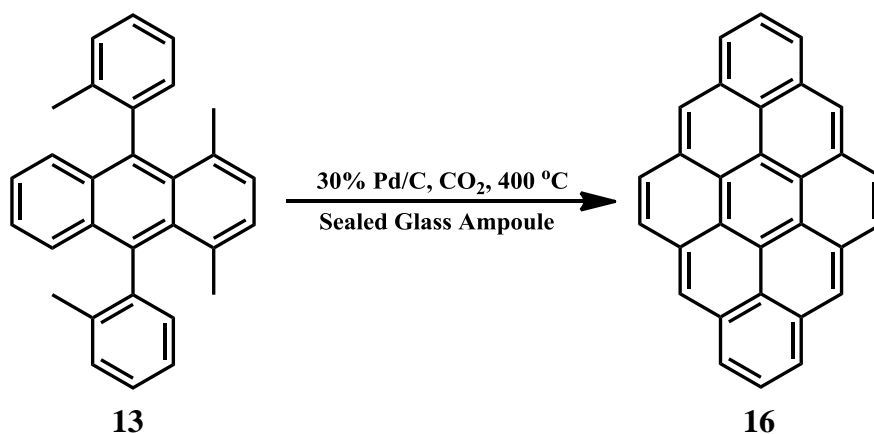


Figure 3.4 Synthetic scheme for the synthesis of dibenzo[*bc,kl*]coronene (**16**) from 1,4-dimethyl-9,10-di-*o*-tolylanthracene (**13**).

3.3 Results

The synthesis of the above compounds proved challenging, with the exception of dibenzo[*cd,lm*]perylene, which followed the literature procedure. In the case of dibenzo[*bc,kl*]coronene, Scholl and Meyer⁷ had reported the synthesis of the compound in 1932, although their synthesis required many steps, making it cumbersome and impractical. In 1960 Clar reported a straightforward synthesis⁶ in which the starting material 1,4-dimethyl-9,10-di-*o*-tolylanthracene (**13**) was slowly sublimed in an air-free CO₂ current over lumps of 15% palladium on charcoal held at 400 °C to afford mostly unchanged starting material (**13**) and dibenzo[*bc,kl*]coronene (**16**) as the product with a 0.4-0.6% conversion. Experiments showed that the best results were obtained when all the starting materials were sealed in a glass ampoule or in a closed environment. As the experiments were conducted, the following was observed:

- a) **Choice of isomer:** Our experiments showed that only 1,4-dimethyl-9,10-di-*o*-tolylanthracene produced the desired product (**Figure 3.5**). This outcome points to a higher reactivity of 1,4-dimethyl-9,10-di-*o*-tolylanthracene (**13**) as compared to its isomer 9,10-bis(2,6-dimethylphenyl)anthracene (**4a**). This higher reactivity

was further probed by the Diels-Alder reaction of each isomer with 1-dodecyl-1*H*-pyrrole-2,5-dione (**20**). Only isomer (**13**) formed the Diels-Alder adduct.

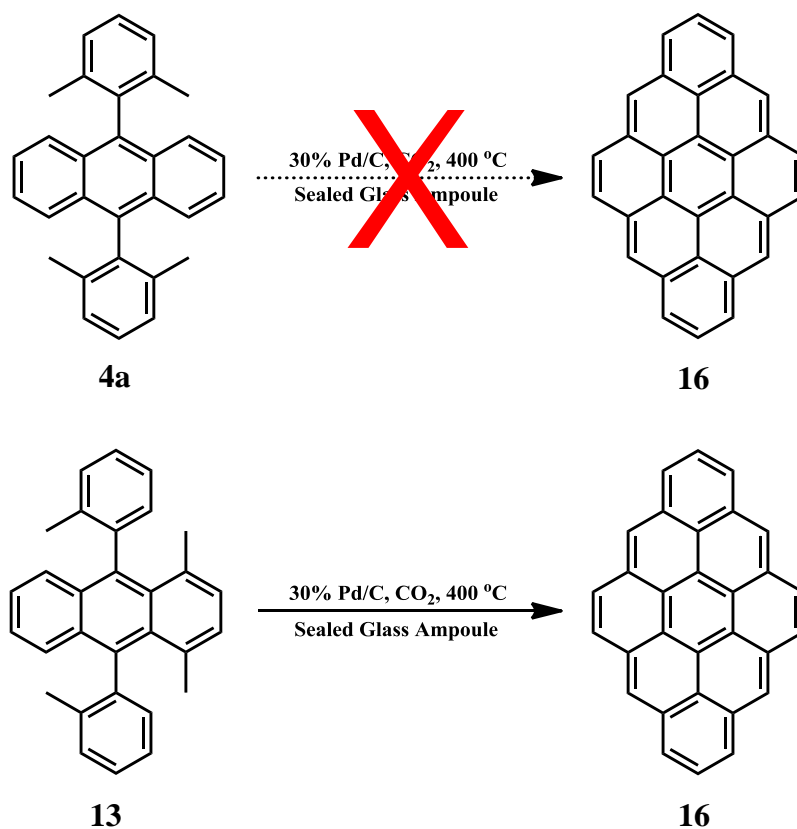


Figure 3.5 Synthesis of dibenzo[bc,kl]coronene (**16**). This reaction takes place only with 1,4-dimethyl-9,10-di-*o*-tolylanthracene (**13**) and not 9,10-bis(2,6-dimethylphenyl)anthracene (**4a**) as the starting material.

Isomer (**4a**) did not react with (**20**) to form (**23**) even when higher temperatures were used (**Figure 3.6**). ¹H-NMR analysis of the crude product from the reaction of (**13**) and (**20**) shows the formation of the Diels-Alder adduct (**21**) and/or (**22**). In accordance with this, the UV-vis spectrum of the crude product (**Figure 3.7**) also points to the formation the Diels-Alder adduct(s). The absorbance bands for the starting material (**13**) are almost completely absent and in its place new absorbance bands have appeared at 297 nm, 287 nm, 277 nm, consistent with that of a naphthalene derivative and in agreement with structures (**21**) or (**22**).

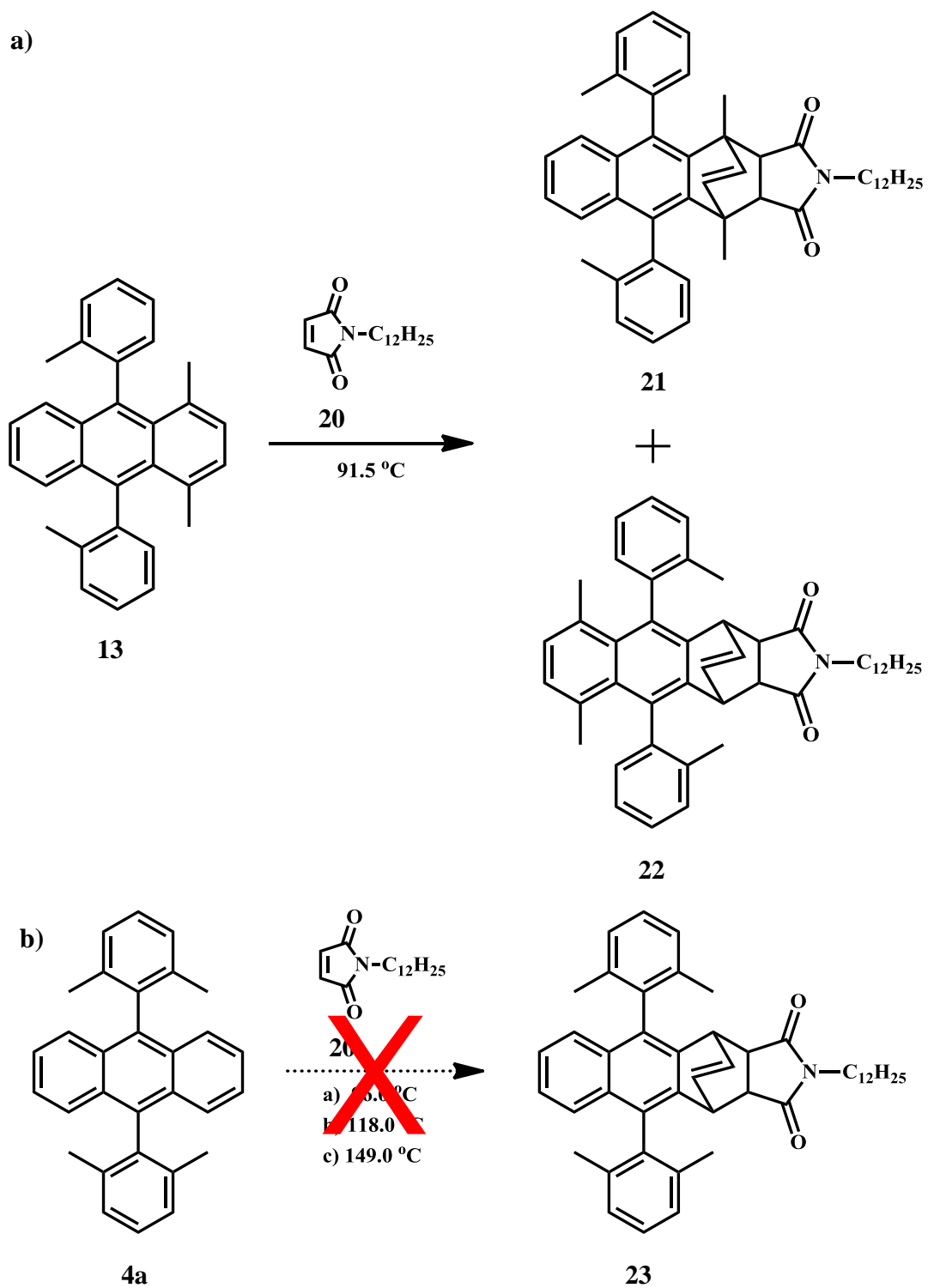


Figure 3.6 Reactivity of anthracene derivatives (a) 1,4-dimethyl-9,10-di-o-tolylanthracene (**13**) and 1-dodecyl-1*H*-pyrrole-2,5-dione (**20**) react to form the Diels-Alder adduct (**21**) and or (**22**) (b) 9,10-bis(2,6-dimethylphenyl)anthracene (**4a**) and 1-dodecyl-1*H*-pyrrole-2,5-dione (**20**) do not react and Diels-Alder adduct (**23**) is not formed.

Furthermore, the EI mass spectra of the crude product shows peaks at 265.2 m/z, 386.1 m/z and a 651.7 [M+] consistent with SM (**20**) and (**13**) and product(s) (**21**) and (**22**). These results point to the effect that the methyl groups have on the reactivity of the molecules at least in the case of the Diels-Alder reaction of (**13**) and (**4a**) with (**20**).

- b) **Temperature:** As for the temperature, the reaction only takes place at 400 °C. At temperatures of 200 °C and 300 °C, (**19**) is formed with no detectable formation of (**16**).
- c) **Catalyst:** Experiments are only successful in producing (**16**) with 30% Pd/C. Only the starting material is recovered when 10% Pd/C is used.
- d) **Gas:** The use of CO₂ is crucial in the formation of (**16**). Only the starting material is recovered when experiments were performed under vacuum. One can speculate that the role of CO₂ might be that as in the water-gas shift reaction in which CO and H₂O are formed from CO₂ and H₂.

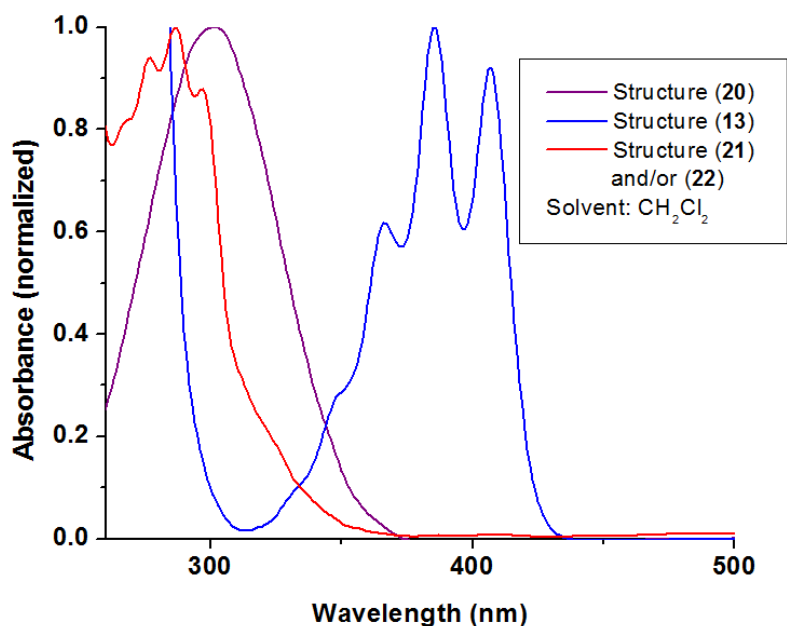


Figure 3.7 UV-vis spectrum of 1-dodecyl-1*H*-pyrrole-2,5-dione (**20**), 1,4-dimethyl-9,10-dio-tolylanthracene (**13**), and Diels-Alder adduct (**21**) an/or (**22**).

3.3.1 UV Spectral Characteristics of PAHs

The UV spectral characteristics of each PAH are unique.⁸ This quality makes the UV spectra of PAHs one of their most important features. In general, the UV spectra of PAHs contain a number of well defined peaks divided in three different groups, namely α , β/β' , and p. These groups are related to various transitions between their molecular orbitals. Typically, benzenoid PAHs (alternant PAHs) have more well defined UV spectra than PAHs containing one or more five-membered rings (non-alternant PAHs).⁹⁻¹³ Often, the p-band peaks in alternant PAHs increase with increasing wavelength whereas for non-alternant PAHs this is not necessarily the case. Another important distinction between non-alternant and alternant PAHs is that usually the ratio of the highest β/β' peak to the highest p-band peak is 3:1 for the former while this ratio is smaller and often less than one for the latter.⁹⁻¹⁴ These characteristics, consistent with an alternant PAH, are observed in the UV-vis spectrum obtained from our experiments (**Figure 3.8**).

The p-band peaks at 451, 477, and 510 nm clearly show an increase in height as the wavelength increases. Also, the terminal p-band peak (510 nm) is higher than that of the β -band. All this suggests the compound to be that of a benzenoid or alternating PAH. This analysis and comparison to that published by Clar⁶ (**Figure 3.9**) suggest the synthesized compound to be dibenzo[*bc,kl*]coronene (**16**).

Fluorescence spectroscopy measurements also point to the formation of the molecule and its reactivity. This compound is highly fluorescent in the green (**Figure 3.8**)^{8,15} which suggest a more rigid structure than that of the starting material. When a solution of dibenzo[*bc,kl*]coronene in 1-methylnaphthalene is exposed to air in the absence of light, the absorption spectrum remains unchanged, but once the solution is exposed to air and light, the p-bands start to diminish and after 24 hrs the p-bands have decreased to more than half their intensity. After 48 hours, they are completely absent (**Figure 3.10**).

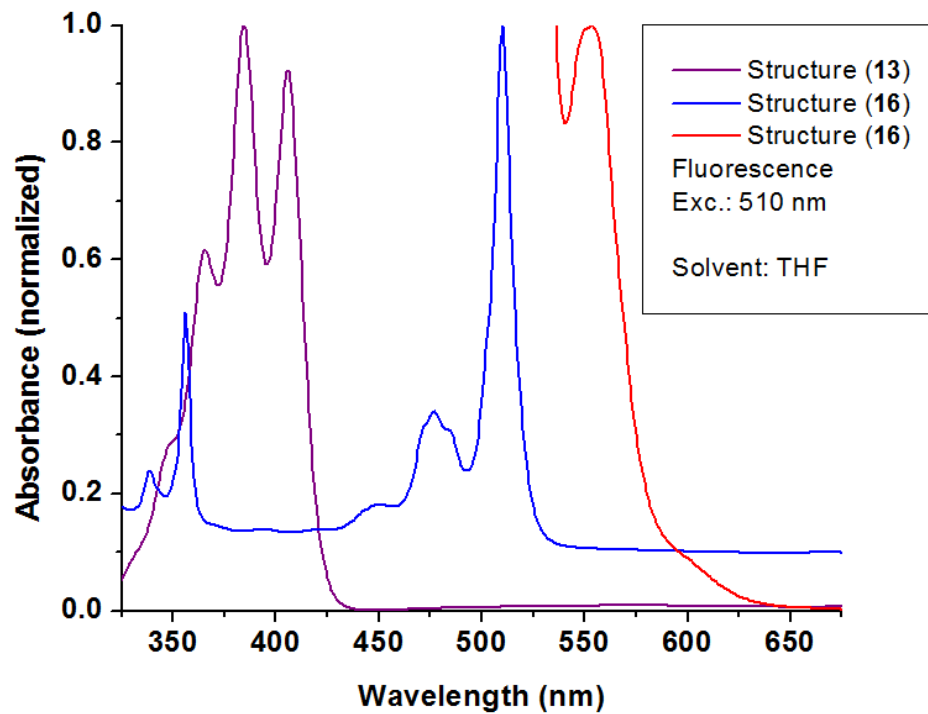


Figure 3.8 UV-vis spectrum of 1,4-dimethyl-9,10-di-o-tolylanthracene (**13**) and dibenzo[bc,kl]coronene (**16**). Fluorescence obtained at 510 nm.

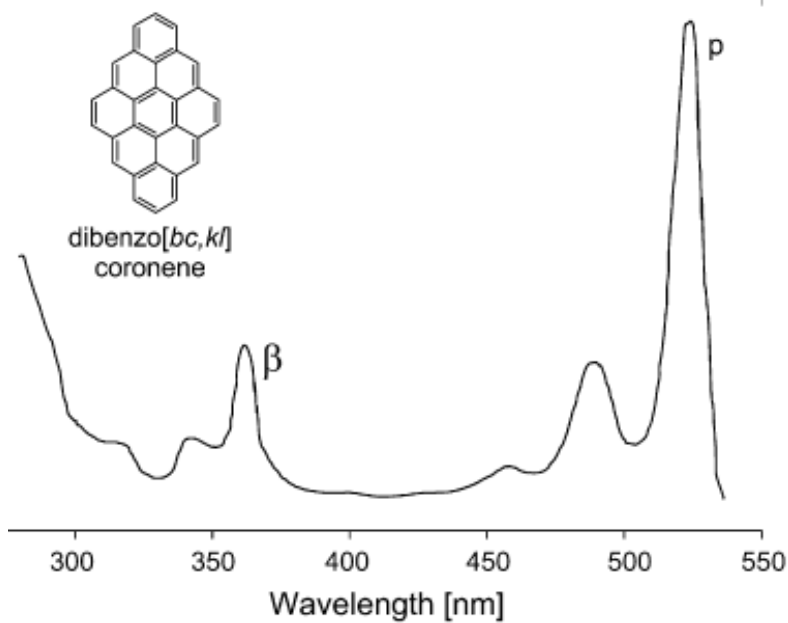


Figure 3.9 UV-vis spectrum of dibenzo[bc,kl]coronene (**16**) in 1-methylnaphthalene.^{8,15}

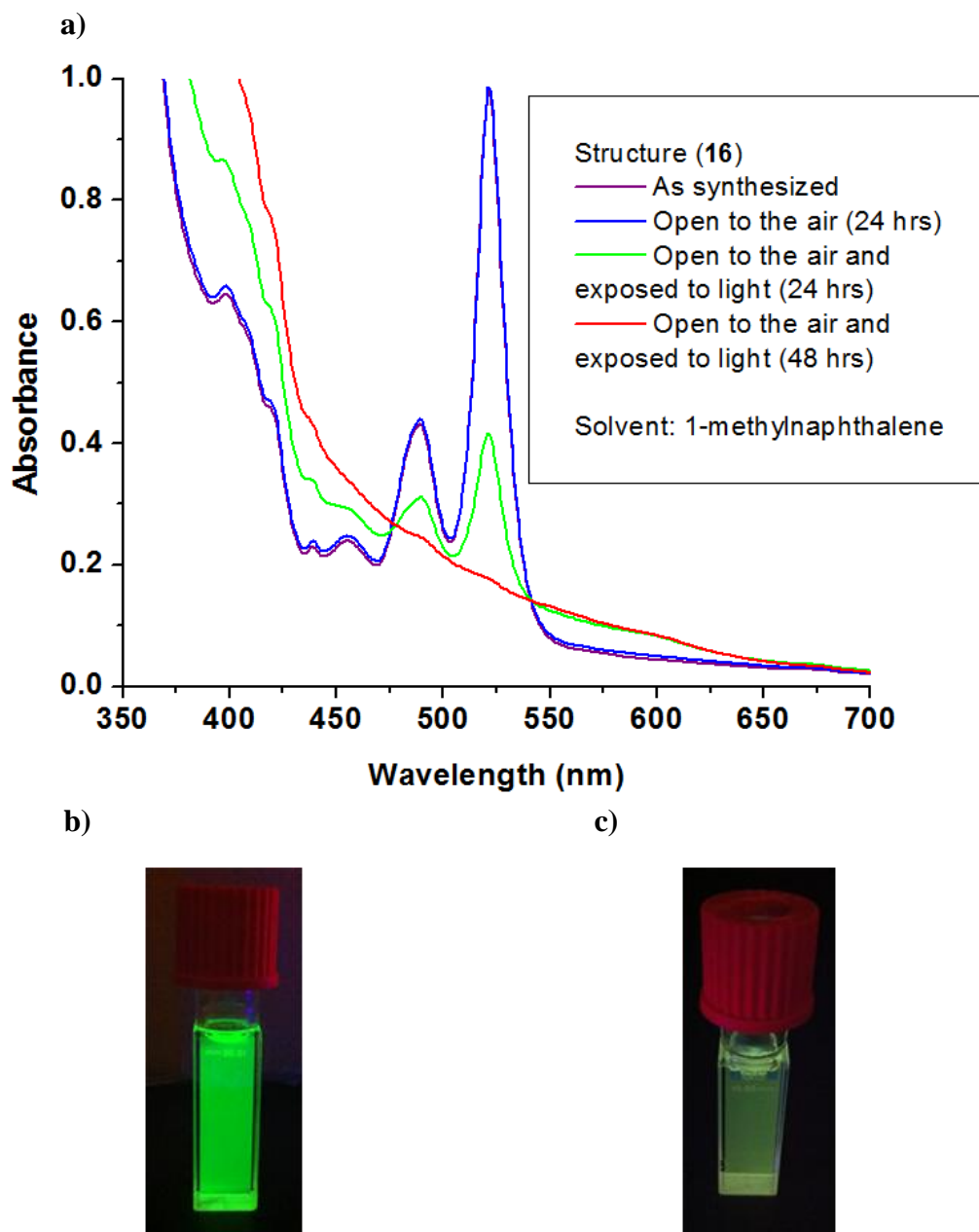


Figure 3.10 Decomposition of (16) in air and light. a) UV-vis spectrum of (16). When the solution is only exposed to air, there is no change in the spectra as shown by the purple and blue spectra. The p-band structure disappears as the solution is exposed to air and light over a period of 48 hrs as seen by the green and red spectra. b) Fluorescence of solution under a UV lamp before experiment. c) Fluorescence of solution under same UV light after experiment.

This suggests **(16)** to be photo-reactive as expected from a material of its class. Fluorescence has almost completely disappeared after 48 hr. Crystals were also obtained as long, thin needles (**Figure 3.11**), as described by Clar.⁶

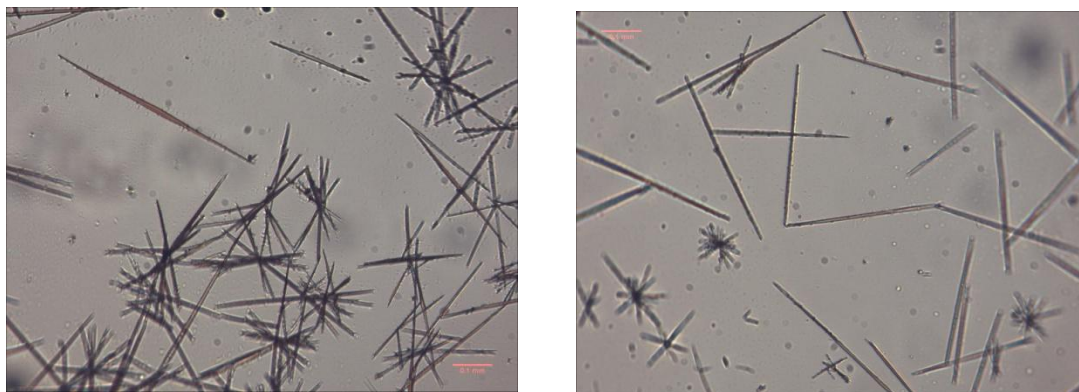


Figure 3.11 Long thin needles of **(16)**.

It should be mentioned that many attempts were made at synthesizing dibenzo[*bc,kl*]coronene **(16)** from other precursors, including 9,10-bis(2,6-bis(bromomethyl)phenyl)anthracene **(5)** and dibenzo[*cd,lm*]perylene **(18)**. All these attempts resulted in a mixture of products difficult to isolate and characterize.

As an interesting side note, 1,12-dimethylnaphtho[1,2,3,4-*rst*]pentaphene **(19)** was recovered during attempts to synthesize dibenzo[*bc,kl*]coronene **(16)** at lower temperatures. This product suggests that coupling of the 1,4-dimethylantracene methyl groups to the 9,10-ditolyl rings occurs faster than that of the tolyl methyl groups to the anthracene.

3.4 Conclusions

In conclusion, the synthesis of dibenzo[*bc,kl*]coronene was accomplished by a modification of the Clar procedure.⁶ This modification resulted in a large increase in the

percentage yields which allowed for amounts to be synthesized in sufficient quantities for further study. This study also shows that this material can only be synthesized from 1,4-dimethyl-9,10-di-o-tolylanthracene, but not from 9,10-bis(2,6-dimethylphenyl)anthracene under the same conditions. This points to the difference in reactivity between these two isomers, which was further explored by the Diel-Alder reaction between each of the starting materials and 1-dodecyl-1*H*-pyrrole-2,5-dione. As the results show, only 1,4-dimethyl-9,10-di-o-tolylanthracene formed the Diels-Alder adduct, pointing to a higher reactivity than that of its isomer. This study also points to the importance of CO₂ for the synthesis of dibenzo[*bc,kl*]coronene. Every attempt made at synthesizing this compound without CO₂ resulted in the recovery of only the starting material. Finally, these results also point to the reactivity of dibenzo[*bc,kl*]coronene, since it was shown to decompose in 48 hr when exposed to light and air.

3.5 References

- [1] Yu, Q.; Jauregui, L. A.; Wu, W.; Colby, R.; Tian, J.; Su, Z.; Cao, H.; Liu, Z.; Pandey, D.; Wei, D.; Chung, T. F.; Peng, P.; Guisinger, N. P.; Stach, E. A.; Bao, J.; Pei, S. S.; Chen, Y. *P. Nat. Mater.* **2011**, *10*, 443–449.
- [2] Yuan, Q.; Gao, J.; Shu, H.; Zhao, J.; Chen, X.; Ding, F. *J. Am. Chem. Soc.* **2012**, *134*, 2970–2975.
- [3] Wan, X.; Chen, K.; Liu, D.; Chen, J.; Miao, Q.; Xu, J. *Chem. Mater.* **2012**, *24*, 3906–3915.
- [4] Yu, J.; Sumathi, R.; Green, W. H. *J. Am. Chem. Soc.* **2004**, *126*, 12685-12700.
- [5] Pogodin, S.; Agranat, I. *J. Am. Chem. Soc.* **2003**, *125*, 12829-12835.
- [6] Clar, E. Fell, G. S.; Ironside, C. T.; Balsillie, A. *Tetrahedron*, **1960**, *10*, 26-36.

- [7] Scholl, R.; Meyer, K. *Ber. Desch. Chem. Ges.* **1932**, *65*, 902.
- [8] McClaine, J. W.; Oña, J. O.; Wornat, M. J. *J. Chromatogr. A* **2007**, *1138*, 175–183.
- [9] J. C. Fetzer, *Large (C_≥24) Polycyclic Aromatic Hydrocarbons: Chemistry and Analysis*, Wiley-Interscience, New York, 2000.
- [10] E. Clar, *Polycyclic Hydrocarbons*, Academic Press, New York, 1964.
- [11] E. Clar, *The Aromatic Sextet*, Wiley-Interscience, New York, 1972.
- [12] Photoelectric Spectrometry Group, Institut für Spectrochemie und Angewandte Spektroskopie, *UV Atlas of Organic Compounds*, Plenum Press, New York, 1966.
- [13] R.A. Friedel, M. Orchin, *Ultraviolet Spectra of Aromatic Compounds*, John Wiley and Sons, New York, 1951.
- [14] Zander, M.; Franke, W. H. *Chem. Ber.* **1966**, *99*, 1275.
- [15] McClaine, J. W. Zhang, X.; Wornat, M. J. *J. Chromatogr. A* **2006**, *1127*, 137–146.

CHAPTER 4

SYNTHESIS OF GRAPHENE BY CHEMICAL VAPOR DEPOSITION ON COPPER

The research highlighted in this chapter was carried out in collaboration between the Tolbert lab and the Henderson lab. The carbon precursors used in this research come from commercial sources or were synthesized within the Tolbert lab. The work on the synthesis of graphene by chemical vapor deposition (CVD) was completed within the Tolbert and Henderson labs. Data analysis was equally shared between the two collaborating labs.

4.1 Introduction

As stated in the introductory chapter, several effective methods have been developed for the synthesis of graphene since it was first isolated.^{1,2} As of the date of this dissertation, mechanical exfoliation^{1,3,4} still remains the best method for the production of small quantities of high quality graphene but due to the nature of the process, this method is not economically scalable. Other methods developed for the synthesis of graphene are not without faults. Epitaxial growth from SiC suffers from the need of expensive SiC single crystals wafers⁵⁻⁸ and the need for high temperatures and vacuum.^{7,9} Layer control and non-uniformity still remains an issue affecting this method.¹⁰ The reduction of graphene oxide¹¹⁻¹⁴ and liquid exfoliation of graphite^{15,16} offer large volume processing but the low quality and size of the graphene flakes produced are still an issue that needs to be resolved.^{17,18}

Much work has been done on the synthesis of graphene by CVD on different metal substrates.¹⁹⁻²⁷ Most of this work makes use of hydrogen as the carrier gas and, if

high quality graphene is desired, the use of ultra high or high vacuum is needed. Also the temperature at which graphene is synthesized has remained pretty much the same (~1000 °C) with some examples of low temperature growth found in the literature.²⁸⁻³⁰ Although several commercially available materials have been used successfully to grow graphene, methane still remains the most used carbon source at this time.

As stated several times in this dissertation, the main objective of this work was the synthesis of graphene at low temperatures by CVD without the need of dangerous concentrations of hydrogen and under moderate vacuum. Most syntheses of graphene by CVD have been accomplished by the use of methane as the carbon source. As mentioned above, methane still remains the most used carbon source for the synthesis of graphene by CVD. The main drawback for using this carbon source is the high concentrations of hydrogen (10-20 %) and the high temperature at which graphene is grown, i.e., 1000 °C. In this chapter experiments were conducted to synthesize graphene at low temperatures from commercial and synthesized carbon sources.

It should be noted that two techniques were used for graphene growth, namely, evaporation of the carbon source into the heating chamber (CVD) and therefore onto the metal substrate, i.e., copper and pyrolysis of the carbon source previously spin-coated on a metal substrate. These two different approaches for the synthesis of graphene were performed in order to compare the results from both methods since reports in the literature suggest that pyrolysis of organic molecules produces good quality graphene.³¹

The synthesis of graphene by CVD remains the most promising method for the production of large single layer graphene sheets. In order to use this method successfully, five different variables have to be taken into consideration:

- a) **Temperature:** Needed in order to (i) anneal the metal substrate (900 °C-1050 °C), (ii) grow graphene on the metal substrate (300 °C to 1000 °C), and (iii) evaporate the carbon source into the system.

- b) **Vacuum:** Needed in order to grow good quality graphene. Reports in the literature vary from the use of ultrahigh vacuum systems,²⁸ to moderate,³¹ and those with no vacuum at all (ambient pressure).^{32,33}
- c) **Gas carrier:** In this particular case, everything seems to indicate that hydrogen is crucial for the formation of graphene on copper. The pre-treatment of the metal substrate under a reducing atmosphere seems to be needed in order to reduce the metal oxides from the surface and in this way activate it. Once the surface has been activated, the hydrogen might play a role on the activation of the carbon source and in the removal of any undesired carbon deposits.³⁴
- d) **Metal substrate:** Graphene has been shown to grow in a variety of metal substrates such as ruthenium (0001), iridium (111), platinum (111), palladium (111), rhenium (0001), rhodium (111), nickel (111), cobalt (0001), and copper (111) and copper (001). It should be noted that in the case of gold and copper, the graphene-metal interaction is relatively weak and polycrystalline graphene grows even if single crystal substrates are used.³⁵
- e) **Carbon source:** Many carbon sources have been used for the synthesis of graphene, the most predominant one being methane. Other carbon sources include: methanol, ethanol, propanol,³⁶ hexane,³⁷ benzene,²⁹ toluene,³⁰ etc. Tour *et al* showed that graphene can be grown from such unconventional carbon sources as: Girl Scout cookies, grass, dog feces, cockroach legs, plastic, and chocolate.³⁸

All these parameters affect the quality of the graphene produced as well as the number of layers formed. As it can be seen from above, the temperatures used for annealing and growth are unacceptable for industrial scale applications as well as the use

of hydrogen at concentrations that might cause explosions if not monitored properly. The choice of the carbon source also plays an important role on the quality of graphene as well as the temperature needed for growth to occur.

This research was conducted using forming gas as the reductive source. This allowed for safer conditions for the production of graphene since dangerous concentrations of hydrogen were not needed. Since the choice of the carbon source seems to play an important role in the synthesis of graphene at low temperatures, as reports in the literature suggest,²⁸⁻³⁰ then it is reasonable to approach the low temperature growth problem by focusing on the use of molecules with characteristics that might induce the growth of graphene at low temperatures. This chapter highlights the use of said molecules, either commercially available or synthesized in our laboratories, as carbon sources for the synthesis of graphene at low temperatures by the CVD method. The synthesis, results, and discussion will be the topic of the next sections.

4.2 Experimental Protocol

General Experimental

All liquid and solid carbon materials from commercial sources were used as received. TGA traces were obtained with a TGAQ500. Raman spectra were recorded with a Nicolet Almega XR Raman spectrometer using a 25 mW, 2.4 eV excitation source (488 nm) through a 24 μM pinhole aperture and 100x objective.

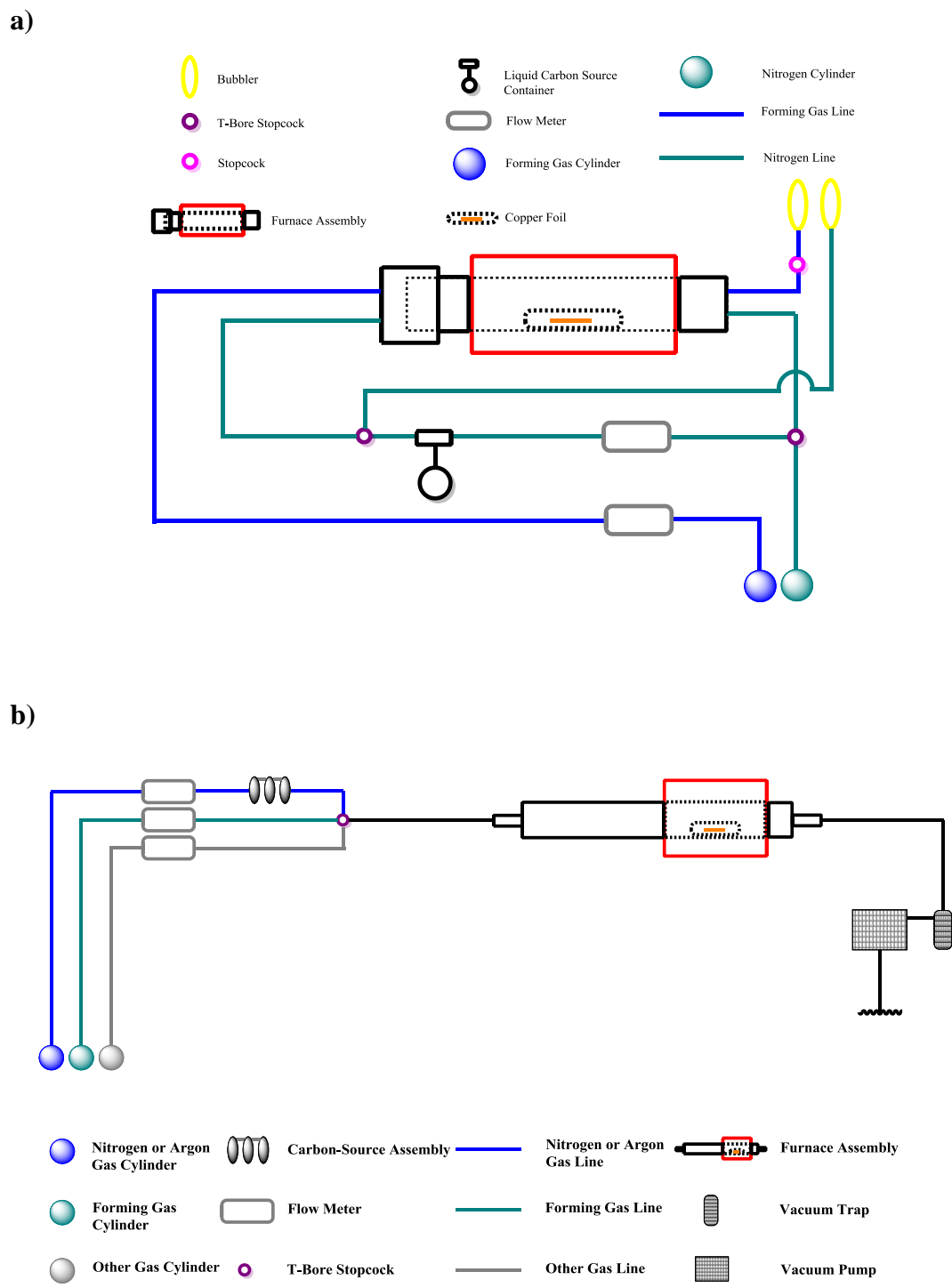
Graphene was grown on 25 μM thick copper foils (Alfa Aesar item No. 46365 cut into 1 cm^2 squares) in a hot furnace consisting of a 46 mm ID fused silica tube heated in a Thermolyne F21100 tube furnace. The general growth processes are as follow:

Chemical vapor deposition at atmospheric pressure (APCVD): (1) Load the fused silica tube with the copper foil on a fused silica boat; (2) flow forming gas for one hour (127 sccm); (3) heat furnace to 1000 °C; (3) add liquid carbon source for a desired period of time (4) cool furnace to room temperature. Figure 4.1 shows the schematic for the setup used.

Chemical vapor deposition under vacuum (CVD): (1) Load the fused silica tube with the copper foil on a fused silica boat; (2) evacuate under vacuum to 20 mTorr, back fill with forming gas (H_2/N_2 or H_2/Ar) to 1 Torr (5 cycles); (3) refill with forming gas (25 sccm, ~1 Torr); (4) let pressure reach 20 mTorr or 1 Torr (25 sccm); (5) Heat furnace to 1000 °C and maintain for 30 min; (6) add solid carbon source for a desired period of time; (7) cool furnace to room temperature. Figure 4.2 shows the schematic for the setup used.

It should be noted that three different ways were used to expose the carbon source to the metal substrate.

- 1) The first way consisted of spin-coating a copper foil with a solution of the carbon source of choice and pyrolyse it at 600 °C or 1000 °C for 10 minutes under vacuum (20 mTorr) or with forming gas flow (1 Torr). The sample was then removed from the hot zone to cool down as fast as possible (**Table 4.1** entries 3,4,6,7, 11, and 15 for 1000 °C experiments and **Table 4.2** entries 4, 5, 11, 14, and 15 for 600 °C experiments).



- 2) The second way consisted of annealing a copper sample for 30 minutes at 1000 °C under forming gas while a second copper sample previously spin-coated with a solution of the carbon source of choice was held outside of the furnace hot zone. The spin-coated sample would be introduced into the hot zone under vacuum (20 mTorr) or forming gas flow (1 Torr) and held inside for a period of ten minutes at which time the samples would be allowed to cool to room temperature (**Table 4.1** entries 5, 8, 9, 12, and 16). In the case of low temperature experiments, the temperature would be lowered to 600 °C after the copper foil had been annealed at 1000 °C (**Table 4.2** entries 6, 7, 12, 16, and 17).
- 3) The third way consisted in annealing a copper sample for 30 minutes at 1000 °C under forming gas. The carbon source would then be evaporated into the chamber for a period of ten minutes under vacuum (20 mTorr) or forming gas flow (1 Torr) at which time the copper would be allowed to cool to room temperature (**Table 4.1** entries 10, 13, and 14). In the case of low temperature experiments, the temperature was lowered to 600 °C after the copper foil had been annealed at 1000 °C (**Table 4.2** entries 3, 8, 9, 10, 13, 18, and 19). TGA was used here to assist in identifying the temperature range at which the carbon source could be introduced into the furnace hot zone.

4.3 Results

4.3.1 APCVD

Attempts at growing graphene at atmospheric pressure were performed in order to move away from the use of pure hydrogen and vacuum in the growing process. As is common in our approach, forming gas was used as the carrier gas to avoid the use of dangerous concentrations of hydrogen. The study focused on the synthesis of graphene at 1000 °C from liquid carbon sources that have previously been reported in the literature to

grow graphene under hydrogen and vacuum conditions. Benzene, toluene, *p*-xylene and styrene were chosen as the carbon source. The first two solvents have been previously reported to grow graphene under hydrogen and vacuum conditions. Styrene and *p*-xylene were chosen since they are similar in molecular structure. It should be noted that only liquid carbon sources were used for this part of the study since the setup would not allow any solid carbon sources to be introduced into the system once the temperature had reached 1000 °C.

At the end of this study, only benzene and toluene produced single layer graphene with very poor quality.

Analysis of the Raman spectra of samples grown from benzene (**Figure 4.2**) and toluene (**Figure 4.3**) show sharp 2D peaks (second order of the D peak) at 2720 cm⁻¹ and 2724 cm⁻¹ for benzene and toluene respectively, indicative to the formation of single layer graphene while the D-peaks (breathing modes of sp² carbon atoms in rings) at 1360 cm⁻¹ and 1375 cm⁻¹ for benzene and toluene respectively, are broad and intense which suggest the low quality of the graphene formed.

The SEM picture (**Figure 4.4**) of the benzene sample shows small graphene domains. As can be seen from the picture, the graphene produced is not continuous and highly defective, in agreement with the Raman results described above.

Although many attempts were made at obtaining good quality graphene by this method, no such results were observed. No matter the amount of time that the system was evacuated with forming gas, the results always suggested that copper oxide or cuprous oxide was present on the samples indicating the presence of oxygen in the system or the poor quality of the annealed copper substrate. Due to these poor results, the focus of the graphene growth was switched to a system where vacuum could be implemented and carbon sources other than liquid could be used.

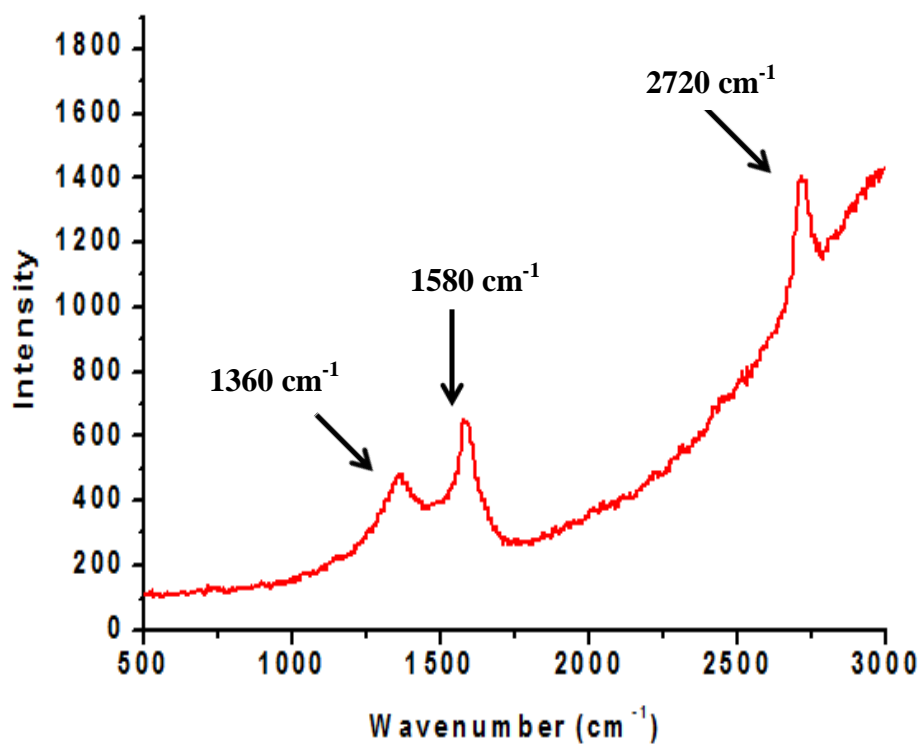


Figure 4.2 Raman spectrum of graphene from benzene on copper foil. Growth conditions: temperature: 1000 °C, H₂/N₂ flow: 123 sccm. Benzene/N₂ flow: 16 sccm (10 min).

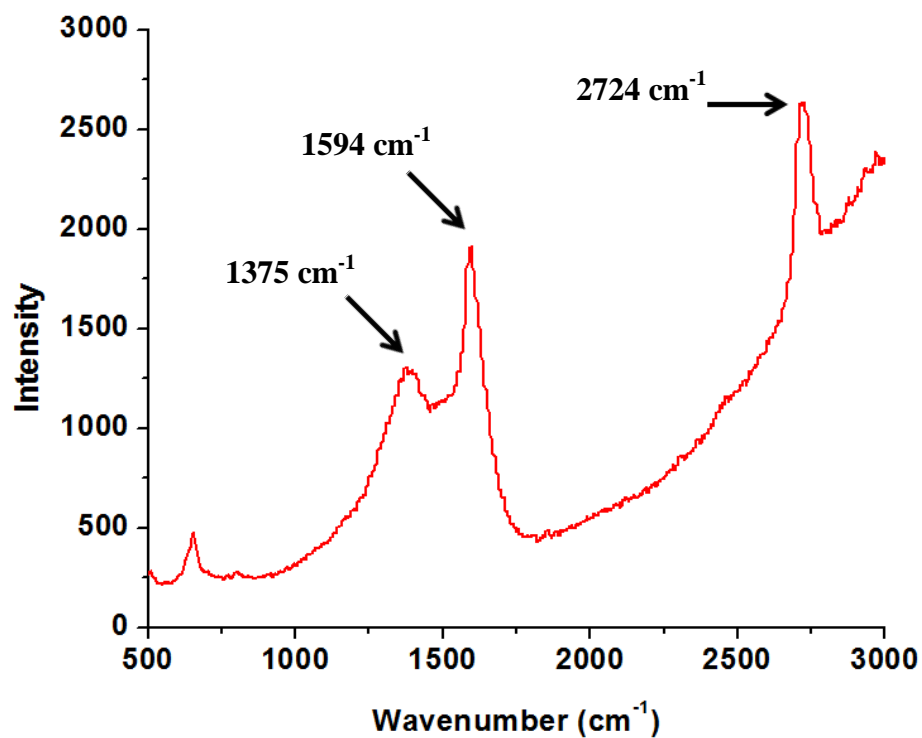


Figure 4.3 Raman spectrum of graphene from toluene on copper foil. Growth conditions: temperature: 1000 °C, H₂/Ar flow: 64 sccm. Toluene/N₂ flow: 54 sccm (10 min).

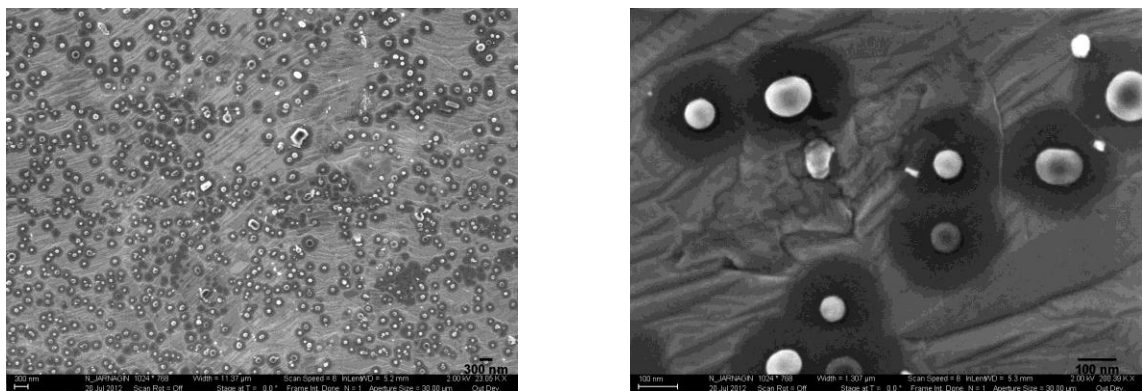


Figure 4.4 SEM image of graphene on copper foil by APCVD. Benzene used as the carbon source. Left image width = 11.37 μm , right image width = 1.307 μm .

4.3.2 CVD

Graphene was grown on copper substrates following the method described in the experimental protocol section. Several solid carbon sources were used including poly(methyl methacrylate) (PMMA) (**24**, **Figure 4.5**) and coronene (**25**, **Figure 4.5**) along with materials synthesized in the previous chapters. PMMA³¹ and coronene²⁸ were chosen in order to duplicate reports in the literature where graphene was successfully grown from these materials at 1000 °C and 550 °C respectively. By reproducing their results with our setup, a procedure was developed for the growth of graphene by other carbon sources.

Single layer graphene was successfully grown on copper foil from different carbon sources at a temperature of 1000 °C (**Table 4.1**). In contrast to the literature where single layer graphene was grown with hydrogen concentration of about 10%³¹, our samples were formed under forming gas with hydrogen concentrations of only 3%.

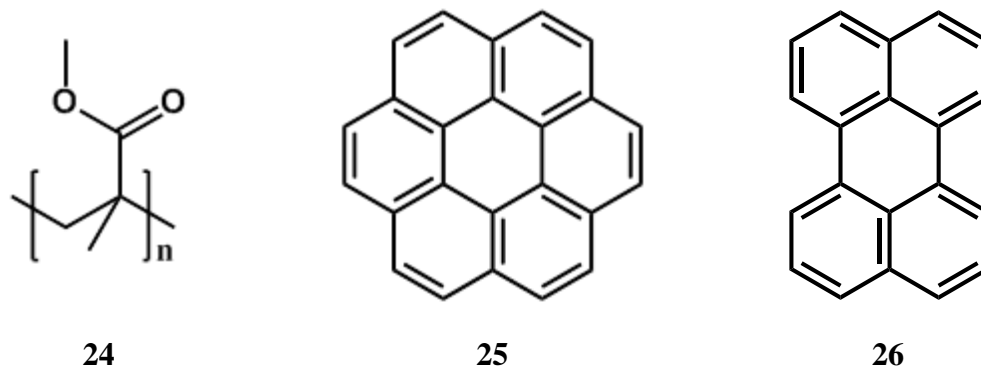


Figure 4.5 Molecular structures of Poly(methyl methacrylate) (**24**), coronene (**25**) and perylene (**26**).

Different pressures were also tested with the best results obtained when the pressure was 20 mTorr or 1 Torr in agreement with literature reports³¹. Above 1 Torr only amorphous carbon on the copper substrate was observed.

Comparison of the Raman spectra from graphene samples reported in the literature³¹ (**Figure 4.6**) and those produced from our experiments (**Figure 4.7**) where PMMA was used as the carbon source, show that the quality of the graphene produced in our setup is similar to that reported in the literature³¹. The lack of a D peak at $\approx 1360\text{ cm}^{-1}$ shows the formations of defect-free graphene at least in the domain where the measurements are taken. On the other hand, when 1,4-dimethyl-9,10-di-o-tolylanthracene (**13**) is used as the carbon source, the Raman spectrum (**Figure 4.8**) shows the characteristic D peak for defective single layer graphene at 1360 cm^{-1} . This result is interesting since both samples were grown under the same conditions with the only difference being the carbon source. In the case of PMMA, it is obvious that extensive rearrangement of the molecules had to take place in order to form graphene but in the case of (**13**), much less rearrangement is necessary.

Both spectra (**Figure 4.7** and **Figure 4.8**) show the G peak at 1590 cm^{-1} and a sharp 2D peak at 2720 cm^{-1} in agreement with single layer graphene. These

representative spectra for single layer graphene are observed in all samples prepared from different carbon sources under our growth conditions (**Table 4.1**). Although all carbon sources produce single layer graphene, the quality of the graphene obtained is not always as that derived from PMMA. This outcome clearly indicates that the choice of a carbon source has a major direct influence in the quality of the graphene produced and is a subject that deserves further study.

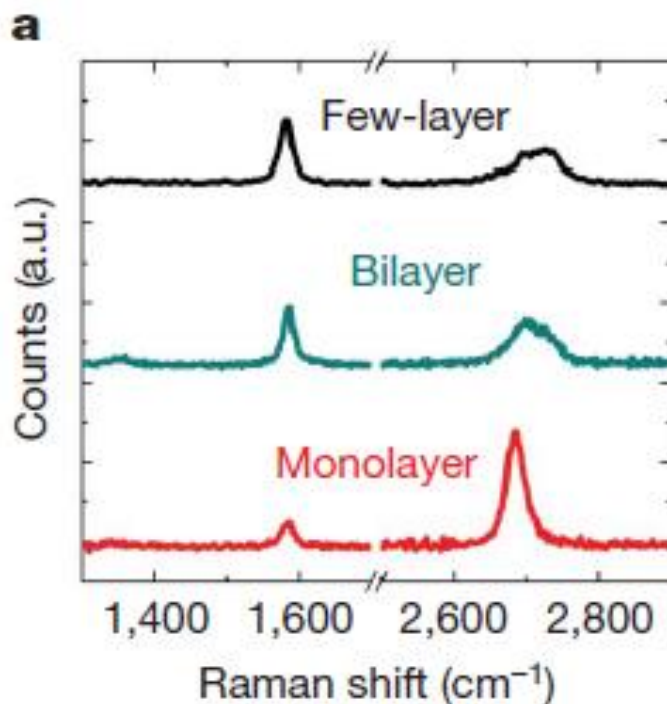


Figure 4.6 Controllable growth of pristine PMMA-derived graphene films. Difference in Raman spectra from PMMA-derived graphene samples with controllable thicknesses derived from different flow rates of H₂.³¹

The use of 9,10-diphenylanthracene (**27**, **Figure 4.9**) as a carbon source should be noted. This molecule was chosen since the molecular structure is similar to that of (**4a**) and (**13**) but without any of the methyl groups attached to it. If graphene is formed under the same conditions as those used for (**4a**) and (**13**) but using (**27**) as the carbon source then this might indicate that breaking of the phenyl and anthracene bonds is taking place and some sort of rearrangement occurs.

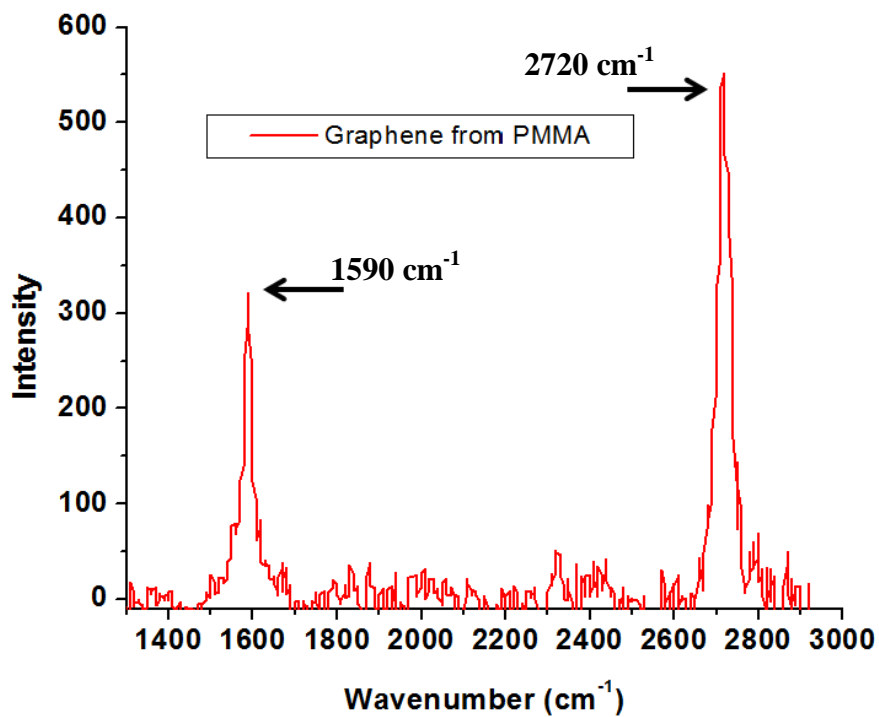


Figure 4.7 Raman spectrum of graphene grown from PMMA (**24**) at 1000 °C.

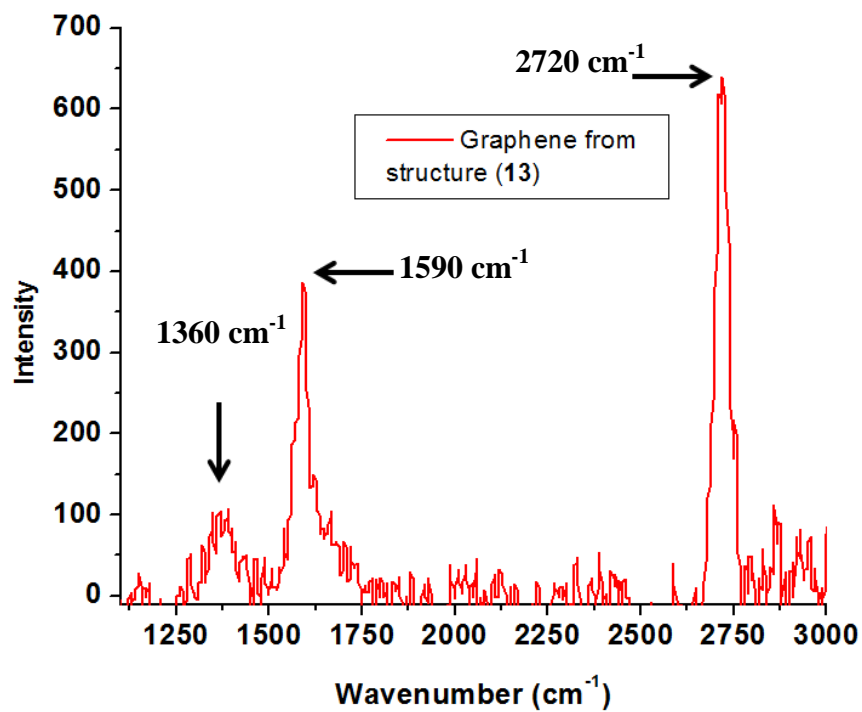


Figure 4.8 Raman spectrum of graphene grown from 1,4-dimethyl-9,10-di-o-tolylanthracene (**13**) at 1000 °C.

Table 4.1 Single layer graphene grown on copper foil at different pressures and from different carbon sources. ¹Carbon source spin-coated onto the copper substrate and introduced in this way into the hot zone held at 1000 °C. ²Carbon source spin-coated onto copper foil and introduced into the furnace held at 1000 °C after a second uncoated copper foil had been annealed under forming gas for a period of 30 min. at 1000 °C. Introduction of spin-coated sample was done under vacuum (20 mTorr) or with forming gas flow (1 Torr) ³The carbon source was evaporated into the hot zone containing uncoated copper foil held at 1000 °C for 30 minutes under vacuum and forming gas flow.

Run	Substrate	Temp. (°C)	Pressure (mTorr)	Gas	Growth Time (min)	Carbon Source	Graphene Layers
1	Copper	1000	20	H ₂ /Ar	10	-	-
2	Copper	1000	1000	H ₂ /Ar	10	-	-
3	Copper	1000	20	H ₂ /Ar	10	24 ¹	Single
4	Copper	1000	1000	H ₂ /Ar	10	24 ¹	Single
5	Copper	1000	1000	H ₂ /Ar	10	24 ²	Single
6	Copper	1000	20	H ₂ /Ar	10	13 ¹	Single
7	Copper	1000	1000	H ₂ /Ar	10	13 ¹	Single
8	Copper	1000	20	H ₂ /Ar	10	13 ²	Single
9	Copper	1000	1000	H ₂ /Ar	10	13 ²	Single
10	Copper	1000	1000	H ₂ /Ar	10	13 ³	Single
11	Copper	1000	1000	H ₂ /Ar	10	25 ¹	Single
12	Copper	1000	1000	H ₂ /Ar	10	25 ²	Single
13	Copper	1000	1000	H ₂ /Ar	10	25 ³	Single
14	Copper	1000	1000	H ₂ /Ar	10	26 ³	single
15	Copper	1000	20	H ₂ /Ar	10	27 ¹	Single
16	Copper	1000	20	H ₂ /Ar	10	27 ²	Single

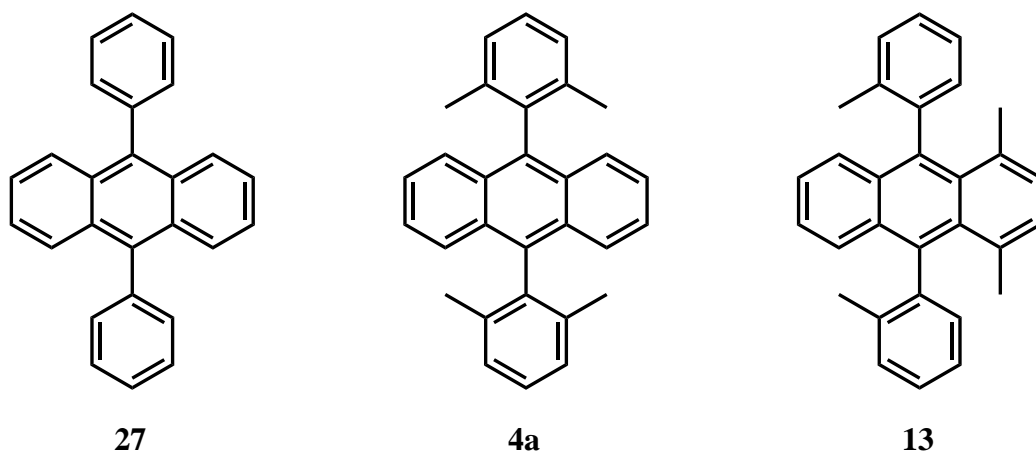


Figure 4.9 Anthracene derivatives.

On the other hand, if graphene does not form from (27) then this might imply that breaking of the bonds between the phenyl and anthracene groups does not take place. This last result would point to the advantage of using carbon sources with molecular structures that closely resemble that of graphene. Results from this experiment show that this carbon source (27) also forms graphene at 1000 °C, which suggests that some sort of rearrangement does take place. Given the previous results, unsubstituted PAHs might be a better choice for graphene growth.

Attempts at growing graphene at lower temperatures were performed. As with the previous experiments, coronene (25) was chosen as a carbon source in order to reproduce the results by the Xu group.²⁸ By reproducing their results with our setup, a procedure would be developed for the growth of graphene by other carbon sources at low temperatures. It should be noted that the Xu group used ultra high vacuum (UHV) and higher concentrations of hydrogen (20%) in their experiments. Our system on the other hand had a maximum vacuum of 20 mTorr. All experiments conducted under the conditions stated earlier in the experimental protocol failed to produce graphene at temperatures of 600 °C (**Table 4.2**) and resulted in the formation of only amorphous carbon. The failure to synthesize graphene at 600 °C is most likely the result of changing two parameters in our procedure as compared to

Table 4.2 Results from experiments of graphene growth on copper foil at 600 °C at different pressures and from different carbon sources. ¹Carbon source spin-coated onto the copper substrate and introduced in this way into the hot zone held at 600 °C under vacuum (20 mTorr) or under forming gas flow (1 Torr). ²Carbon source spin-coated onto copper foil and introduced into the furnace held at 600 °C under vacuum (20 mTorr) or forming gas flow (1 Torr) after a second uncoated copper foil inside the furnace had been annealed under forming gas for a period of 30 min. at 1000 °C. ³The carbon source was evaporated into the hot zone containing uncoated copper foil held at 600 °C. The copper foil had been annealed previously at 1000 °C for 30 minutes under vacuum (20 mTorr) or forming gas flow (1 Torr).

Run	Substrate	Temp. (°C)	Pressure (mTorr)	Gas	Growth Time (min)	Carbon Source	Graphene Layers
1	Copper	600	20	H ₂ /Ar	10	-	-
2	Copper	600	1000	H ₂ /Ar	10	-	-
3	Copper	600	20	H ₂ /Ar	10	12 ³	Amorphous
4	Copper	600	20	H ₂ /Ar	10	13 ¹	Amorphous
5	Copper	600	1000	H ₂ /Ar	10	13 ¹	Amorphous
6	Copper	600	20	H ₂ /Ar	10	13 ²	Amorphous
7	Copper	600	1000	H ₂ /Ar	10	13 ²	Amorphous
8	Copper	600	20	H ₂ /Ar	10	13 ³	Amorphous
9	Copper	600	1000	H ₂ /Ar	10	13 ³	Amorphous
10	Copper	600	1000	H ₂ /Ar	10	4a ³	Amorphous
11	Copper	600	1000	H ₂ /Ar	10	16 ¹	Amorphous
12	Copper	600	20	H ₂ /Ar	10	16 ²	Amorphous
13	Copper	600	20	H ₂ /Ar	10	16 ³	Amorphous
14	Copper	600	20	H ₂ /Ar	10	25 ¹	Amorphous
15	Copper	600	1000	H ₂ /Ar	10	25 ¹	Amorphous
16	Copper	600	20	H ₂ /Ar	10	25 ²	Amorphous
17	Copper	600	1000	H ₂ /Ar	10	25 ²	Amorphous
18	Copper	600	20	H ₂ /Ar	10	25 ³	Amorphous
19	Copper	600	1000	H ₂ /Ar	10	25 ³	Amorphous

that of the literature. The literature reports the growth of graphene from coronene (**25**) at 10^{-6} to 10^{-7} Torr and annealing of the copper foil at 1000 °C in 20% hydrogen and 80% Argon flow. One could argue that the use of forming gas with concentrations of 3% hydrogen and 97% Ar might not be sufficient for the annealing and activation of the metal substrate and subsequent formation of graphene but the successful growth of graphene at 1000 °C from different carbon sources under concentrations of 3% hydrogen and 97% Ar point to the contrary (**Table 4.1**). On the other hand, all our attempts at growing graphene at 600 °C were done under a maximum vacuum of 20 mTorr. The possible effect of the vacuum change on the graphene growth is still a matter of debate. At the end, the failure to grow graphene at a temperature of 600 °C might be due to any of these changes or to a combination of both. These experimental results are suggestive of the importance of hydrogen and vacuum for the synthesis of graphene at low temperatures from solid carbon sources.

4.4 Conclusions

In conclusion, our experiments show that good quality graphene can be grown from commercially available and synthesized materials. It seems that any carbon source regardless of the molecular structure will grow graphene at temperatures of 1000 °C and under vacuum. This is in accordance with literature where good quality graphene has been grown from a number of carbon sources at this temperature. Our experiments also point to the importance of a vacuum system capable of producing high or ultrahigh vacuum in order to synthesize graphene at low temperatures from solid carbon sources. It should be noted that the copper substrate still needs to be annealed at 1000 °C under forming gas in order to activate the copper surface. Low temperature growth means only that the graphene growth took place at temperatures lower than 1000 °C.

On the other hand our experiments showed that high concentrations of hydrogen are not needed in order to grow good quality graphene at least at temperatures of 1000

°C. Under these conditions, the much safer forming gas is enough to produce good quality graphene.

Attempts to grow graphene at low temperature (600 °C) failed to form graphene, producing only amorphous carbon on the copper substrate and on the walls of the fused silica tube. This is in no way indicative that graphene cannot be synthesized at this temperature with the carbon sources used here. The failure of our setup to reproduce the work from the Xu group does not allow us to draw a conclusion indicating that our carbon sources do not grow graphene at this temperature. The fact that higher concentrations of hydrogen and UHV were not used in our setup might be enough cause to prevent the formation of graphene at these temperatures. In order to investigate the influence of the vacuum system in the synthesis of graphene at low temperatures further studies need to be conducted with high or UHV with all other parameters in our procedure unchanged.

4.5 References

- [1] Novoselov, K.S.; Geim, A.K.; Morozov, S. V.; Jiang, D.; Zhang, Y.; Dubonos, S. V.; Grigorieva, I. V.; Firsov, A. A. *Science* **2004**, *306*, 666–669.
- [2] Geim, A. K.; Novoselov, K. S. *Nat. Mater.* **2007**, *6*, 183–191.
- [3] Geim, A. K.; MacDonald, A. H. *Phys. Today* **2007**, *60*, 35.
- [4] Singh, V.; Joung, D.; Zhai, L.; Das, S.; Khondaker, S. I.; Seal, S. *Prog. Mater. Sci.* **2011**, *56*, 1178–1271.
- [5] Berger, C.; Song, Z.; Li, X.; Wu, X.; Brown, N.; Naud, C.; Mayou, D.; Li, T.; Hass, J.; Marchenkov, A. N.; Conrad, E. H.; First, P. N. de Heer, W. A. *Science* **2006**, *312*.1191.

- [6] Faugeras, C.; Nerrière, A.; Potemski, M.; Mahmood, A.; Dujardin, E.; Berger, C.; de Heer, W. A. *Appl. Phys. Lett.* **2008**, *92*, 011914.
- [7] Berger, C. Song, Z.; Li, T.; Li, X.; Ogbazghi, A. Y.; Feng, R.; Dai, Z.; Marchenkov, A. N.; Conrad, E. H.; First, P. N.; de Heer, W. A. *J. Phys. Chem. B* **2004**, *108*, 19912-19916.
- [8] Varchon, F.; Feng, R.; Hass, J.; Li, X.; Nguyen, B. N.; Naud, C.; Mallet, P.; Veuillen, J.-Y.; Berger, C.; Conrad, E. H.; Magaud, L. *Phys. Rev. Lett.* **2007**, *99*, 126805.
- [9] Forbeaux, I.; Themlin, J. M.; Debever, J.M. *Phys. Rev.B* **1998**, *58*, 16396.
- [10] Riedl, C.; Coletti, C.; Starke, U. *J. Phys. D: Appl. Phys.* **2010**, *43*, 374009.
- [11] Some, S.; Kim, Y.; Hwang, E.; Yoo, H.; Lee, H. *Chem. Commun.* **2012**, *48*, 7732-7734.
- [12] Tung, V. C.; Allen, M. J.; Yang, Y.; Kaner, R. B. *Nat Nanotechnol.* **2009**, *4*, 25-29.
- [13] Gao, X.; Jang, J.; Nagase, S. *J. of Phys. Chem. C* **2010**, *114*, 832 – 842.
- [14] Marcano, D.; Kosynkin, D. V.; Berlin, J. M.; Siniskii, A.; Sun, Z.; Slesarev; A.; Alemany, L. B.; Luand, W.; Tour, J. M. *ACS Nano* **2010**, *4*, 8.
- [15] Hernandez, Y.; Nicolosi, V.; Lotya, M.; Blighe, F. M.; Sun, Z.; De, S.; McGovern, I. T.; Holland, B.; Byrne, M.; Gun'Ko, Y. K.; Boland, J. J.; Niraj, P.; Duesberg, G.; Krishnamurthy, S.; Goodhue, R.; Hutchison, J.; Scardac, V.; Ferrari, A.; Coleman, J. *Nat. Nanotechnol.* **2008**, *3*, 563-568.
- [16] Green A. A. Hersam, M. C. *Nano. Lett.* **2009**, *9*, 4031.
- [17] Park, S.; Ruoff, R. S. *Nat. Nanotechnol.* **2009**, *4*, 217-224.
- [18] Coleman, J. N. *Acc. Chem. Res.* **2013**, *46*, 14-22.

- [19] Somani, P. R.; Somani, S. P.; Umeno M. *Chem Phys Lett* **2006**, *430*, 56.
- [20] May, J. W. *Surf. Sci* **1969**, *17*, 267.
- [21] Shelton, J.C, Patil, H. R.; Blakely, J. M. *Surf Sci*, **1974**; *43*, 493.
- [22] Eizenberg, M.; Blakely, J. M. *Surf. Sci.* **1979**, *82*, 228.
- [23] Oshima, C.; Nagashima, A. *J. Phys.: Condens. Matter.* **1997**, *9*, 1.
- [24] Gall, N. R.; Rut'kov, E. V.; Tontegode, A. Y. *Internat. J. Modern Phys. B* **1997**, *11*, 1865.
- [25] Bao, W.; Miao, W. F.; Chen, Z.; Zhang, H.; Jang, W.; Dames, C.; Lau, C. N. *Nat. Nanotechnol.* **2009**, *4*, 562–566.
- [26] Li, X.; Cai, W.; An, J.; Kim, S.; Nah, J.; Yang, D.; Piner, R.; Velamakanni, A.; Jung, I.; Tutuc, E.; Banerjee, S. K. Sanjay, K.; Colombo, L.; Ruoff, R. S. *Science* **2009**, *324*, 1312–1314.
- [27] Kim, K. S.; Zhao, Y.; Jang, H.; Lee, S. Y. Kim, J. M.; Kim, K. S.; Ahn, J. H.; Kim, P.; Choi, J. Y.; Hong, B. H. *Nature* **2009**, *457*, 706.
- [28] Wan, X; Chen, K.; Liu, D.; Chen, J.; Miao, Q.; Xu, J. *Chem. Mater.* **2012**, *24*, 3906–3915.
- [29] Li, Z.; Wu, P.; Wang, C.; Fan, X.; Zhang, W.; Zhai, X.; Zeng, C.; Li, Z.; Yang, J.; Hou, J. *ACS Nano* **2011**, *4*, 3385–3390.
- [30] Zhang, B.; Lee, W. H. Piner, R.; Kholmanov, I. Wu, Y.; Li, H.; Ji, H.; Ruoff, R. S. *ACS Nano*, **2012**, *6*, 2471–2476.
- [31] Sun, Z.; Yan, Z.; Yao, J.; Beitler, E.; Zh, Y.; Tour, J. M. *Nature* **2010**, *468*, 549-552.
- [32] Dong, X.; Wang, P.; Fang, W.; Su, C.-Y. Chen, Y.-H. Li, L.-J.; Huang, W.; Chen, P. *Carbon*, **2011**, *36*, 3672-3678.

- [33] Gao, L.; Ren, W.; Zhao, J.; Ma, L.-P.; Chen, Z.; Cheng, H.-M. *Appl. Phys. Lett.* **2010**, *97*, 183109.
- [34] Ji, H.; Hao, Y.; Ren, Y.; Charlton, M.; Lee, W. H.; Wu, Q.; Li, H.; Zhu, Y.; Wu, Y.; Piner, R.; Ruoff, R. S. *ACS Nano* **2011**, *5*, 7656–7661.
- [35] Batzill, M. *Surf. Sci Rep.* **2012**, *67*, 83–115
- [36] Guermoune, A. Chari, T. Popescu, F. Sabri, S. S. Guillemette, J.; Skulason, H. S. Szkopek, T.; Sij, M. *Carbon*, **2011**, *49*, 4204-4210.
- [37] Srivastava, A.; Galande, C.; Ci, L.; Song, L. Rai, Jariwala, D.; Kelly, K. F.; Ajayan, P. M. *Chem. Mater.*, **2010**, *22*, 3457.
- [38] Ruan, G.; Sun, Z.; Peng, Z.; Tour, J. M. *ACS Nano*, **2011**, *5*, 7601-7607.

CHAPTER 5

SYNTHESIS OF GRAPHENE NANORIBBONS (GNRs) BY ENCAPSULATION IN SINGLE-WALLED ALUMINOSILICATE NANOTUBES

The research in this chapter highlights ongoing work between the Tolbert and Henderson groups. The starting materials for this work are from commercial sources. Synthesized materials will be used as the project continues. Results from commercial sources have provided encouraging results.

5.1 Introduction

As with graphene, graphene nanoribbons (GNRs) are of great interest for many applications due to their electronic properties which can be adjusted by changes on their width and molecular geometry¹⁻¹⁰. Several methods have been developed for the synthesis of GNRs. These methods include, cutting graphene sheets to ribbons by electron¹¹ or ion beams¹², unzipping of carbon nanotubes^{1,13-16}, by deposition and fusion reaction of hydrocarbons on metallic surfaces^{3,11,17,18} and more recently by encapsulation in single-walled carbon nanotubes (SWNTs)^{19,20}. In his work, Talyzin *et al* used thermally induced fusion of coronene (**25**) and perylene (**26**) to form graphene nanoribbons encapsulated in single-walled carbon nanotubes (GNR@SWNT)¹⁹. In this method, hydrogen-terminated GNRs were synthesized at temperatures of 350 - 440 °C from perylene (**26**) with best results at 400 °C and with coronene (**25**) in the range of 470 - 530 °C with best results at 450 - 470 °C.

Because GNRs form inside the SWNT, then it seems clear that the optimum diameter of the SWNT depends on the width of the GNR to be synthesized.

In his paper, Talyzin *et al*, explains how the optimum diameter is 1.4 nm ((10,10) SWNT) for armchair tubes in order to synthesize coronene-based GNRs. Nanotubes with smaller diameters produced GNR@SWNT complexes with higher total energy due to geometrical distortion of the SWNT. Insertion of the ribbons into the nanotubes with larger diameters gave rise to weaker van der Waals interactions between the tubes and the ribbons¹⁹.

The main idea behind encapsulation is to impose geometrical restrictions to the alignment of the reacting molecules prior to thermal fusion and subsequent formation of GNRs. These geometrical restrictions are imposed by the use of SWNT as one-dimensional reactors for the insertion and fusion of polycyclic aromatic hydrocarbons.

Because Raman spectroscopy is one of the main tools for analysis of GNRs then the use of carbon nanotubes as one-dimensional reactors becomes a disadvantage due to the signals produced by the carbon nanotube itself, which can overlap with the Raman spectra of the newly synthesized GNRs. For this reason, a nanotube that could be used as a one-dimensional reactor without producing such signals would be advantageous.

Aluminosilicate single-walled nanotubes (SWNTs), a synthetic version of the nanotubular mineral imogolite²¹⁻²³, are metal oxide nanotubes that are formed of a tubular aluminum(III) hydroxide layer on the outer surface with pendant silanol groups on the inner surface²⁴ (**Figure 5.1a**). It has been hypothesized that because of the high surface density of silanol in the inner wall ($\sim 9.1 \text{ -OH/nm}^2$)^{25,26} the material is highly hydrophilic at ambient conditions²⁷ (**Figure 5.1b**). These nanotubes could provide the desired one-dimensional geometrical restrictions without the signal overlap on the Raman spectra caused by the carbon nanotubes.

It should be noted that the experiments conducted here made use also of coronene (**25**) and perylene (**26**) as starting materials in order to compare the results with those obtained from the literature¹⁹. Once a procedure has been established, other starting

materials, either commercially available or previously synthesized, will be used in order to change the shape of the GNRs produced.

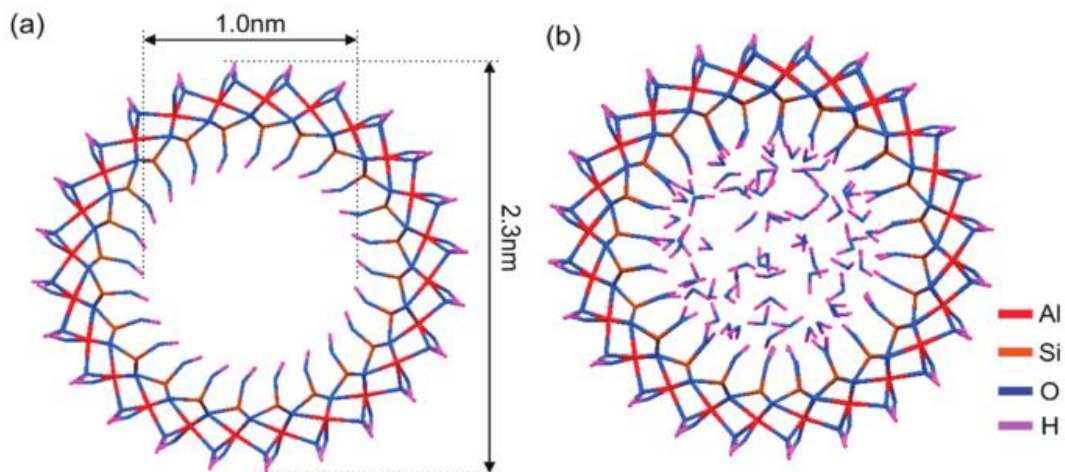


Figure 5.1 Aluminosilicate nanotubes (a) Cross-section of single-walled aluminosilicate nanotube. (b) Example of a model of the hydrated SWNT, with 14 wt% of water physisorbed in the SWNT at ambient conditions.²⁴

5.2 Experimental Protocol

General Experimental

All organic solvents and reagents to synthesize the GNRs were used as received from commercial sources without further purification. Reactions were performed in a Blue M Lindberg tube furnace. Raman spectra were recorded with a Nicolet Almega XR Raman spectrometer using a 25 mW, 2.4 eV excitation source (488 nm) through a 24 μM pinhole aperture and 100x objective.

Synthesis of GNRs General Procedure

Aluminosilicate nanotubes (1 - 2 mg) were added to a glass ampoule and heated (150 °C) in a silicon bath for 1 – 2 hr under Ar. Perylene (**26**) (20 mg, 79 μmol) or coronene (**25**) (20 mg, 66 μmol) was added to the glass ampoule. The reaction mixture was placed under Ar flow for 30 minutes and then sealed under vacuum. The ampoule was heated in a Lindbergh furnace for 3 – 6 hours at 200, 250, and 300 °C for perylene (**26**) and 200, 250, 300, 350, and 400 °C for coronene (**25**). The reaction mixture was allowed to cool to r.t. and extracted with chloroform. Filtration afforded black aluminosilicate nanotubes. The nanotubes were further washed with chloroform and dried under reduced pressure.

5.3 Results

Perylene (**26**) was the only starting material that formed hydrogen terminated GNRs under these conditions. GNRs were obtained at temperatures as low as 200 °C. These results are highly encouraging since the lowest temperature reported in the literature to form GNRs from perylene (**26**) is 350 °C.

Analysis of the Raman spectra of the aluminosilicate nanotubes (**Figure 5.2**), perylene (**26**) (**Figure 5.3**), and the synthesized material (**Figure 5.4**) points to the formation of hydrogen terminated GNR. As expected, none of the peaks from the Raman spectrum of aluminosilicate nanotubes interfered with the Raman spectrum of the synthesized GNRs. In fact, the Raman spectrum of the GNRs synthesized here closely resembles that from the literature (**Figure 5.5**). The peaks observed at 1290 cm^{-1} and 1370 cm^{-1} are exactly as those reported for GNR previously described as polyperinaphthalene (**Figure 5.6**). This is another indication that the narrowest possible armchair nanoribbon is forming as expected for a synthesis where perylene (**26**) is the starting material.²⁸

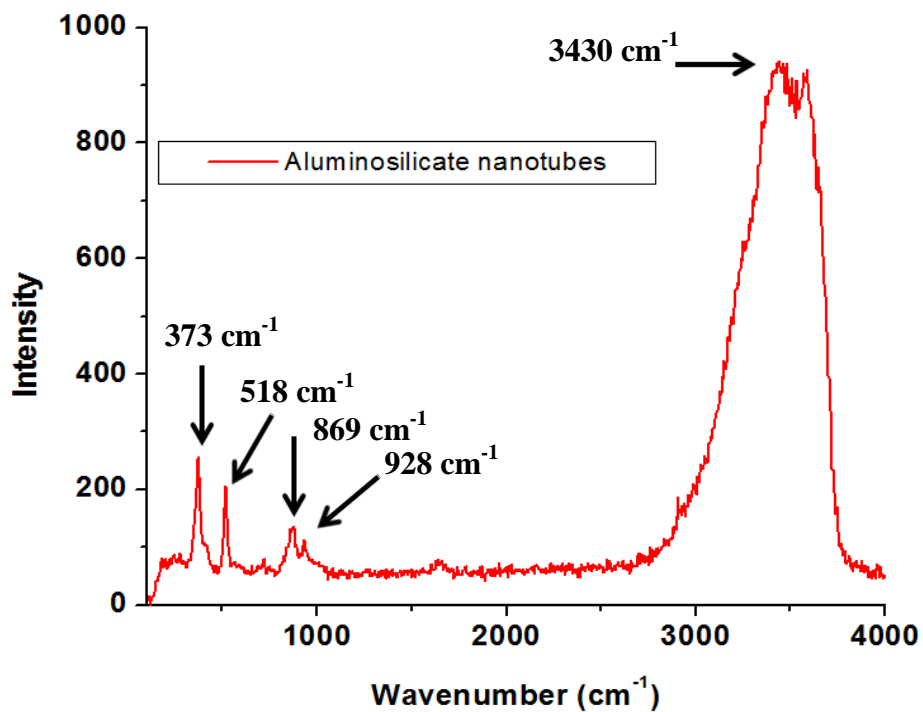


Figure 5.2 Raman spectrum of aluminosilicate nanotubes.

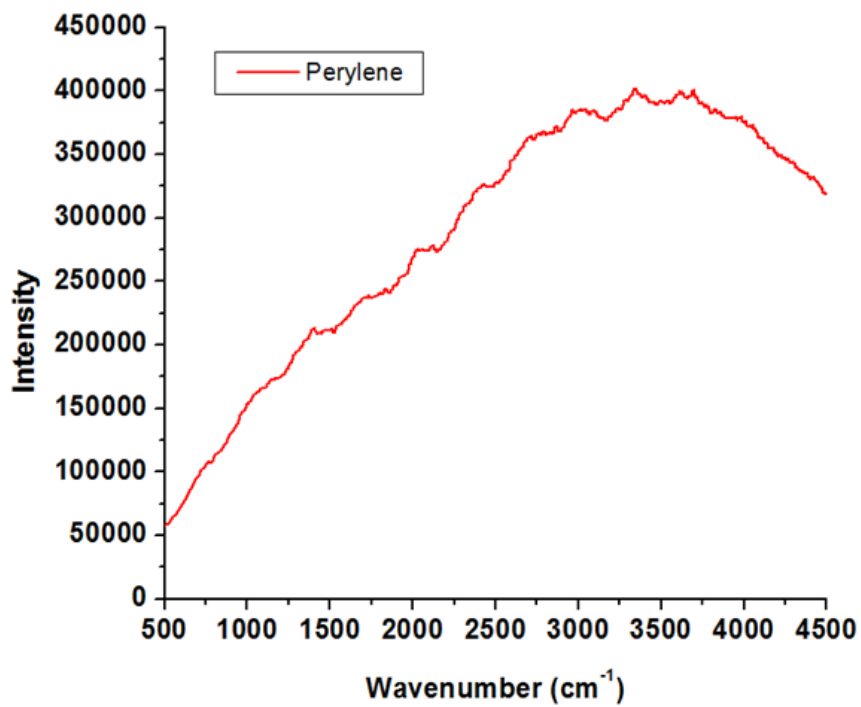


Figure 5.3 Raman spectrum of perylene (26).

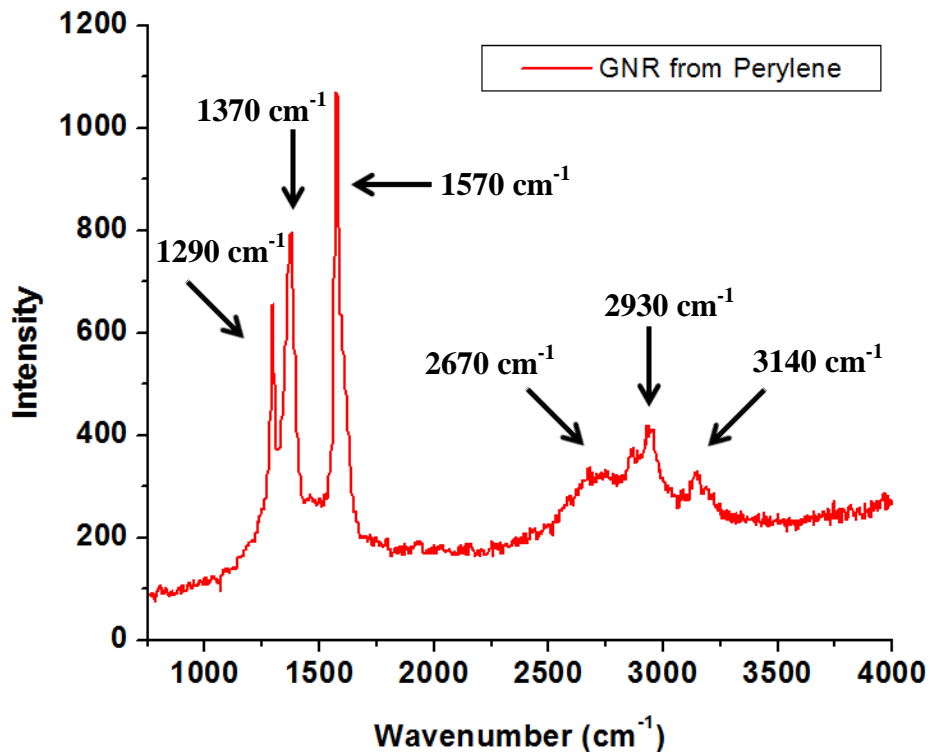


Figure 5.4 Raman spectrum of a graphene nanoribbon (GNR) from perylene (26).

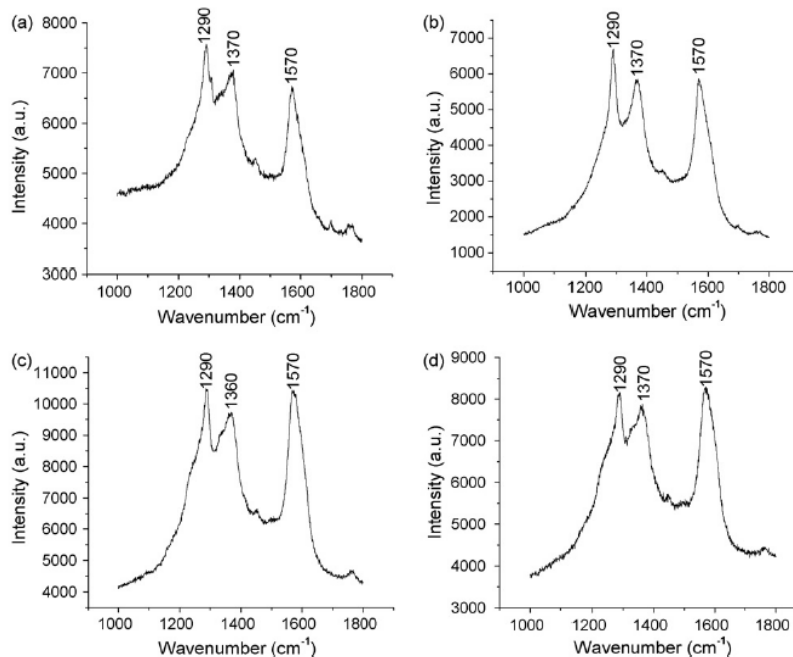


Figure 5.5 Typical micro-Raman spectra in the 1000–1800 cm^{-1} frequency range of PPN films on (a) aluminum, (b) steel, (c) silicon, and (d) ITO conducting glass. The weak feature at 1700 cm^{-1} in spectra (a) and (b) is from the room light.²⁸

Since the molecular structure of perylene (**26**) is composed of carbon and hydrogen, it would not be surprising if the GNRs formed here are also hydrogen terminated.¹⁹ The Raman spectrum of the molecule synthesized from perylene (**26**) (**Figure 5.4**) shows peaks at 2670 cm^{-1} , 2930 cm^{-1} , and 3140 cm^{-1} which are consistent with C-H stretching. This observation corroborates that the molecules synthesized here are indeed hydrogen terminated.

In the case of coronene (**25**), the results are as yet inconclusive but promising, and are the topic of continuous work.

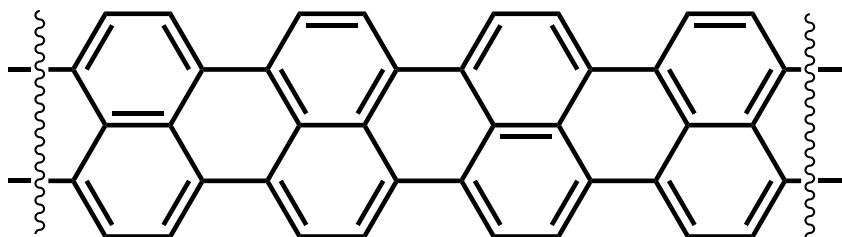


Figure 5.6 Polyperinaphthalene, the narrowest possible armchair nanoribbon.

5.4 Conclusions

In conclusion, our experiments showed that hydrogen terminated GNRs encapsulated in SWNT can be synthesized using other types of nanotubes, i.e. aluminosilicate. These experiments also show that by changing the type of nanotube one can influence the temperature of formation of the GNR and the synthesis can proceed with temperatures as low as $200\text{ }^{\circ}\text{C}$. Another advantage that aluminosilicate nanotubes offer is the fact that the signals from its Raman spectrum do not interfere with those of the synthesized GNRs allowing in this way for an easier interpretation of the spectra. The use of other starting materials, either commercially available or synthesized, is being

explored and in principle could provide for the synthesis of hydrogen terminated GNRs of different shapes and open the door to the synthesis of GNRs at even lower temperatures than those reported as of today.

5.5 References

- [1] Kosynkin, D. V.; Higginbotham, A. L.; Sinitskii, A.; Lomeda, J. R.; Dimiev, A.; Price, B. K.; Tour, J. M. *Nature* **2009**, *458*, 872.
- [2] Jiao, L. Y.; Zhang, L.; Wang, X. R.; Diankov, G.; Dai, H. J. *Nature* **2009**, *458*, 877.
- [3] Cai, J. M.; Ruffieux, P.; Jaafar, R.; Bieri, M.; Braun, T.; Blankenburg, S.; Muoth, M.; Seitsonen, A. P.; Saleh, M.; Feng, X. L.; Mullen, K.; Fasel, R. *Nature* **2010**, *466*, 470.
- [4] Jiao, L. Y.; Zhang, L.; Wang, X. R.; Diankov, G.; Dai, H. J. *Nature*, **2009**, *458*, 877.
- [5] Hirsch, A. *Angew. Chem., Int. Ed.* **2009**, *48*, 6594.
- [6] Shimizu, T.; Haruyama, J.; Marcano, D. C.; Kosinkin, D. V.; Tour, J. M.; Hirose, K.; Suenaga, K. *Nat. Nanotechnol.* **2011**, *6*, 45.
- [7] Balandin, A. A.; Ghosh, S.; Bao, W. Z.; Calizo, I.; Teweldebrhan, D.; Miao, F.; Lau, C. N. *Nano Lett.* **2008**, *8*, 902.
- [8] Ritter, K. A.; Lyding, J. W. *Nat. Mater.* **2009**, *8*, 235.
- [9] Dai, H. J.; Jiao, L. J.; L., Y.; Zhang, L.; Wang, X. R.; Diankov, G. *Nature* **2009**, *458*, 877.
- [10] Shimizu, T. S., T.; Haruyama, J.; Marcano, D. C.; Kosinkin, D. V.; Tour, J. M.; Hirose, K.; Suenaga, K. *Nat. Nanotechnol.* **2011**, *6*, 45.

- [11] Jin, C. H.; Lan, H. P.; Peng, L. M.; Suenaga, K.; Iijima, S. *Phys. Rev. Lett.* **2009**, 102, 205501.
- [12] Lemme, M. C.; Bell, D. C.; Williams, J. R.; Stern, L. A.; Baugher, B. W. H.; Jarillo-Herrero, P.; Marcus, C. M. *ACS Nano* **2009**, 3, 2674.
- [13] Bai, J. W.; Cheng, R.; Xiu, F. X.; Liao, L.; Wang, M. S.; Shailos, A.; Wang, K. L.; Huang, Y.; Duan, X. F. *Nat. Nanotechnol.* **2010**, 5, 655.
- [14] Sprinkle, M.; Ruan, M.; Hu, Y.; Hankinson, J.; Rubio-Roy, M.; Zhang, B.; Wu, X.; Berger, C.; de Heer, W. A. *Nat. Nanotechnol.* **2010**, 5, 727.
- [15] Sinitskii, A.; Dimiev, A.; Kosynkin, D. V.; Tour, J. M. *ACS Nano* **2010**, 4, 5405.
- [16] Jiao, L. J.; L., Y.; Wang, X. R.; Diankov, G.; Wang, H. L.; Dai, H. J. *Nat. Nanotechnol.* **2010**, 5, 321.
- [17] Treier, M.; Pignedoli, C. A.; Laino, T.; Rieger, R.; Mullen, K.; Passerone, D.; Fasel, R. *Nat. Chem.* **2011**, 3, 61.
- [18] Diez-Perez, I.; Li, Z. H.; Hihath, J.; Li, J. H.; Zhang, C. Y.; Yang, X. M.; Zang, L.; Dai, Y. J.; Feng, X. L.; Muellen, K.; Tao, N. J. *Nat Commun.* **2010**, 1, 31.
- [19] Talyzin, A. V.; Anoshkin, I. V.; Krasheninnikov, A. V.; Nieminen, R. M.; Nasibulin, A. G. Jiang, H.; Kauppinen, E.I. *Nano Lett.* **2011**, 11, 4352.
- [20] Chuvilin, A.; Bichoutskaia, E.; Gimenez-Lopez, M. C.; Chamberlain, T. W.; Rance, G. A.; Kuganathan, N.; Biskupek, J.; Kaiser, U.; and Khlobystov, A. N. *Nat. Mater.* **2011**, 687.
- [21] Wada, K.; Yoshinag, N. *Am. Mineral.* **1969**, 54, 50.
- [22] Wada, S. I.; Eto, A.; Wada, K. *J. Soil Sci.* **1979**, 30, 347.
- [23] Farmer, V. C.; Smith, B. F. L.; Tait, J. M. *Clay Miner.* **1979**, 14, 103.

- [24] Dun-Yen Kang, D-Y.; Zang, J.; Wright, E. R. McCanna, A. L.; Jones, C. W.; Nair, S. *ACS Nano* **2010**, *4*, 4897.
- [25] Ying, J. Y.; Mehnert, C. P.; Wong, M. S. *Angew. Chem., Int. Ed.* **1999**, *38*, 56.
- [26] Sayari, A.; Hamoudi, S. *Chem. Mater.* **2001**, *13*, 3151.
- [27] Cheng, C. H.; Bae, T. H.; McCool, B. A.; Chance, R. R.; Nair, S.; Jones, C. W. *J. Phys. Chem. C* **2008**, *112*, 3543.
- [28] Sosnowski, M.; Yu, C.; Wang, S. C.; Iqbal, Z. *Synth. Met.* **2008**, *158*, 425.

CHAPTER 6

SUMMARY AND RECOMMENDATIONS FOR FUTURE WORK

In Chapters two and three, organic molecules were synthesized with the goal in mind to use them as precursors for the synthesis of graphene at low temperature. Chapter three highlights the reactivity of dibenzo[*bc,kl*]coronene as well as that of its precursor. This reactivity could be used to our advantage for the synthesis of graphene at low temperatures. The experiments conducted in chapter four showed that graphene can be synthesized from virtually any carbon source at temperatures of 1000 °C. Although this is consistent with the literature,¹⁻³ the use of forming gas at concentrations of 3% hydrogen differs from published results. These results showed that in principle this safer concentration of hydrogen can be used to synthesize graphene on copper substrates. The failure of our experiments to grow graphene at 600 °C might not be due to the carbon sources used here but instead on the UHV that our system lacked. This argument is based on the fact that according with literature graphene has been synthesized under UHV conditions from coronene at temperatures as low as 550 °C although it should be said that higher concentrations of hydrogen were used to anneal the copper substrate.⁴ On the other hand, the ongoing work on the synthesis of GNRs highlighted in chapter five shows that their synthesis by encapsulation in SWNT is not restricted to the use of only CNTs but that in fact other nanotubes as the ones used in our research can be used. This research also shows that GNR's can be synthesized at temperatures as low as 200 °C. Based on these observations, the following recommendations for future work are derived:

6.1 Synthesis and Study of the Properties and Chemistry of Dibenzo[bc,kl]coronene

The successful synthesis of dibenzo[bc,kl]coronene in sufficient quantities for further study highlighted in chapter three opens the door to investigate the properties and chemistry of this PAH. As of today only the UV-vis spectrum⁵ and mass spectrum of this compound have been obtained as a proof of its existence. Additional research can be focused on the formation of crystals from this material, with this, a crystal structure can be obtained and the question of its synthesis and existence will be settled finally. On the other hand, our research shows this material to decompose when exposed to light and air. Further studies about the chemistry and reactivity of this material can be conducted in order to understand more about the nature of this PAH.

6.2 Synthesis of Graphene at Low Temperatures by CVD on Copper

Much work still remains to be done involving the synthesis of graphene at low temperatures by CVD. As mentioned earlier, the failure to grow graphene at temperatures of 600 °C in no way shows that the carbons sources used in our experiments cannot be successful. Either the lack of an UHV system and/or higher concentrations of hydrogen might be enough to account for these results. Further research needs to be conducted with UHV systems capable of handling higher concentrations of hydrogen than the one used in this research. These studies will provide for a better understanding of the effects that these parameters have on the synthesis of graphene at low temperatures. It is of course necessary to repeat the results found in the literature⁴ to insure the system is capable to grow graphene at least at the temperature reported. Once a procedure has been established and a better understanding of the effects that each parameter has in the overall

results, then new molecules, either commercially available or synthesized, can be used in order to grow graphene at low temperatures.

6.3 Synthesis of GNRs Encapsulated in Aluminosilicate Nanotubes

Much work still remains to be done for the synthesis of GNRs highlighted in chapter five. Studies need to be conducted where other organic molecules, either commercially available or synthesized, are used as the starting material. Since the shape of the nanotubes allows for reactions to take place only in one dimension⁶ then the choice of the organic molecule will have a direct effect on the shape of the GNR formed. This would allow for GNRs of different shapes to be synthesized. Studies on the properties of GNRs with different shapes will provide a better understanding of the effect that the shape of the GNR has on its properties. The results from chapter five also open the door for studies using other types of nanotubes. Since our results showed that the synthesis of GNR by encapsulation is not restricted only to CNTs then, as an extension of this observation, the synthesis of GNRs might not be restricted to only these two types of nanotubes.

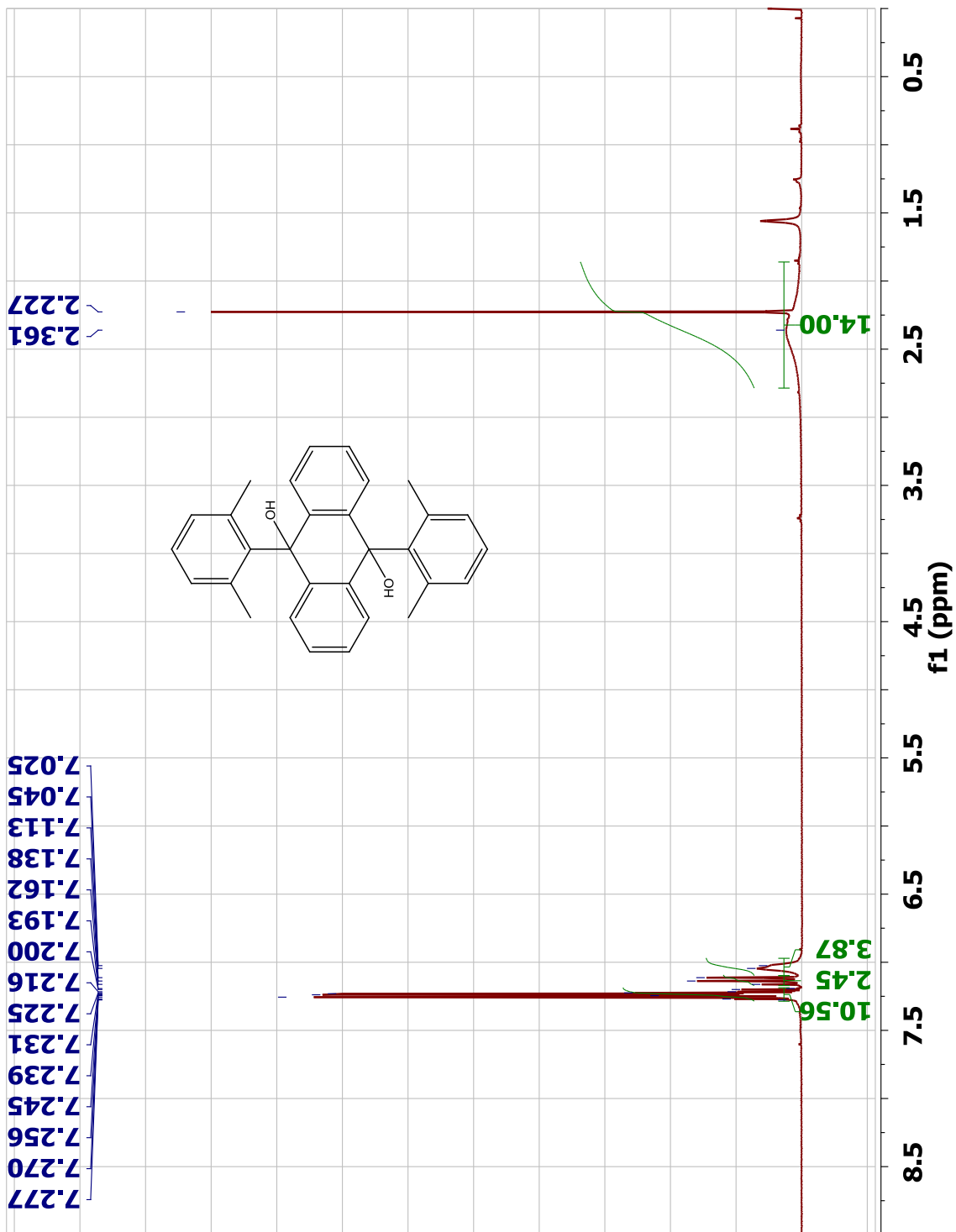
6.4 References

- [1] Li, X.; Cai, W.; An, J.; Kim, S.; Nah, J.; Yang, D.; Piner, R.; Velamakanni, A.; Jung, I.; Tutuc, E.; Banerjee, S. K. Sanjay, K.; Colombo, L.; Ruoff, R. S. *Science* **2009**, *324*, 1312–1314.
- [2] Ruan, G.; Sun, Z.; Peng, Z.; Tour, J. M. *ACS Nano*, **2011**, *5*, 7601-7607.
- [3] Sun, Z.; Yan, Z.; Yao, J.; Beitler, E.; Zh, Y.; Tour, J. M. *Nature* **2010**, *468*, 549-552.

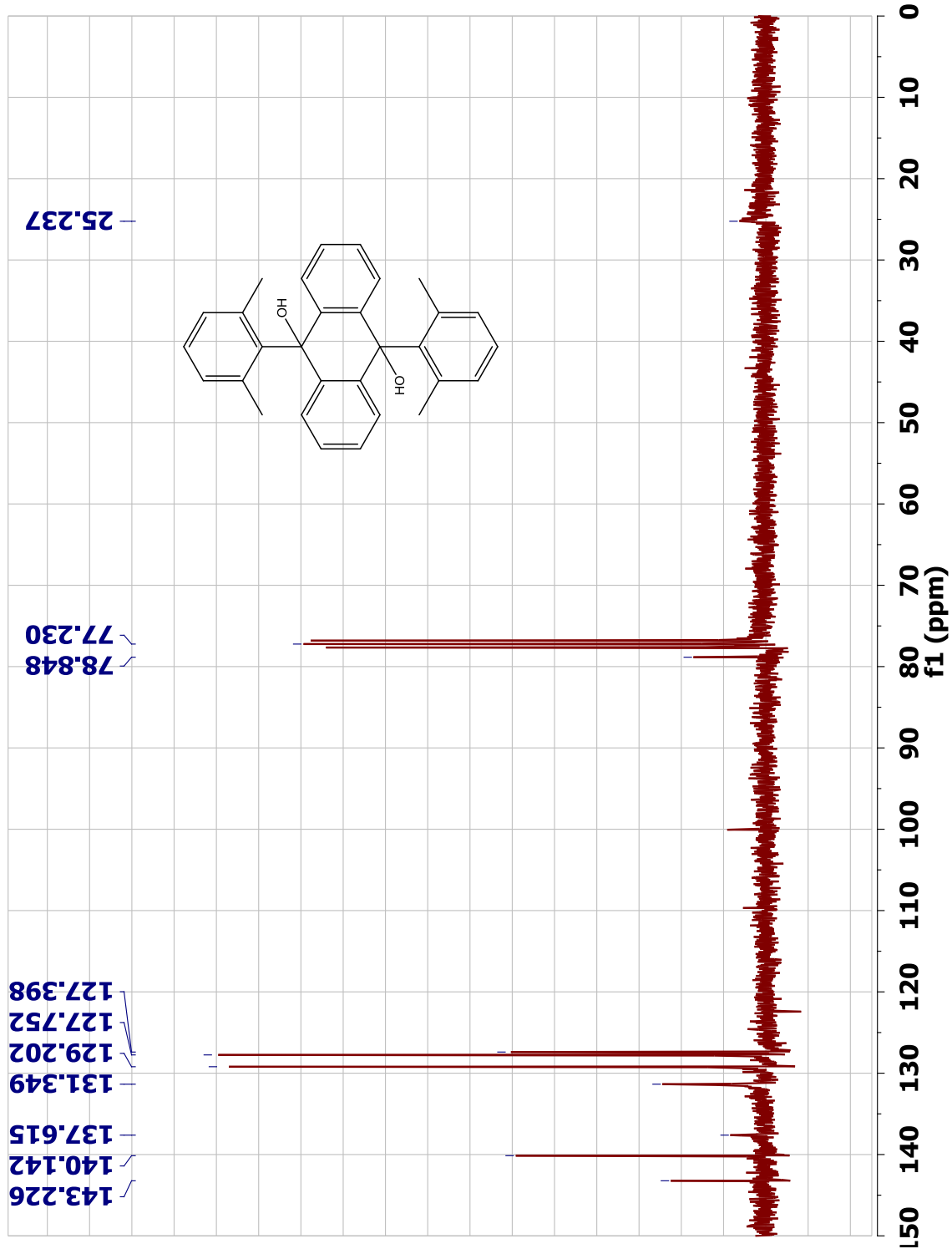
- [4] Wan, X.; Chen, K.; Liu, D.; Chen, J.; Miao, Q.; Xu, J. *Chem. Mater.* **2012**, *24*, 3906–3915.
- [5] Clar, E. Fell, G. S.; Ironside, C. T.; Balsillie, A. *Tetrahedron*, **1960**, *10*, 26-36.
- [6] Talyzin, A. V.; Anoshkin, I. V.; Krasheninnikov, A. V.; Nieminen, R. M.; Nasibulin, A. G. Jiang, H.; Kauppinen, E.I. *Nano Lett.* **2011**, *11*, 4352.

APPENDIX A

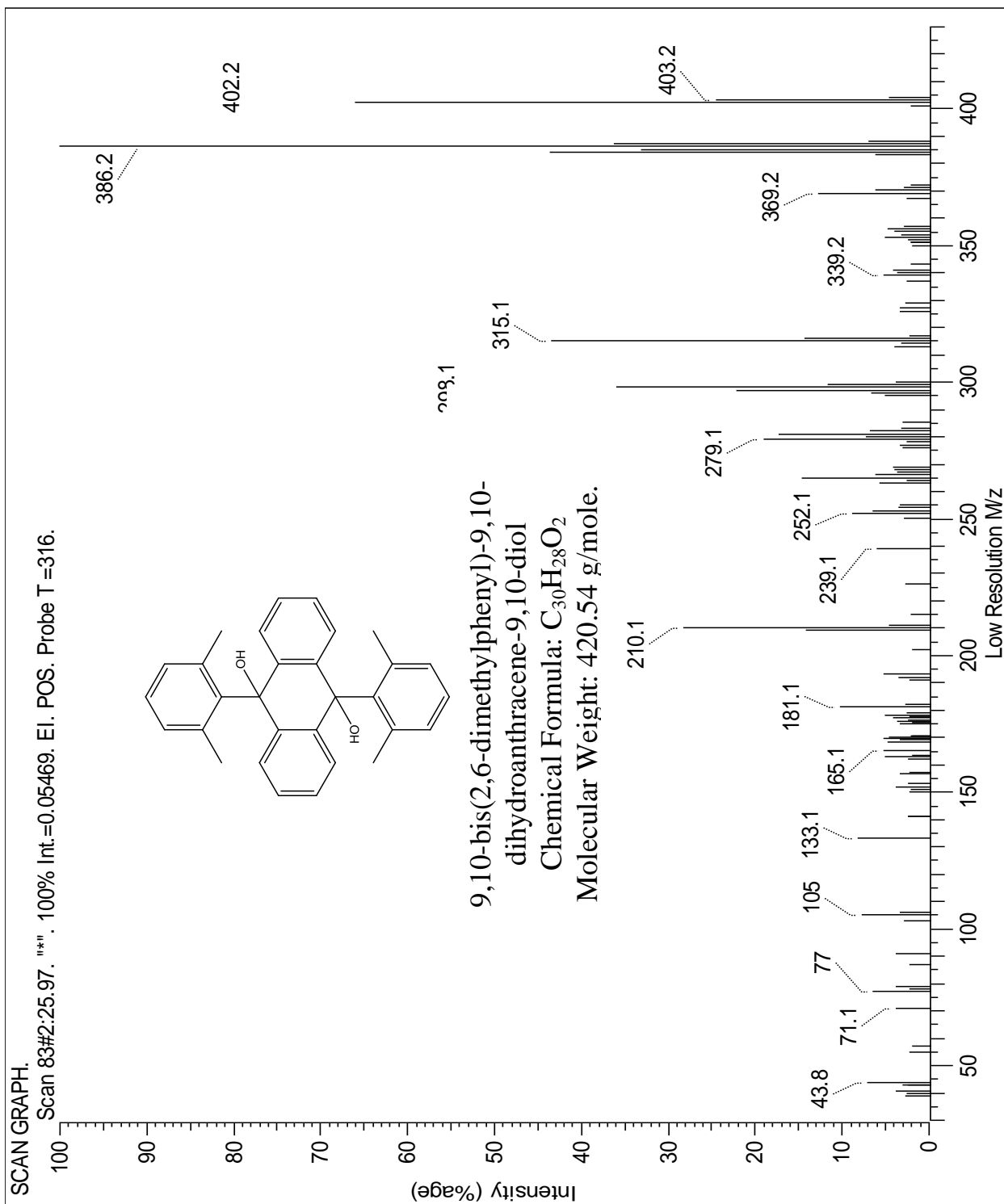
CHARACTERIZATION OF SYNTHESIZED COMPOUNDS



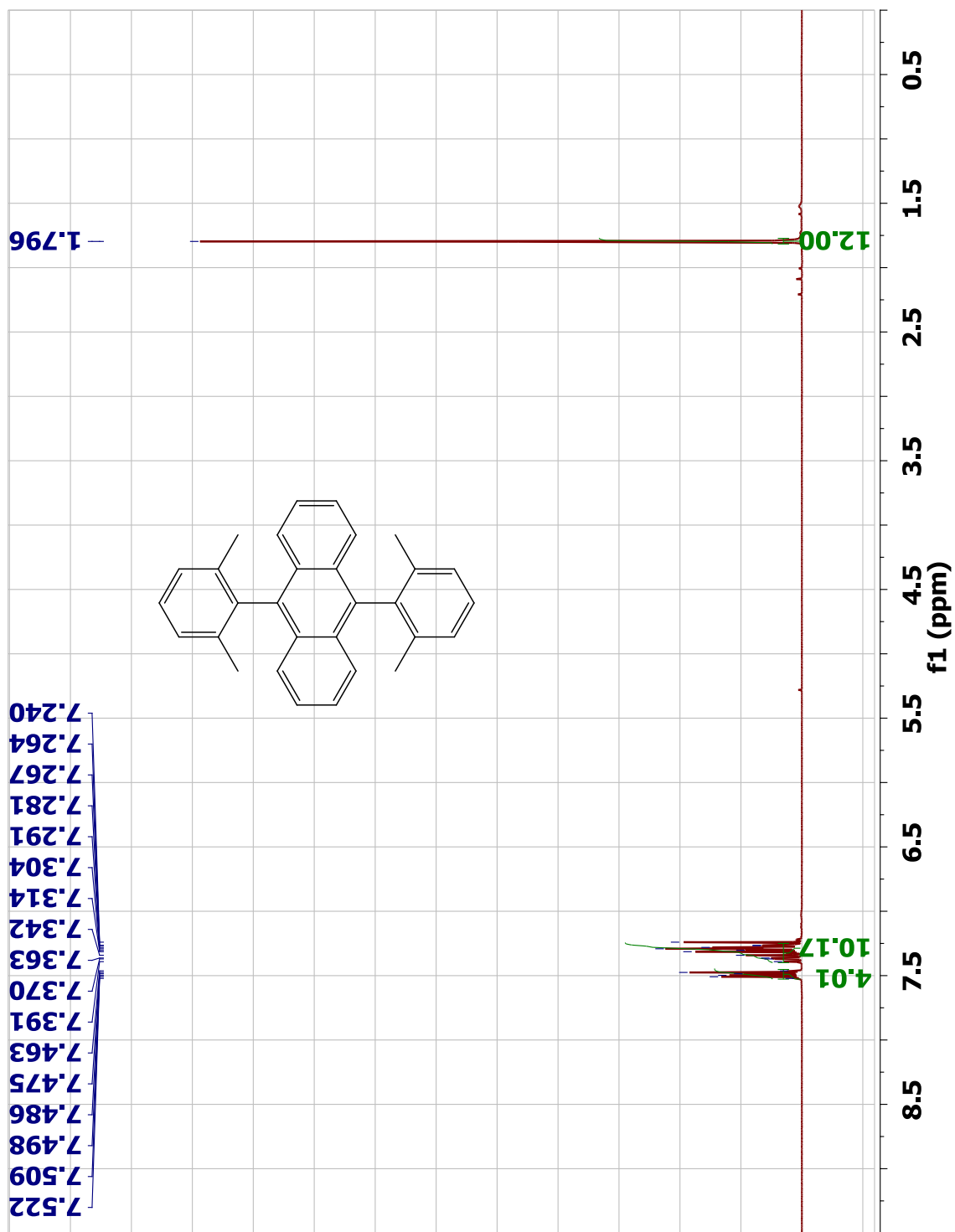
A.1 ¹H-NMR spectrum of 9,10-bis(2,6-dimethylphenyl)-9,10-dihydroanthracene-9,10-diol (3a).



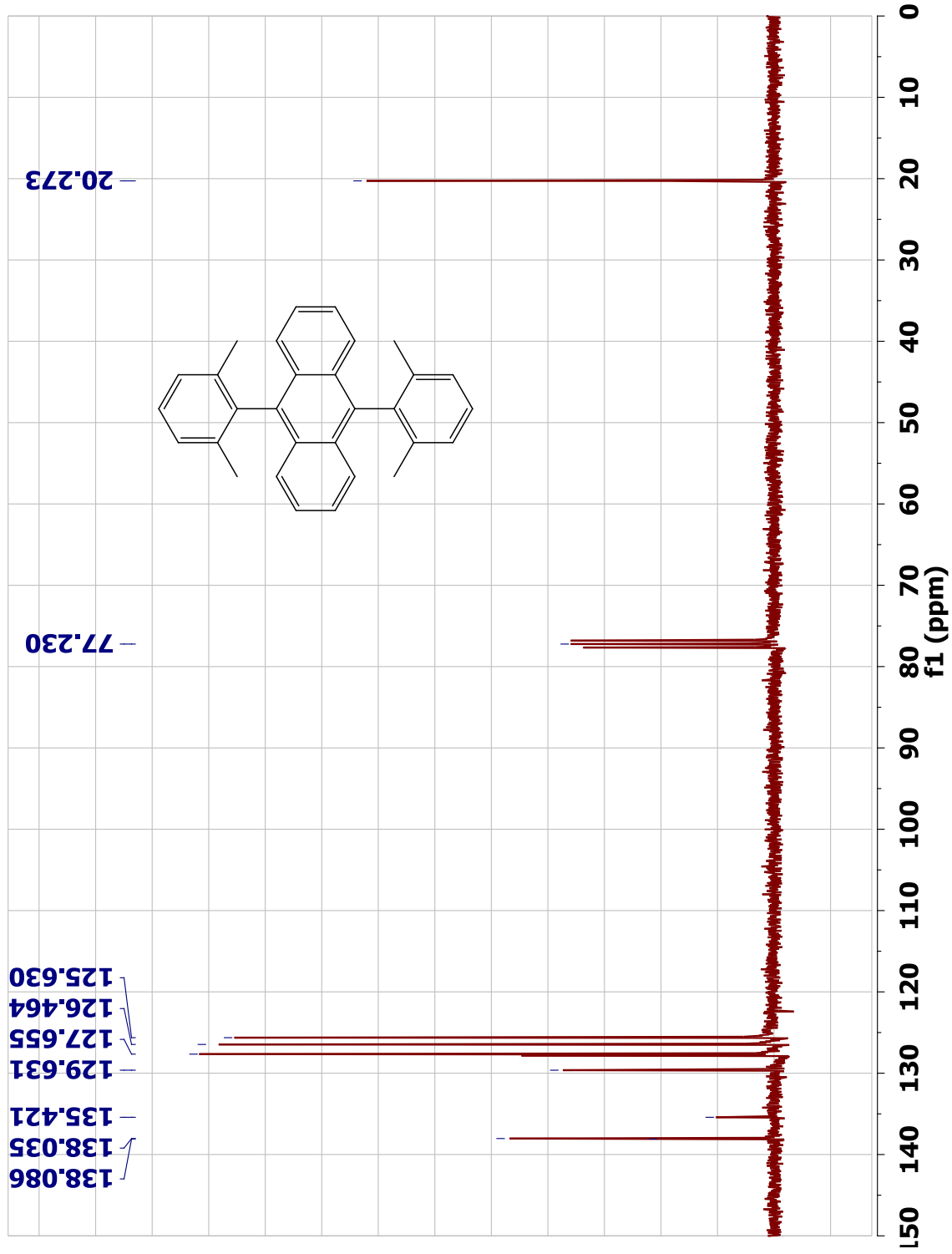
A.2 ^{13}C -NMR spectrum of 9,10-bis(2,6-dimethylphenyl)-9,10-dihydroanthracene-9,10-diol (3a).



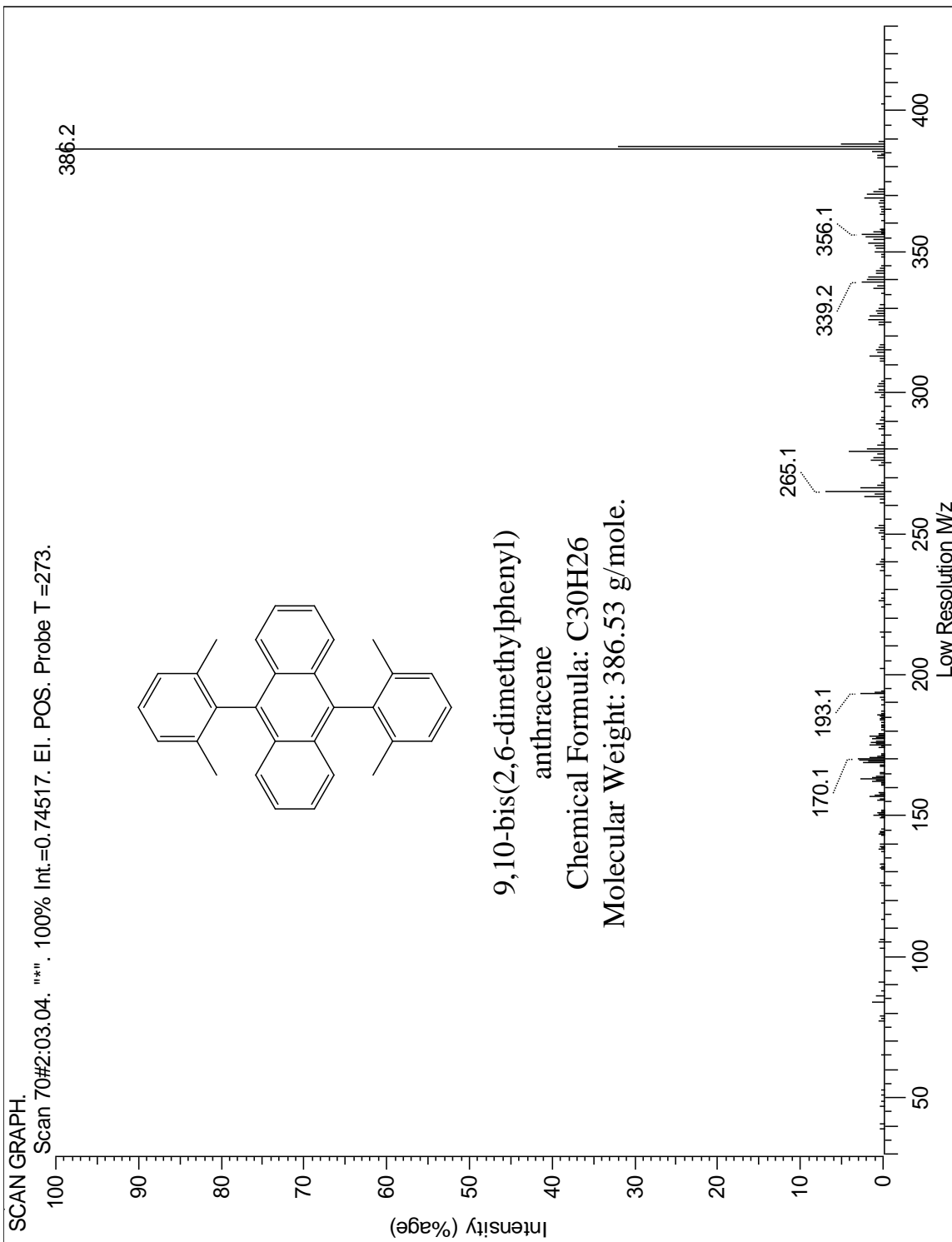
A.3 Mass spectrum of 9,10-bis(2,6-dimethylphenyl)-9,10-dihydroanthracene-9,10-diol (3a).



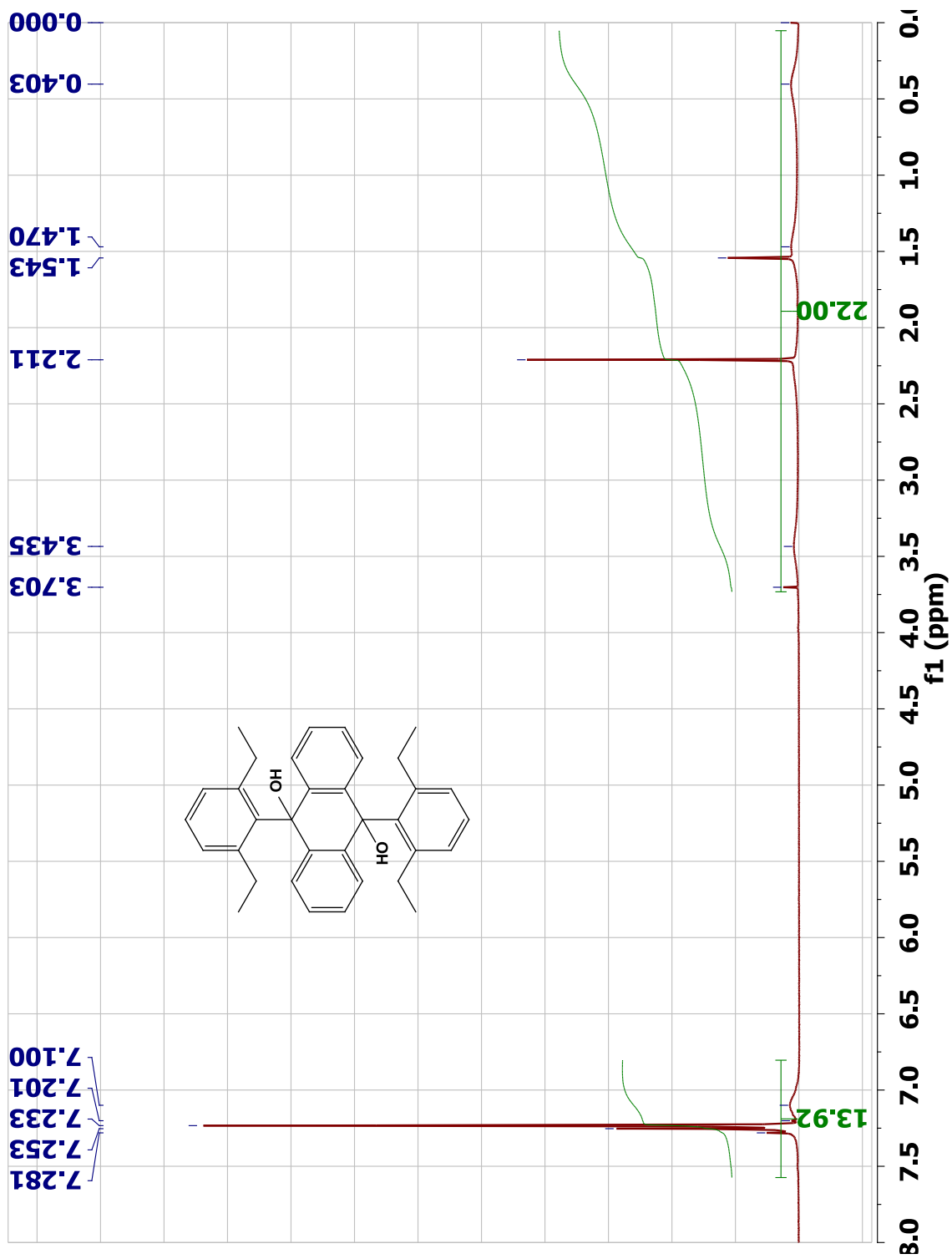
A.4 ¹H-NMR spectrum of 9,10-bis(2,6-dimethylphenyl)anthracene (4a).



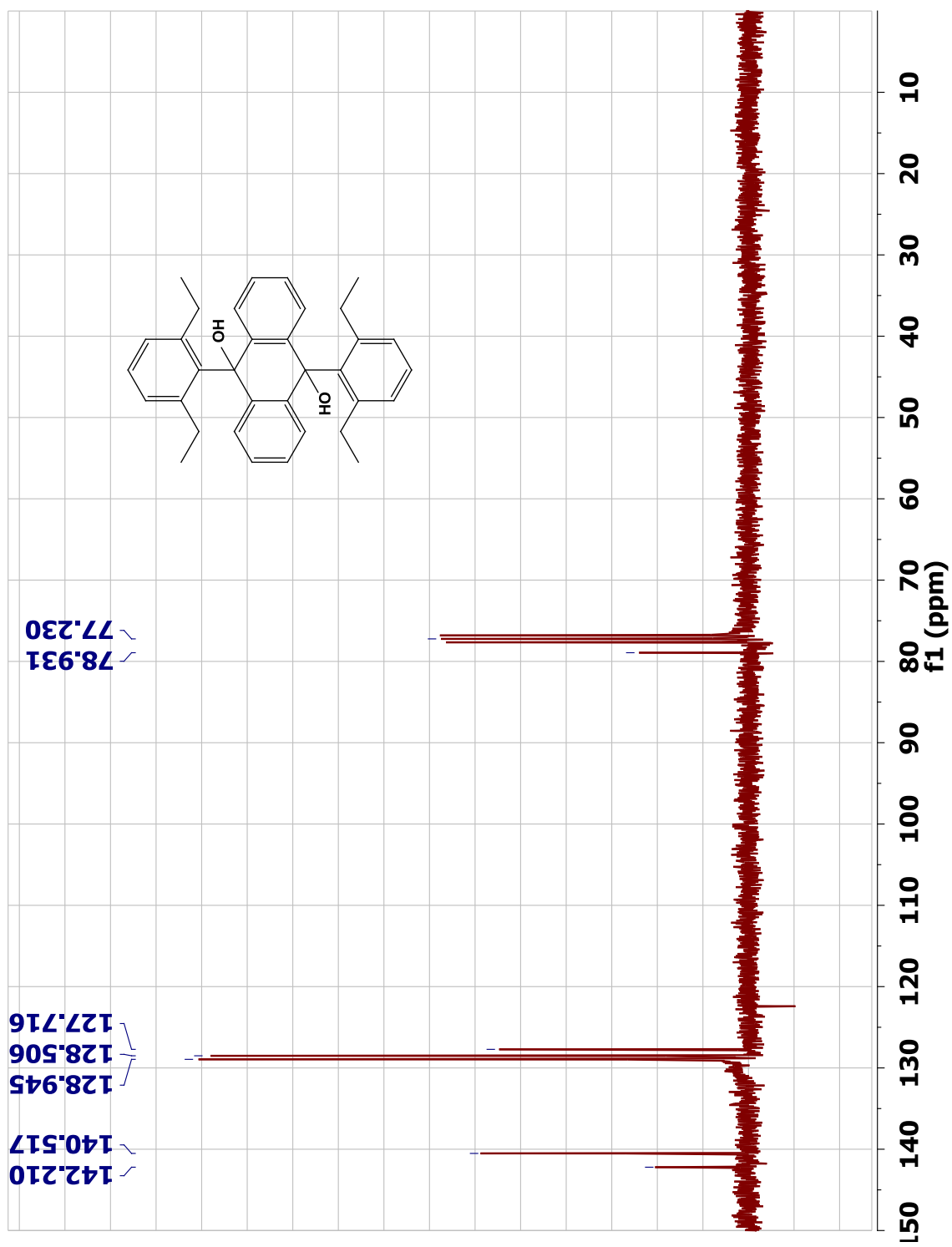
A.5 ^{13}C -NMR spectrum of 9,10-bis(2,6-dimethylphenyl)anthracene (4a).



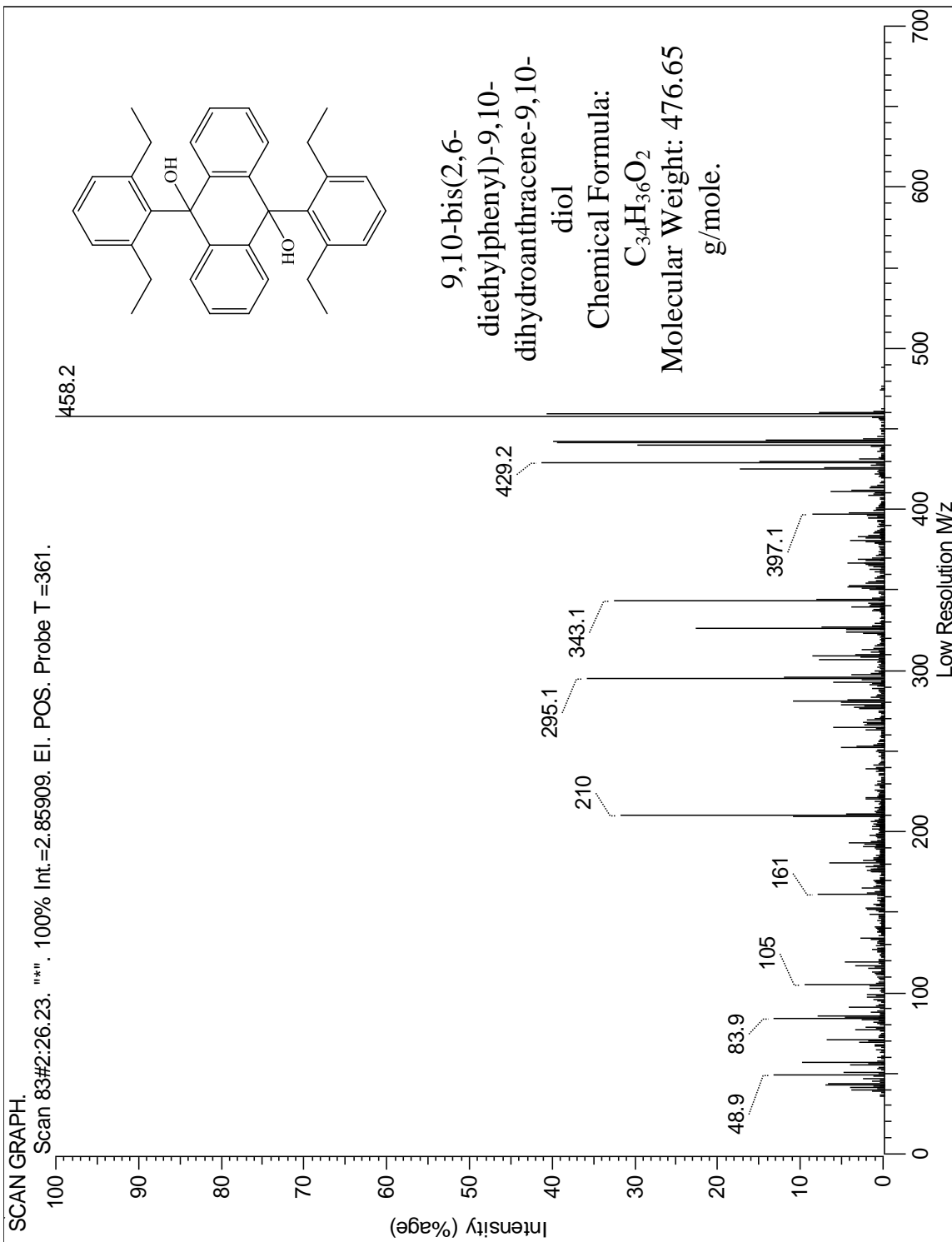
A.6 Mass spectrum of 9,10-bis(2,6-dimethylphenyl)anthracene (**4a**).



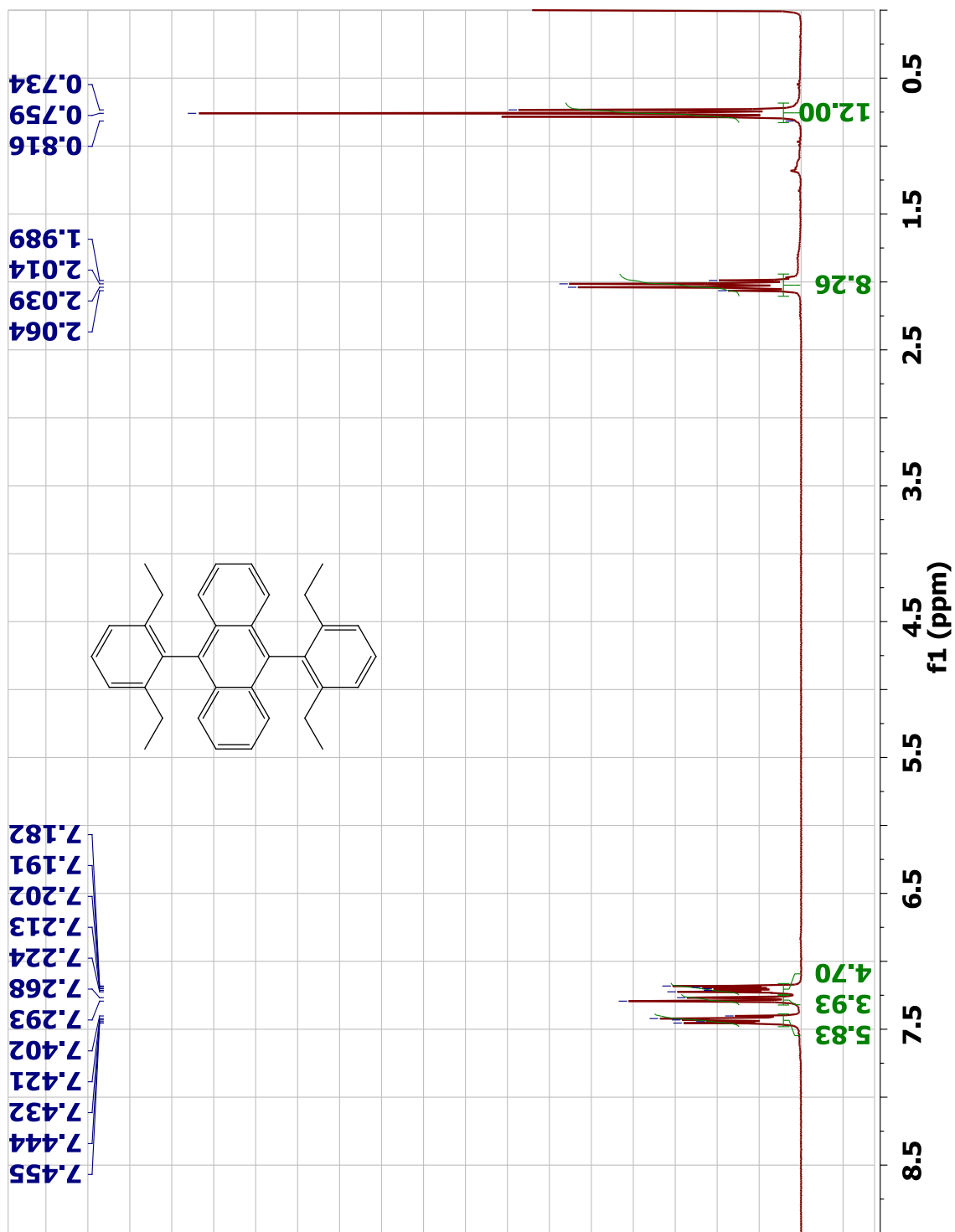
A.7 ¹H-NMR spectrum of 9,10-bis(2,6-diethylphenyl)-9,10-dihydroanthracene-9,10-diol (3b).



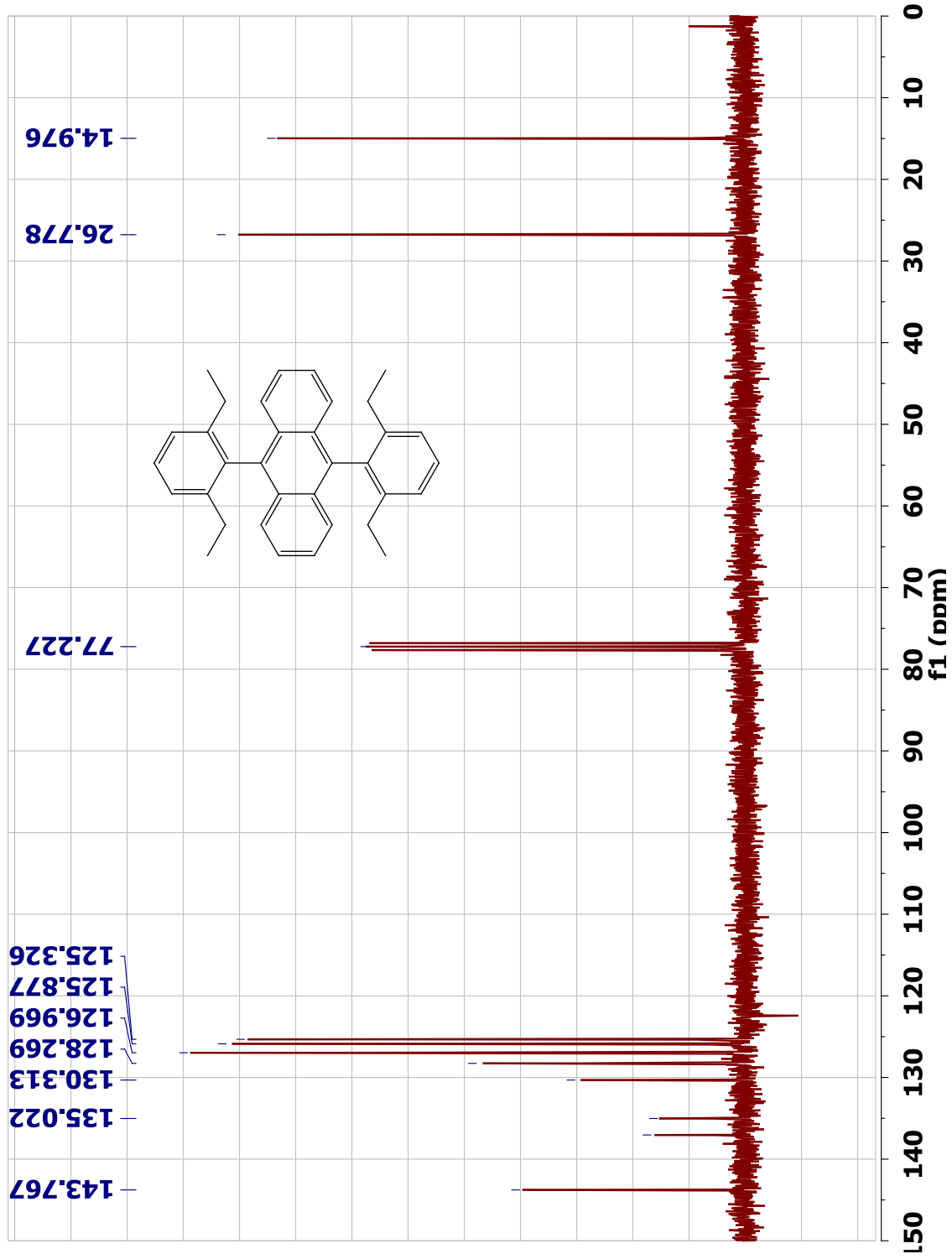
A.8 ¹³C-NMR spectrum of 9,10-bis(2,6-diethylphenyl)-9,10-dihydroanthracene-9,10-diol (3b).



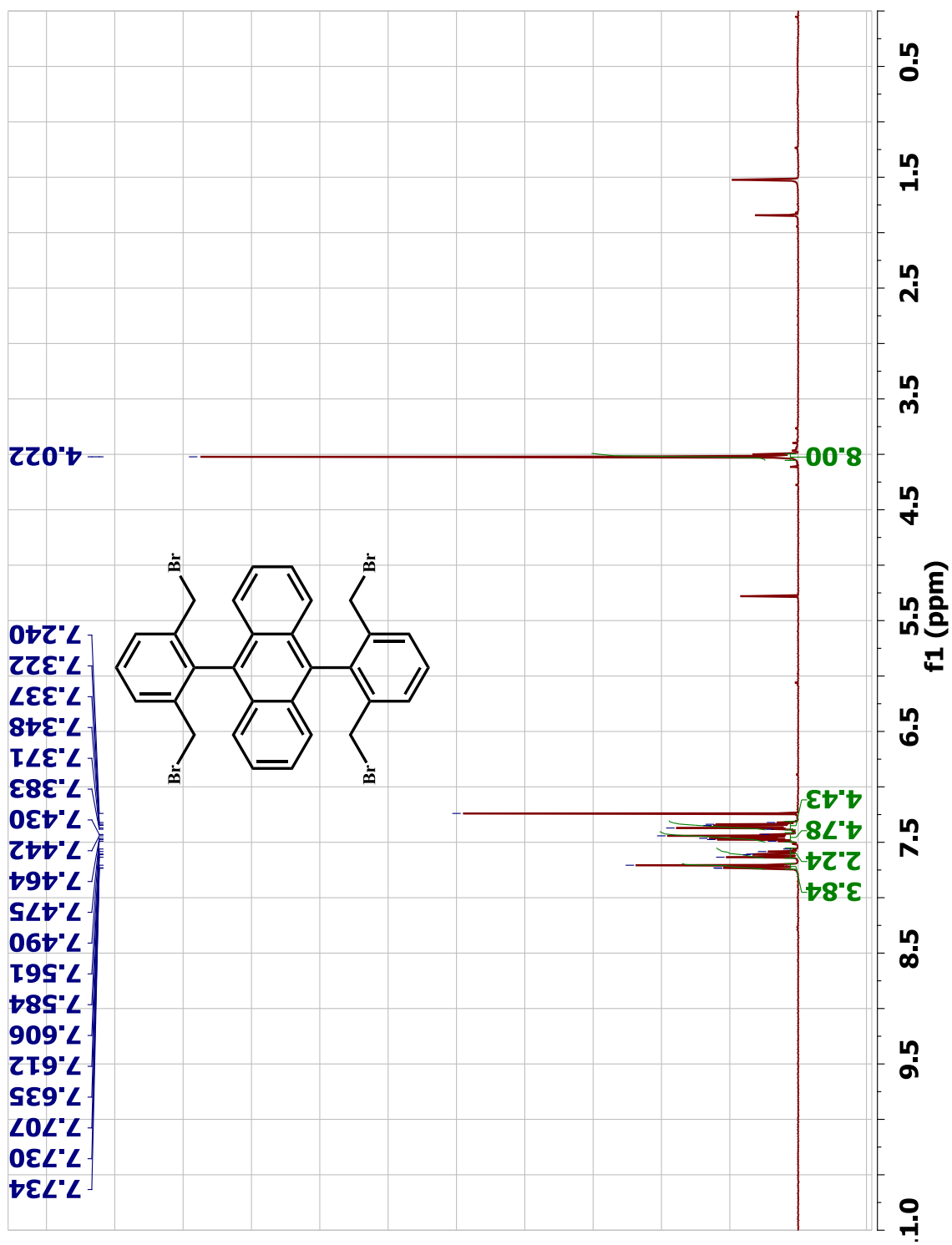
A.9 Mass spectrum of 9,10-bis(2,6-diethylphenyl)-9,10-dihydroanthracene-9,10-diol (**3b**).



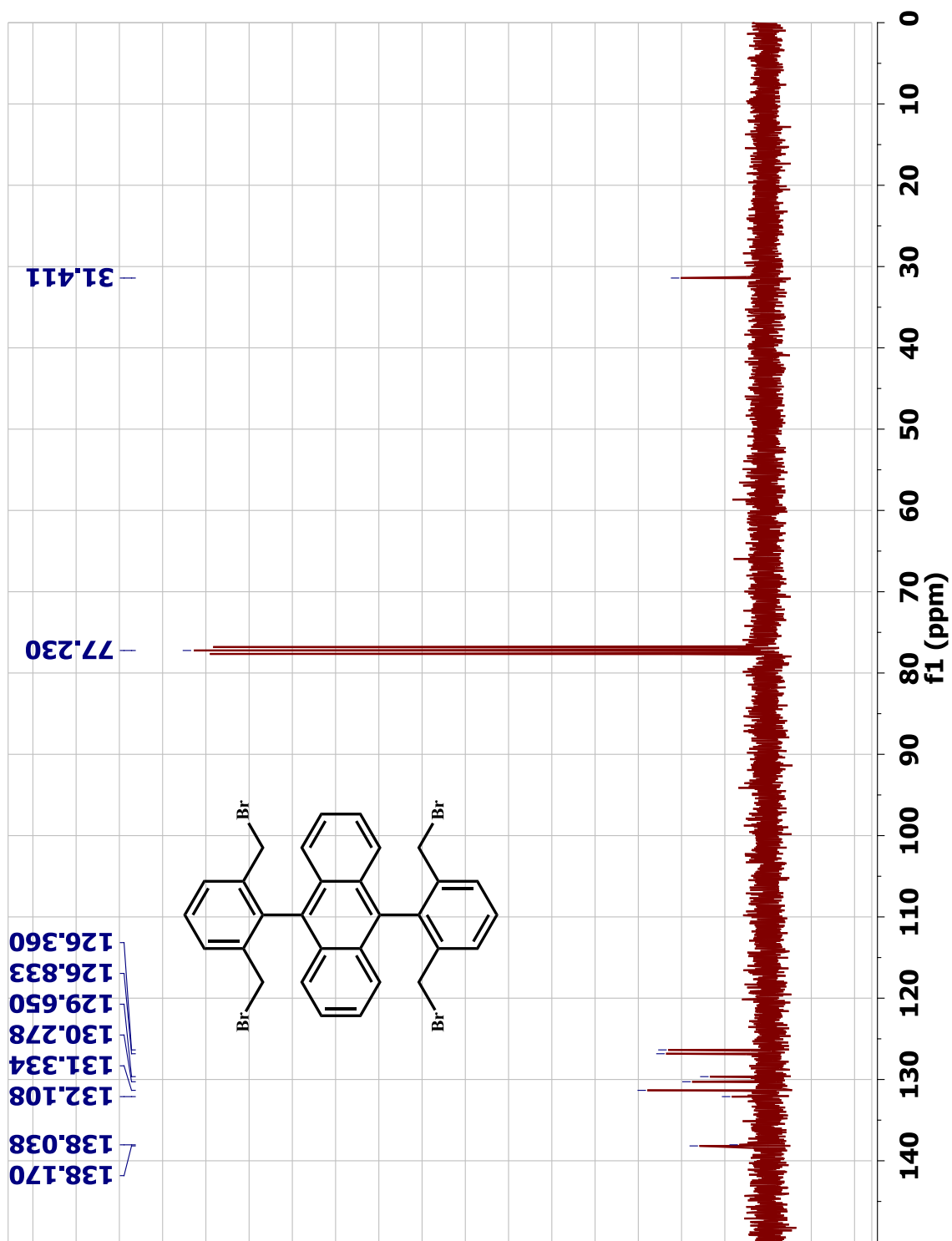
A.10 ¹H-NMR spectrum of 9,10-bis(2,6-diethylphenyl)anthracene (4b).



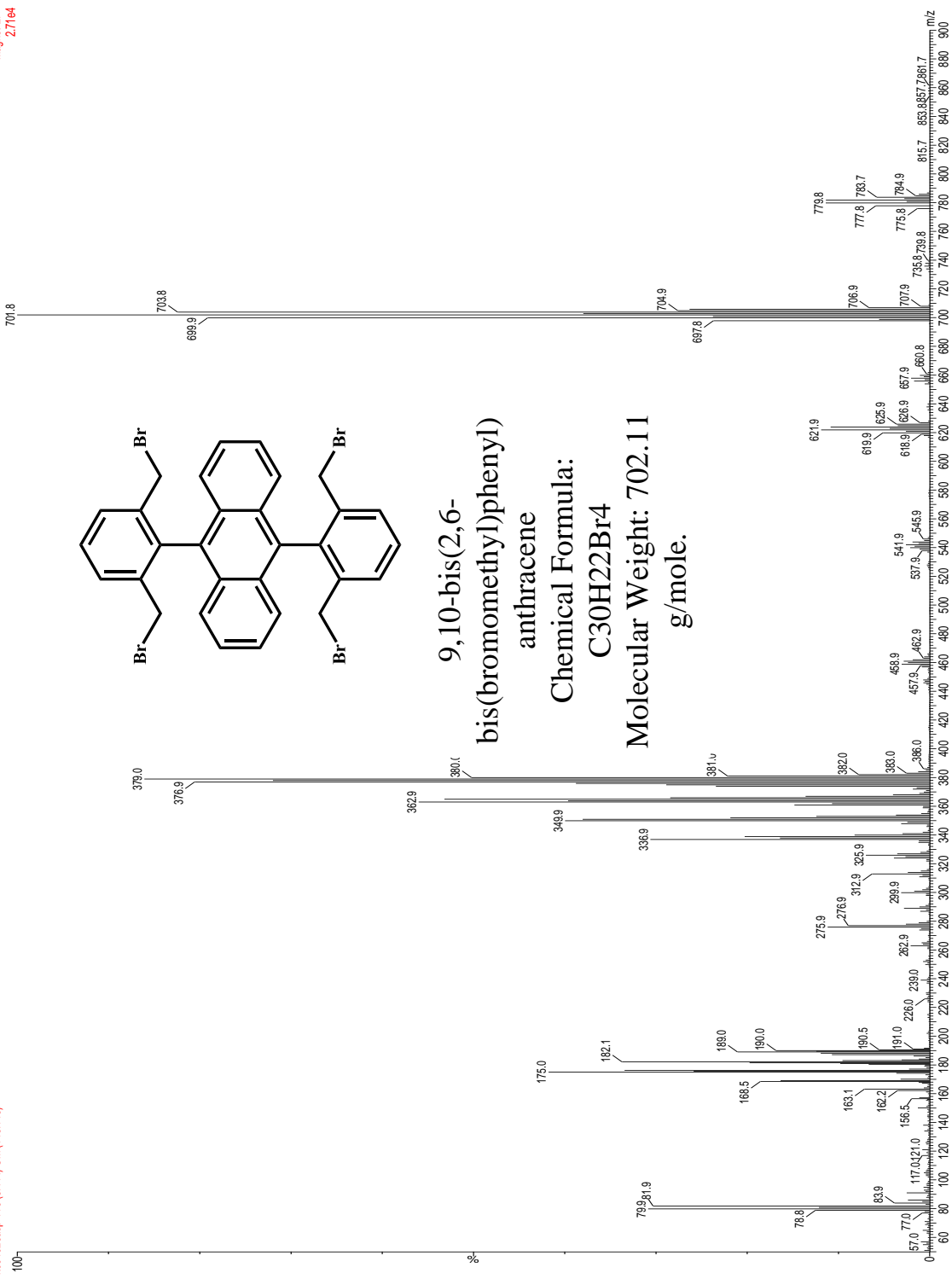
A.11 ¹³C-NMR spectrum of 9,10-bis(2,6-diethylphenyl)anthracene (4b).



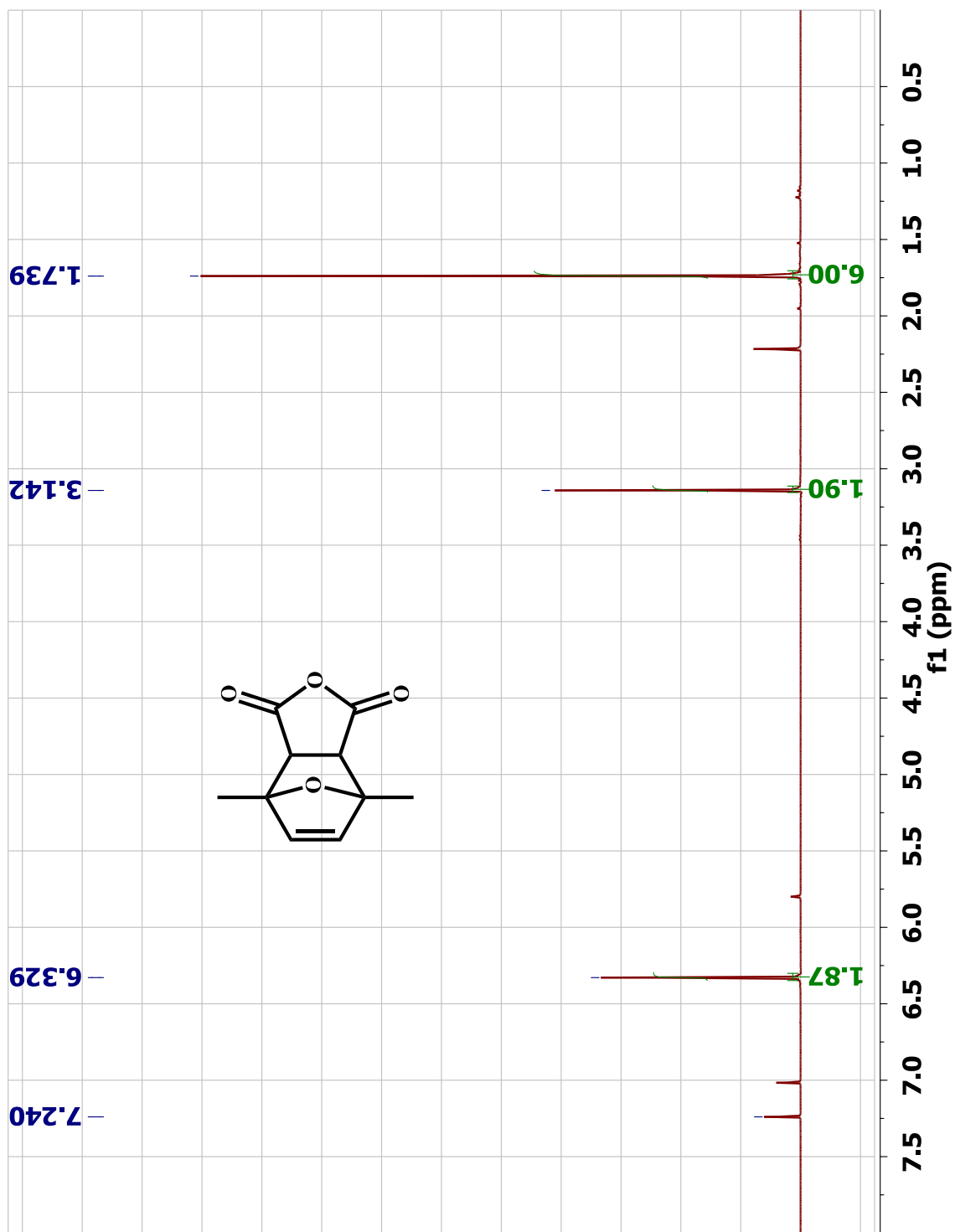
A.12 ¹H-NMR spectrum of 9,10-bis(2,6-bis(bromomethyl)phenyl)anthracene (5).



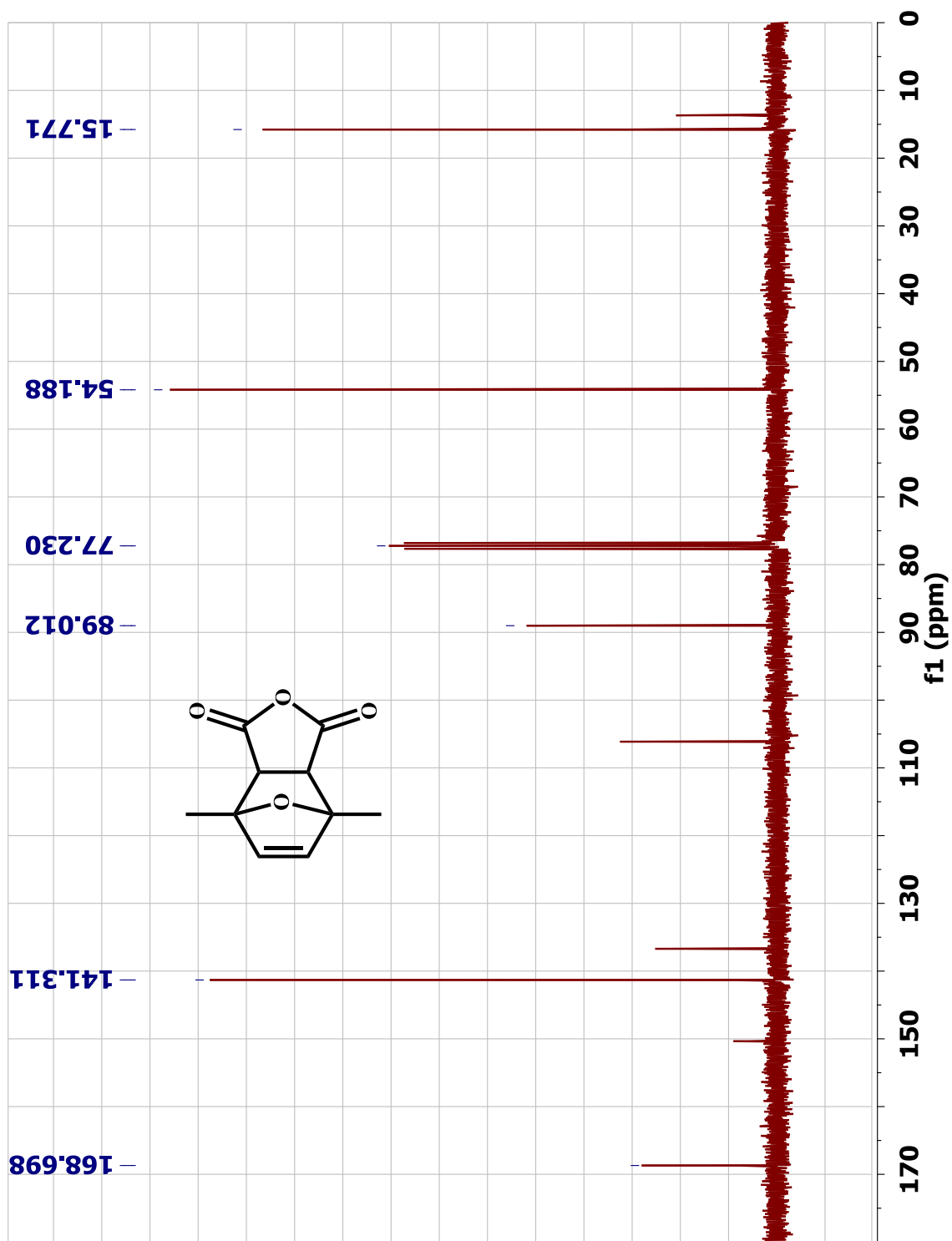
A.13 ^{13}C -NMR spectrum of 9,10-bis(2,6-bis(bromomethyl)phenyl)anthracene (5).



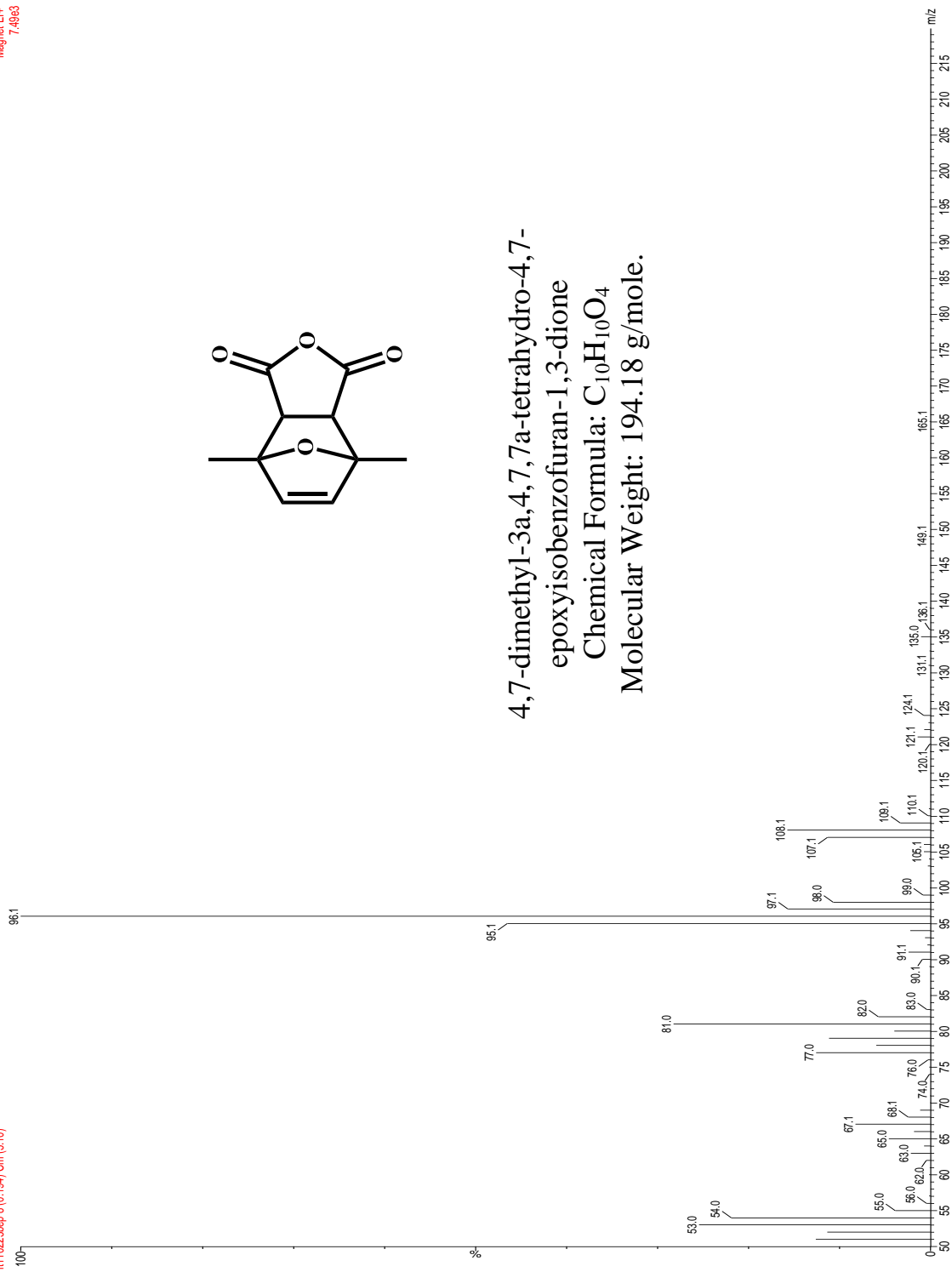
A.14 Mass spectrum of 9,10-bis(2,6-bis(bromomethyl)phenyl)anthracene (5).



A.15 ¹H-NMR spectrum of 4,7-dimethyl-3a,4,7a-tetrahydro-4,7-epoxyisobenzofuran-1,3-dione (8).

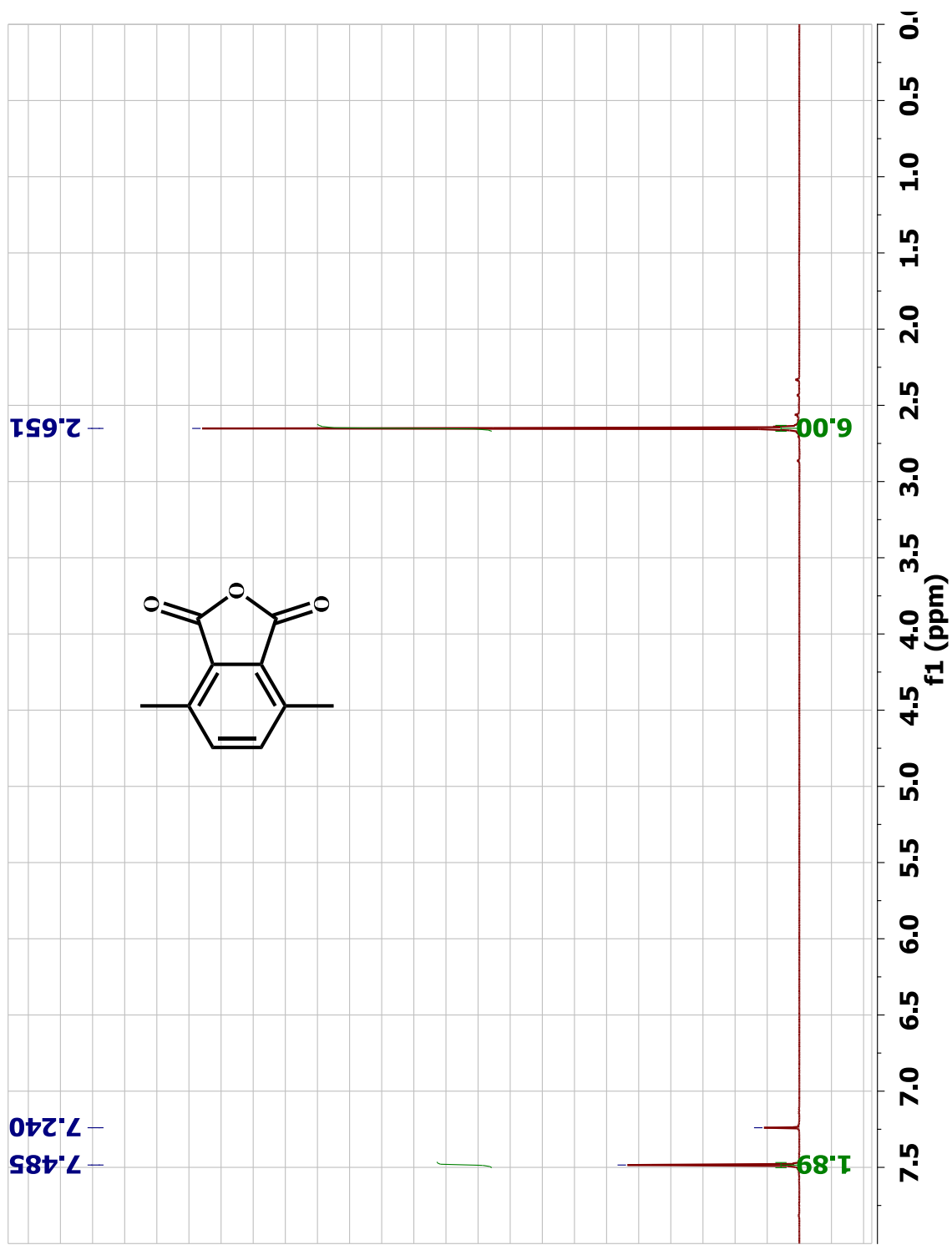


A.16 ^{13}C -NMR spectrum of 4,7-dimethyl-3a,4,7,7a-tetrahydro-4,7-epoxyisobenzofuran-1,3-dione (**8**).

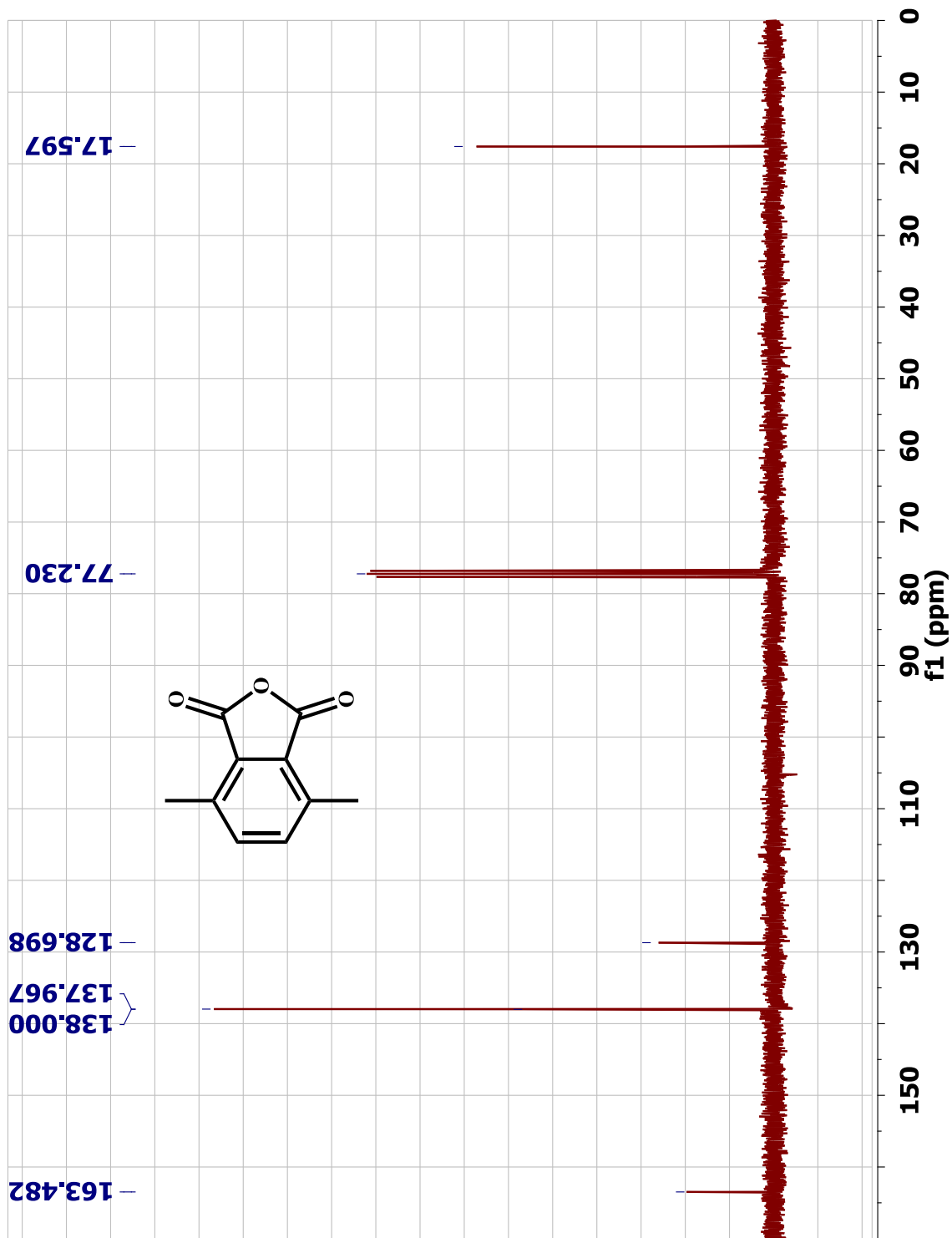


4,7-dimethyl-3a,4,7,7a-tetrahydro-4,7-epoxyisobenzofuran-1,3-dione
Chemical Formula: C₁₀H₁₀O₄
Molecular Weight: 194.18 g/mole.

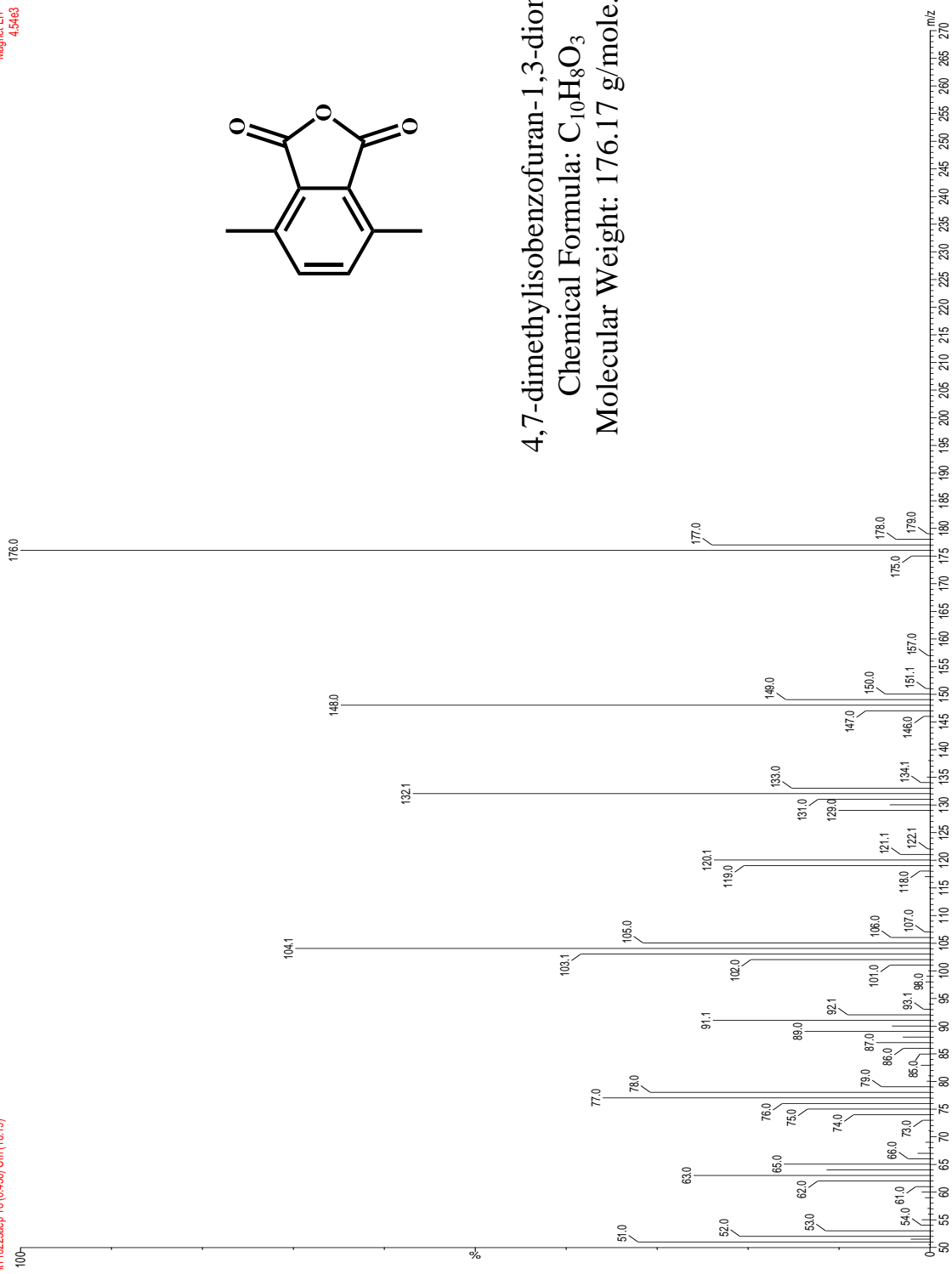
A.17 Mass spectrum of 4,7-dimethyl-3a,4,7,7a-tetrahydro-4,7-epoxyisobenzofuran-1,3-dione (8).



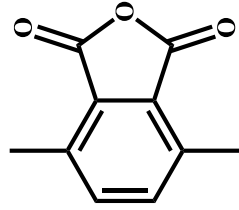
A.18 ¹H-NMR spectrum of 4,7-dimethylisobenzofuran-1,3-dione (9).



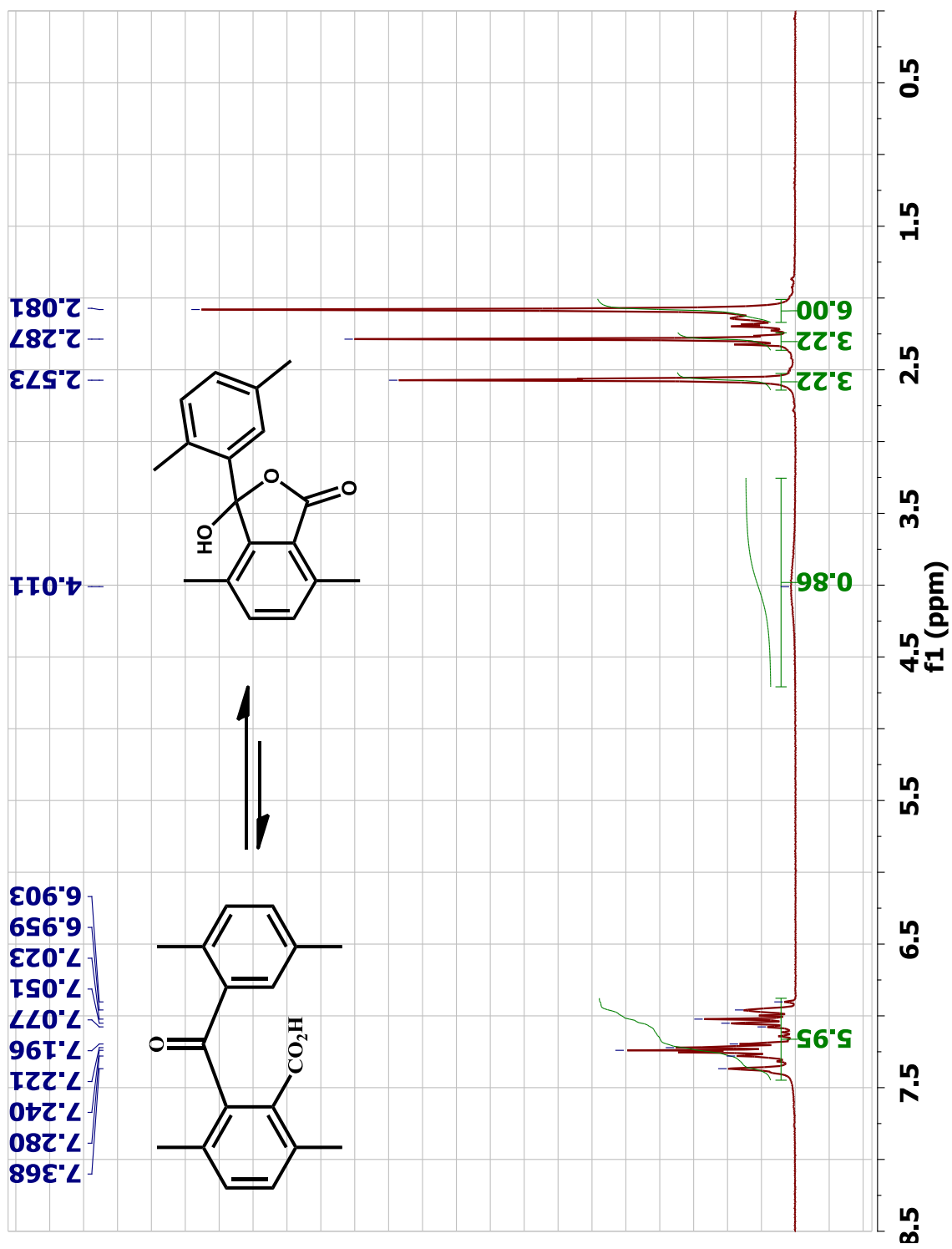
A.19 ^{13}C -NMR spectrum of 4,7-dimethylisobenzofuran-1,3-dione (9).



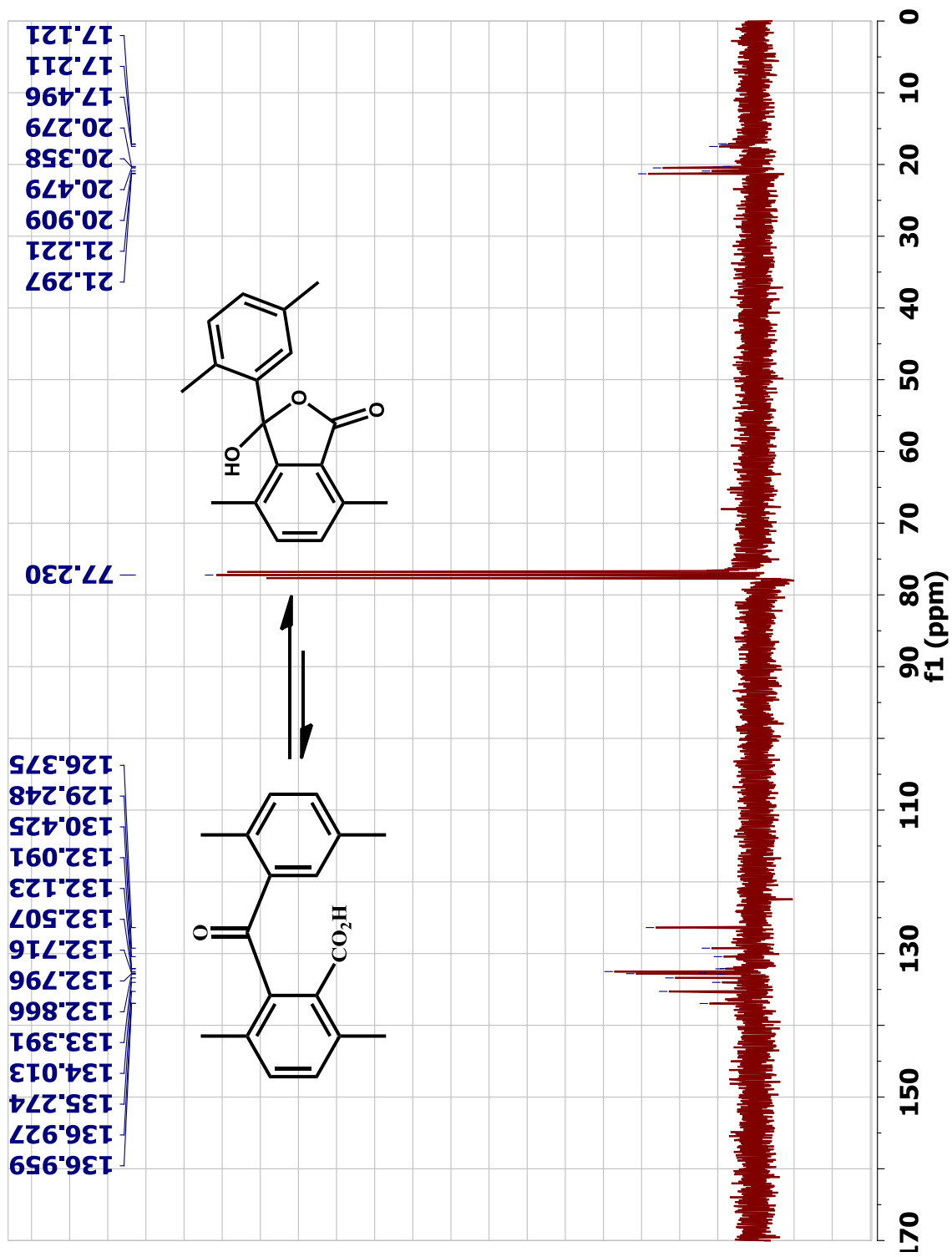
4,7-dimethylisobenzofuran-1,3-dione
Chemical Formula: $C_{10}H_8O_3$
Molecular Weight: 176.17 g/mole.



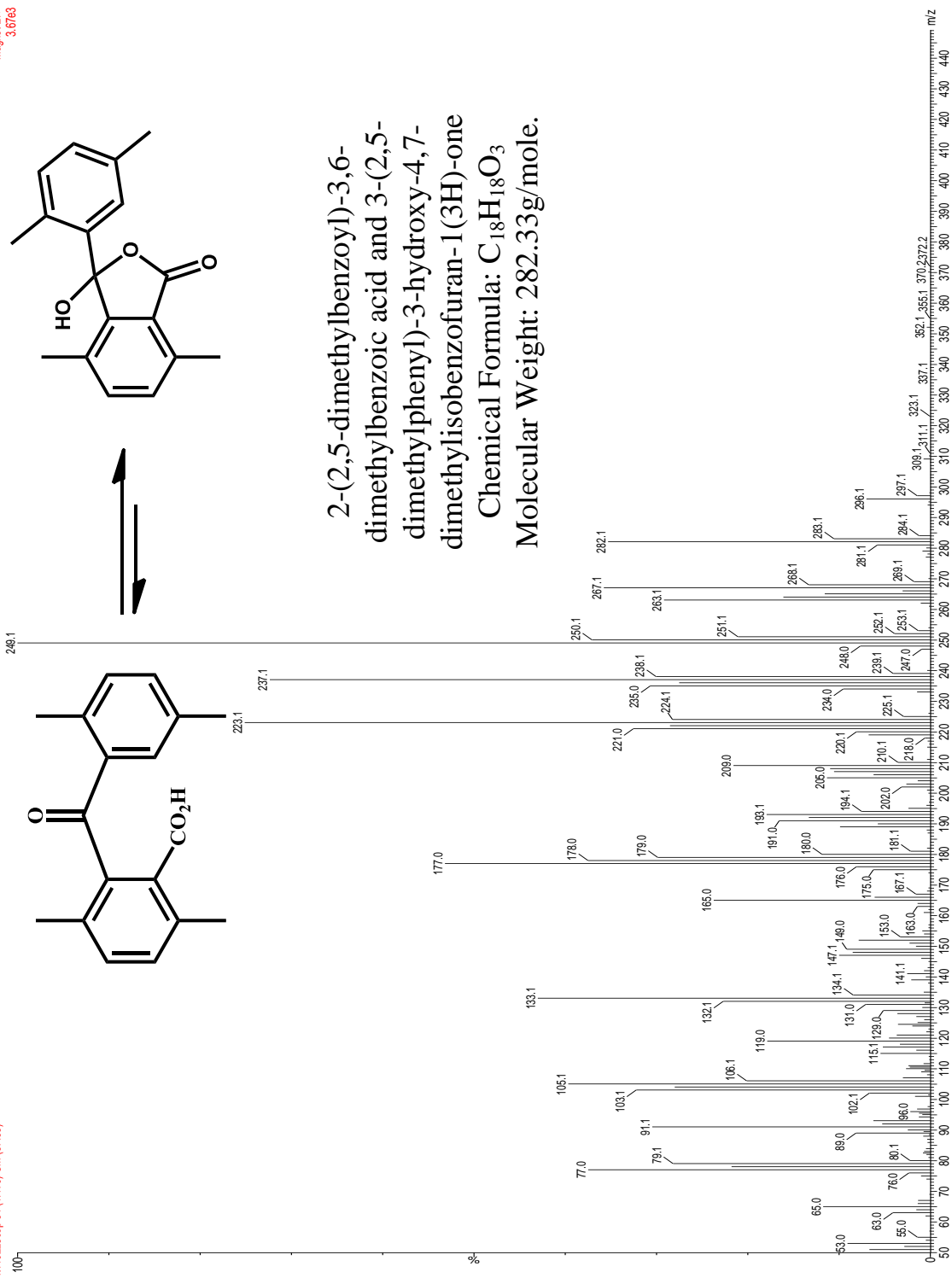
A.20 Mass spectrum of 4,7-dimethylisobenzofuran-1,3-dione (9).



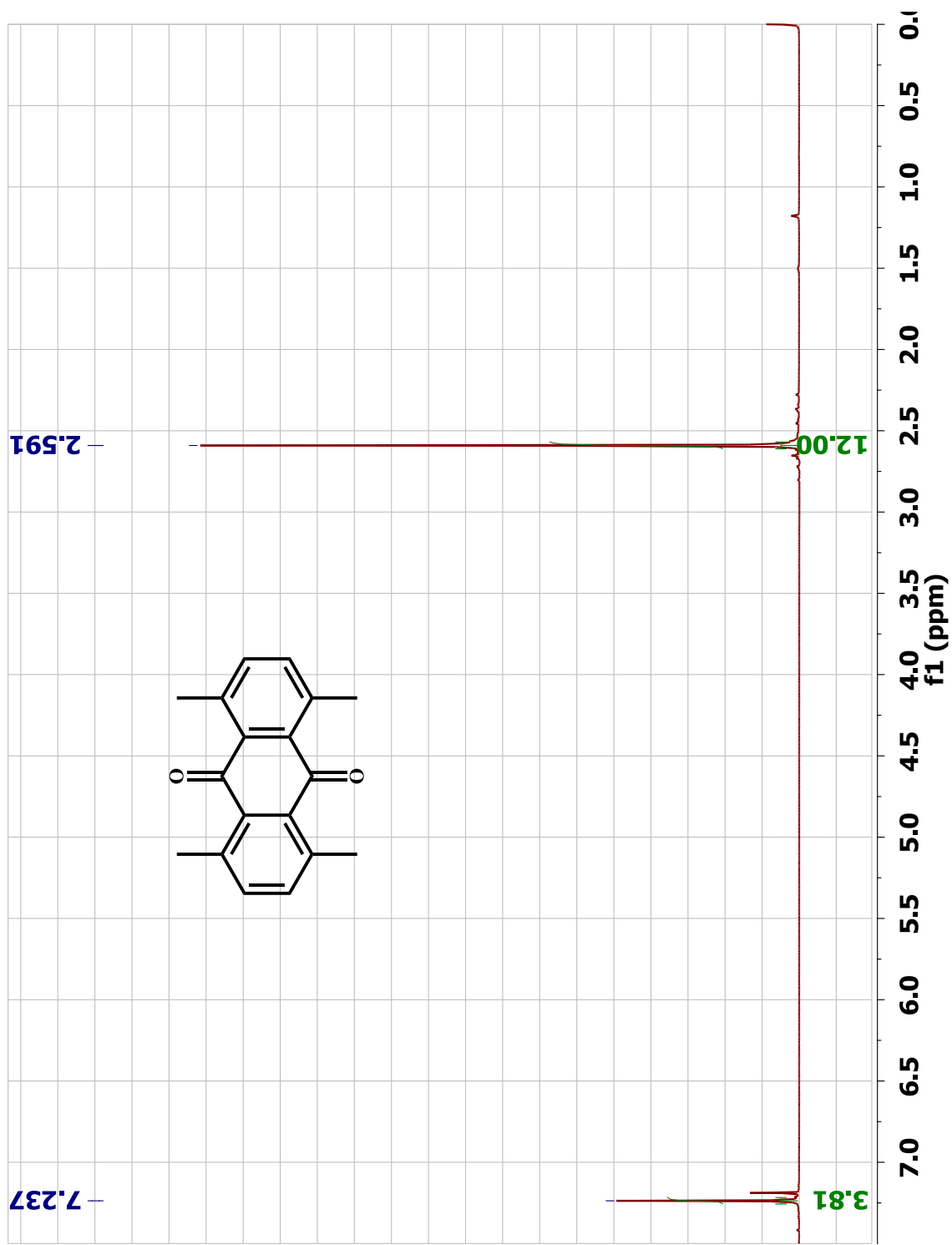
A.21 ¹H-NMR spectrum of 2-(2,5-dimethylbenzoyl)-3,6-dimethylbenzoic acid (10).



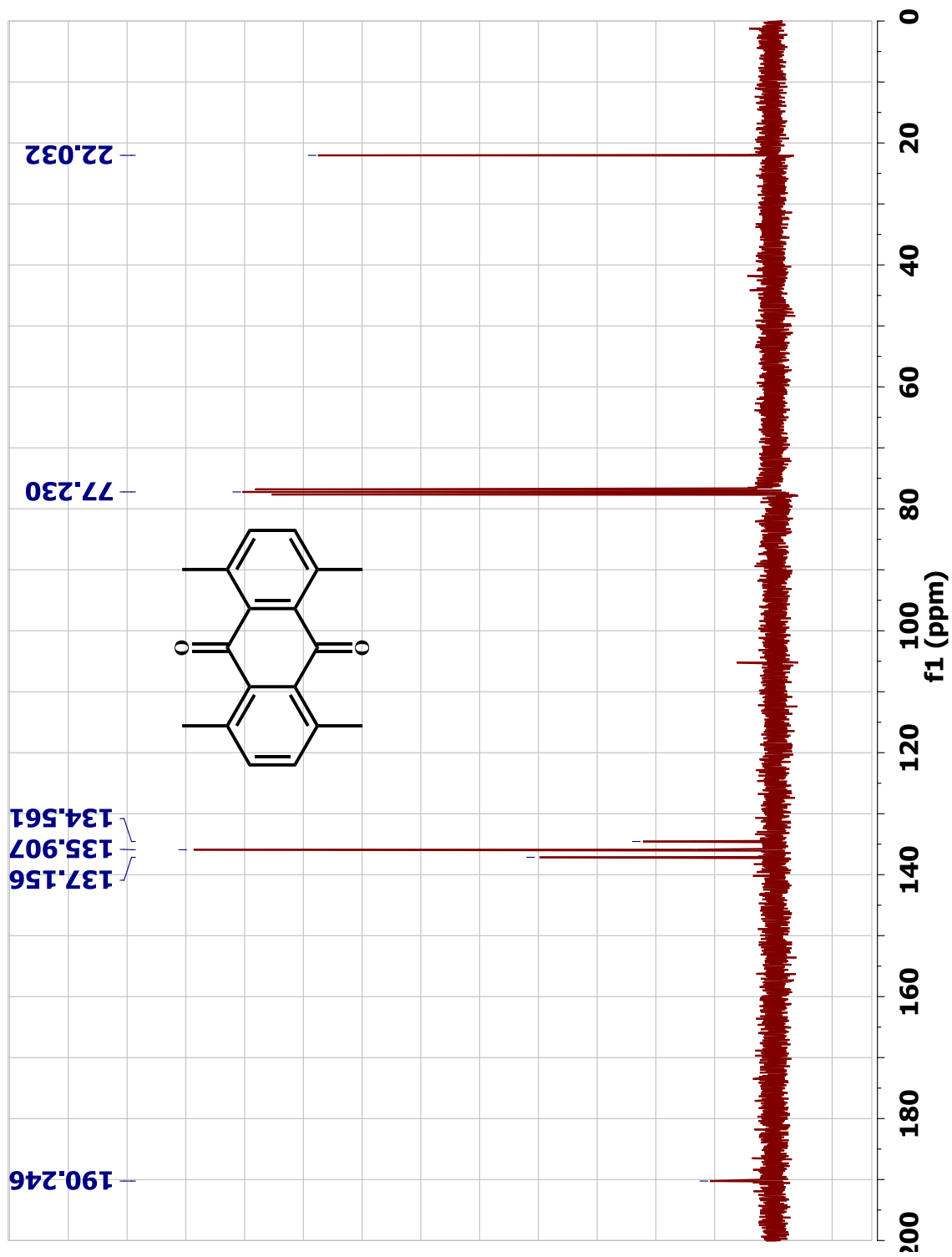
A.22 ^{13}C -NMR spectrum of 2-(2,5-dimethylbenzoyl)-3,6-dimethylbenzoic acid (**10**).



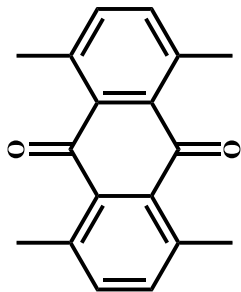
A.23 Mass spectrum of 2-(2,5-dimethylbenzoyl)-3,6-dimethylbenzoic acid (10).



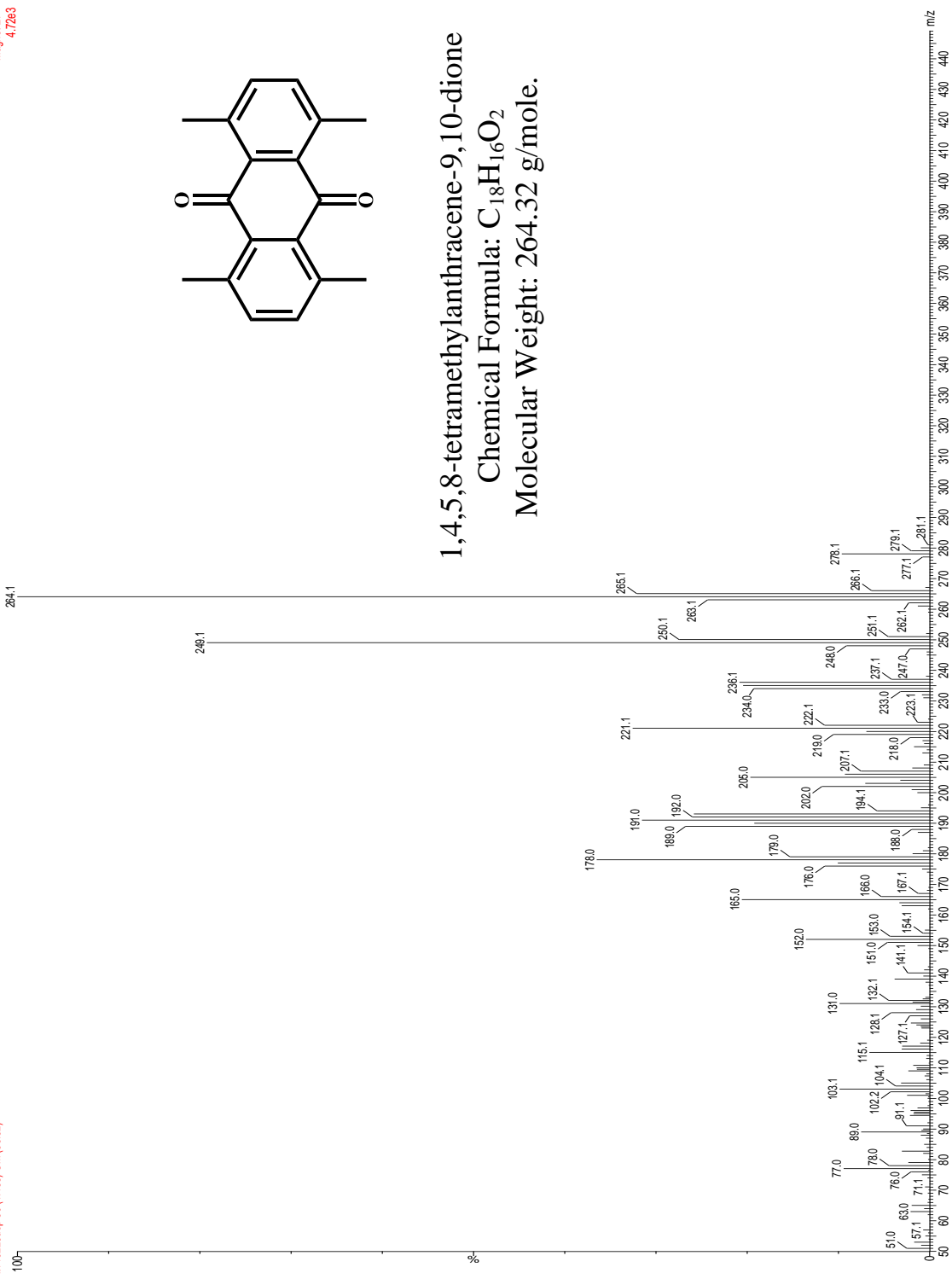
A.24 ¹H-NMR spectrum of 1,4,5,8-tetramethylanthracene-9,10-dione (11).



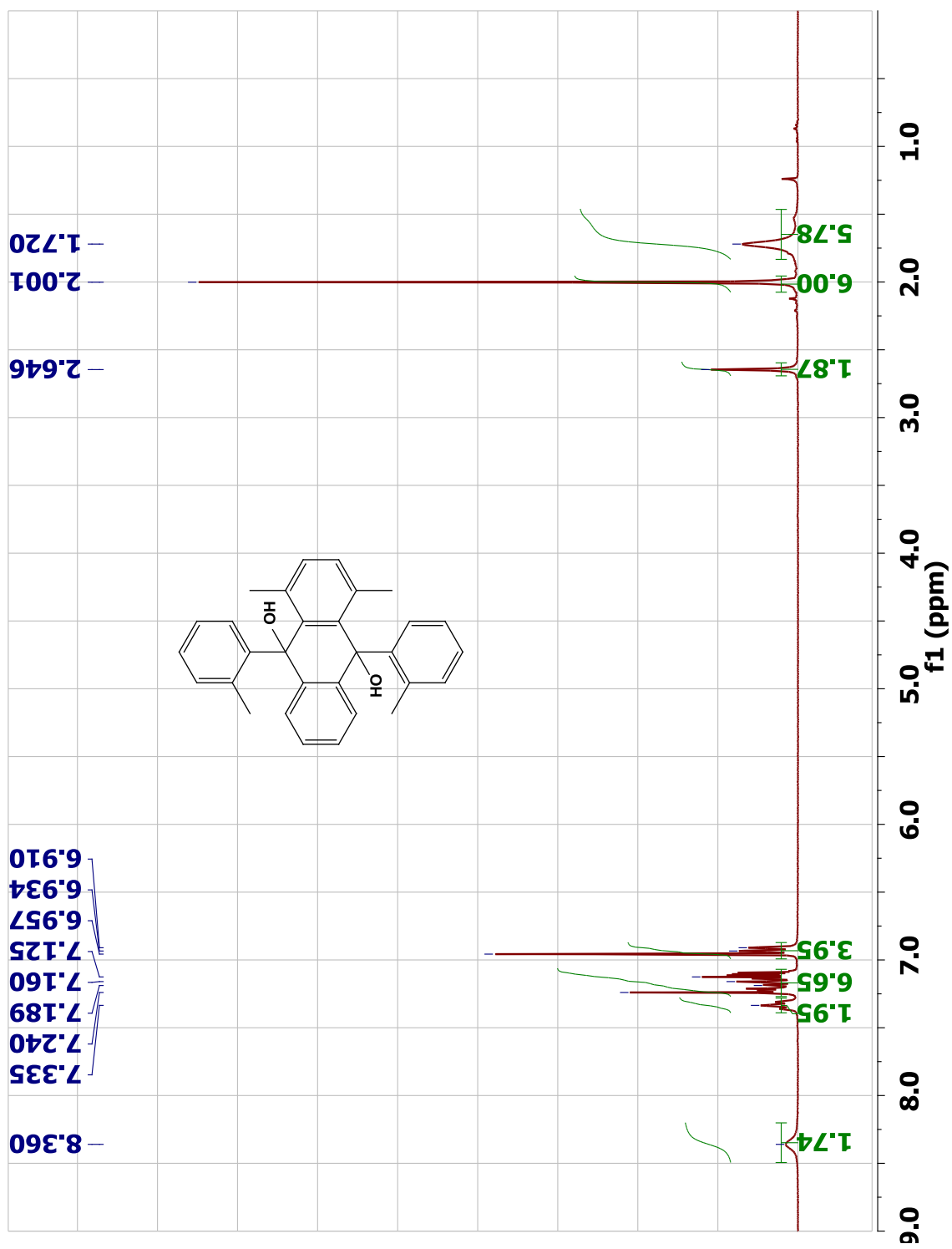
A.25 ^{13}C -NMR spectrum of 1,4,5,8-tetramethylanthracene-9,10-dione (11).



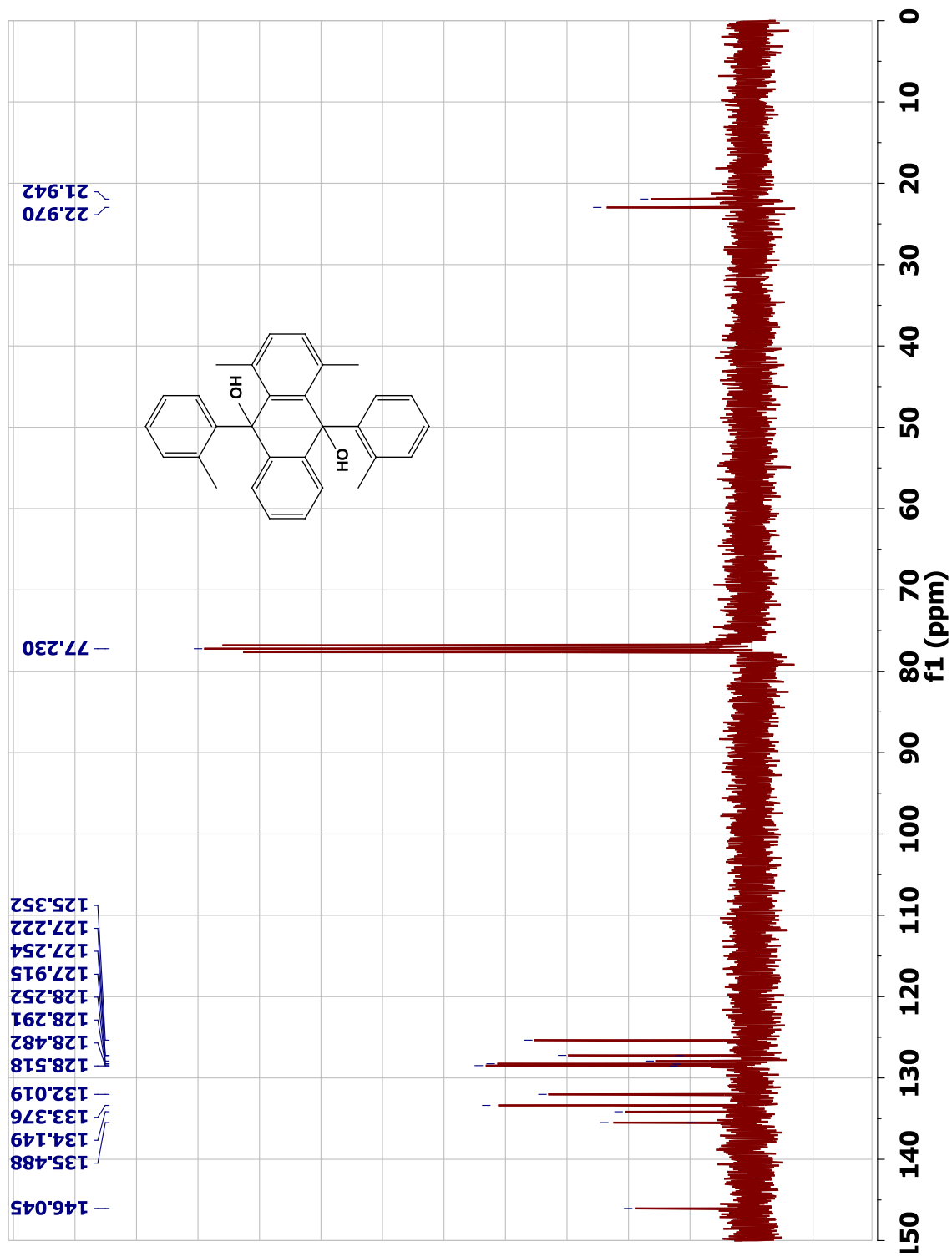
1,4,5,8-tetramethylanthracene-9,10-dione
Chemical Formula: $C_{18}H_{16}O_2$
Molecular Weight: 264.32 g/mole.



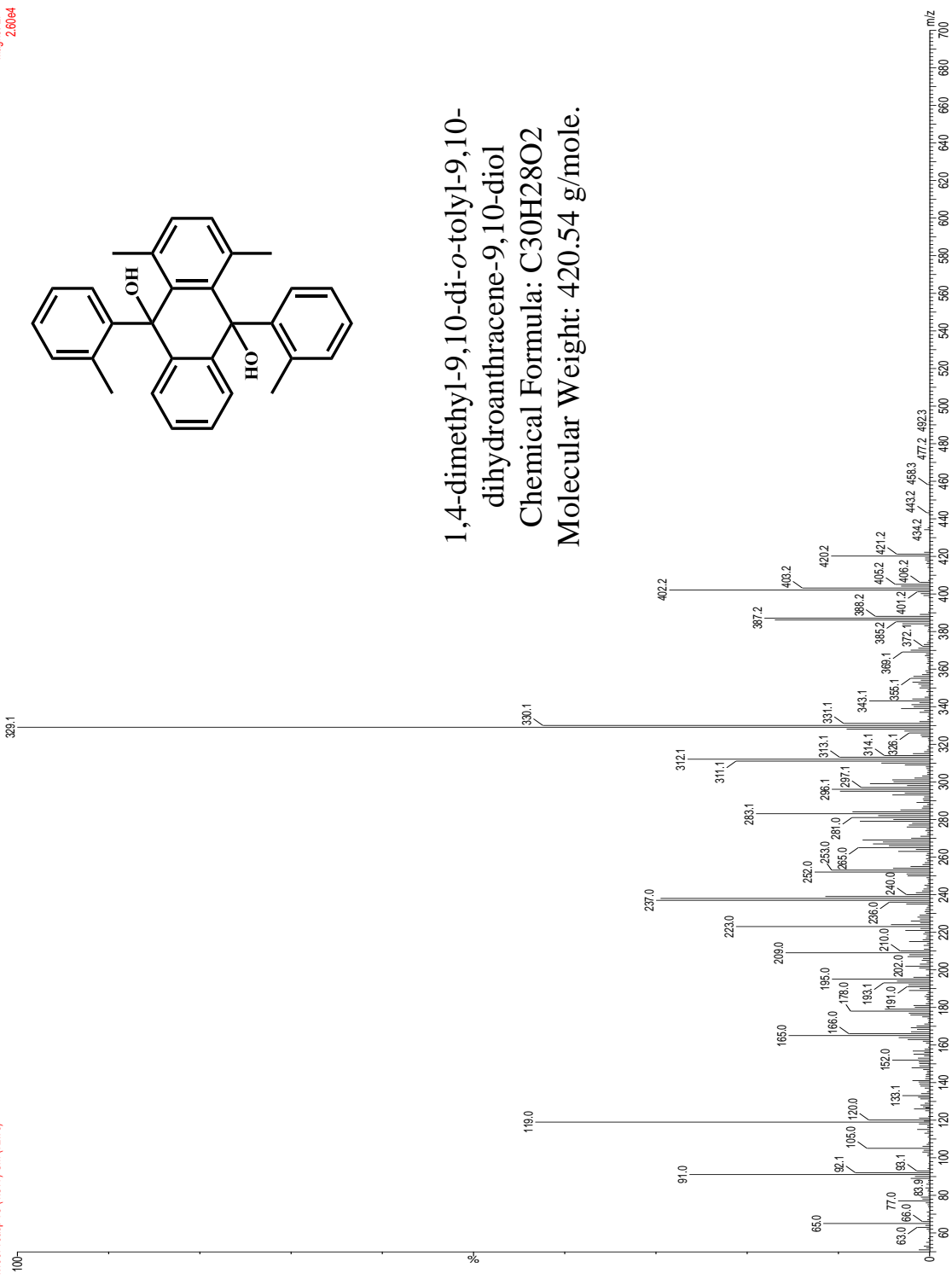
A.26 Mass spectrum of 1,4,5,8-tetramethylanthracene-9,10-dione (11).



A.27 ¹H-NMR spectrum of 1,4-dimethyl-9,10-di-o-tolyl-9,10-dihydroanthracene-9,10-diol (12).

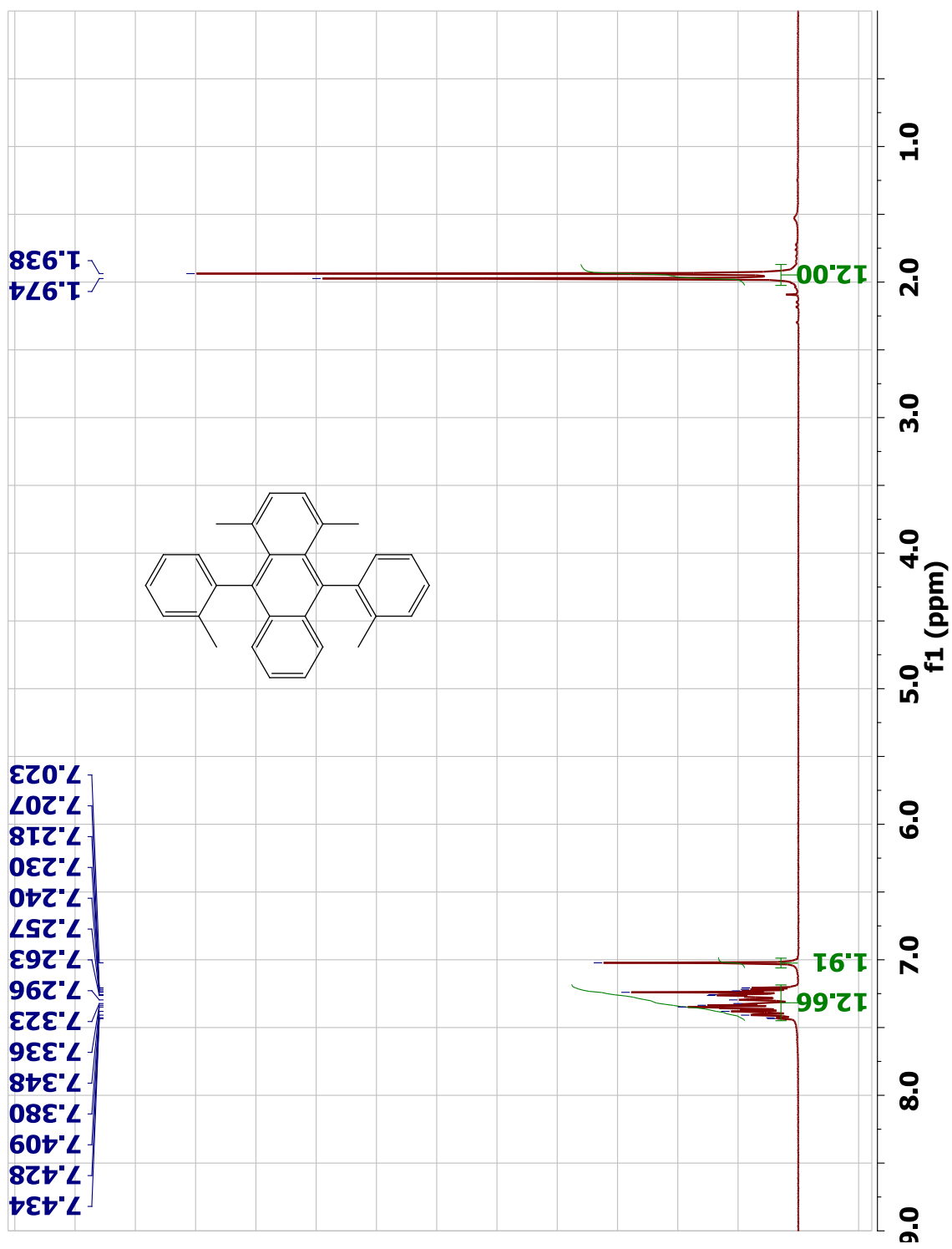


A.28 ¹³C-NMR spectrum of 1,4-dimethyl-9,10-di-o-tolyl-9,10-dihydroanthracene-9,10-diol (12).

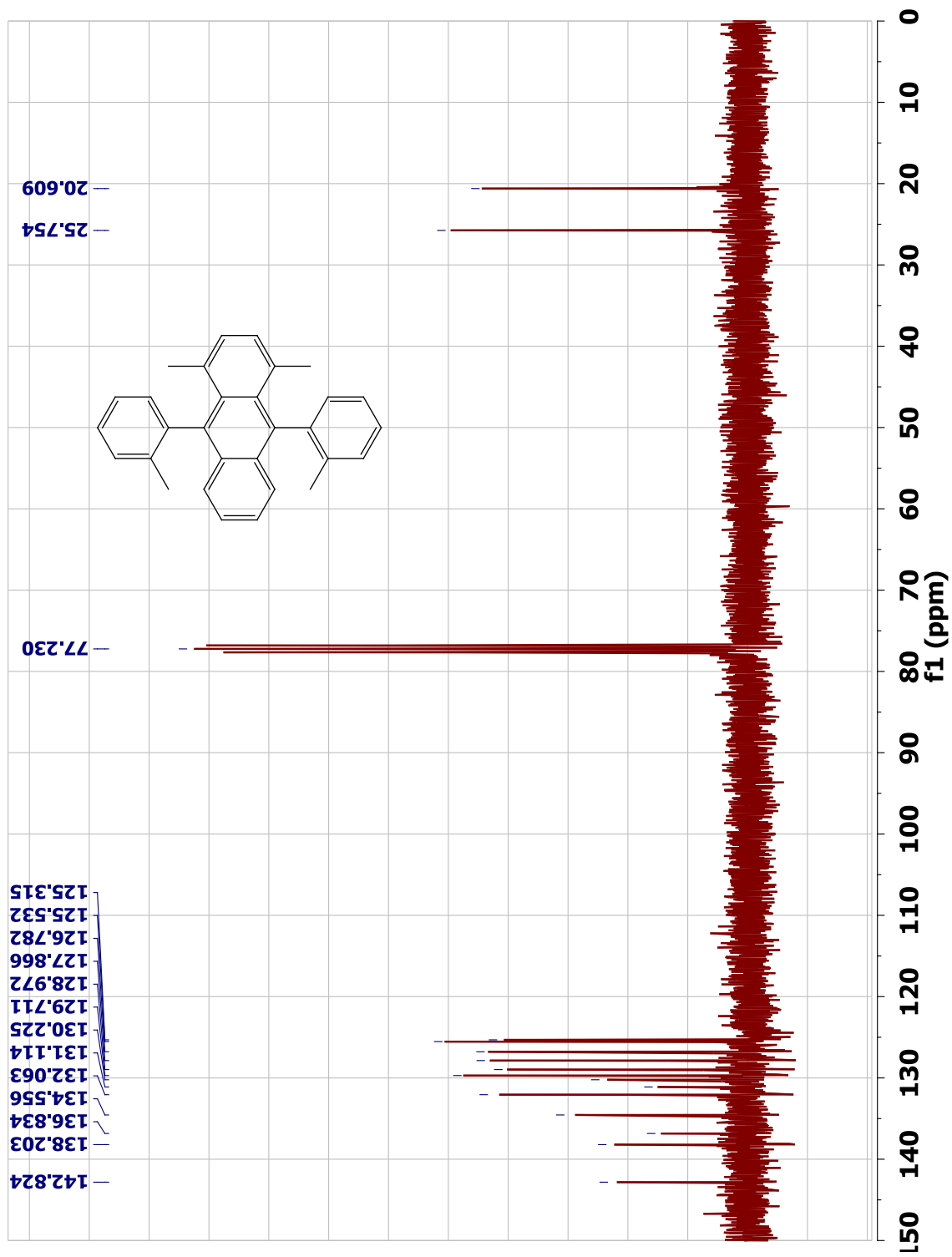


1,4-dimethyl-9,10-di-o-tolyl-9,10-dihydroanthracene-9,10-diol
Chemical Formula: C30H28O2
Molecular Weight: 420.54 g/mole.

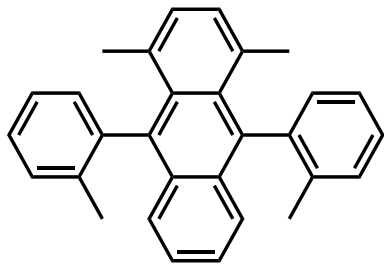
A.29 Mass spectrum of 1,4-dimethyl-9,10-di-o-tolyl-9,10-dihydroanthracene-9,10-diol (12).



A.30 ¹H-NMR spectrum of 1,4-dimethyl-9,10-di-o-tolylanthracene (13).



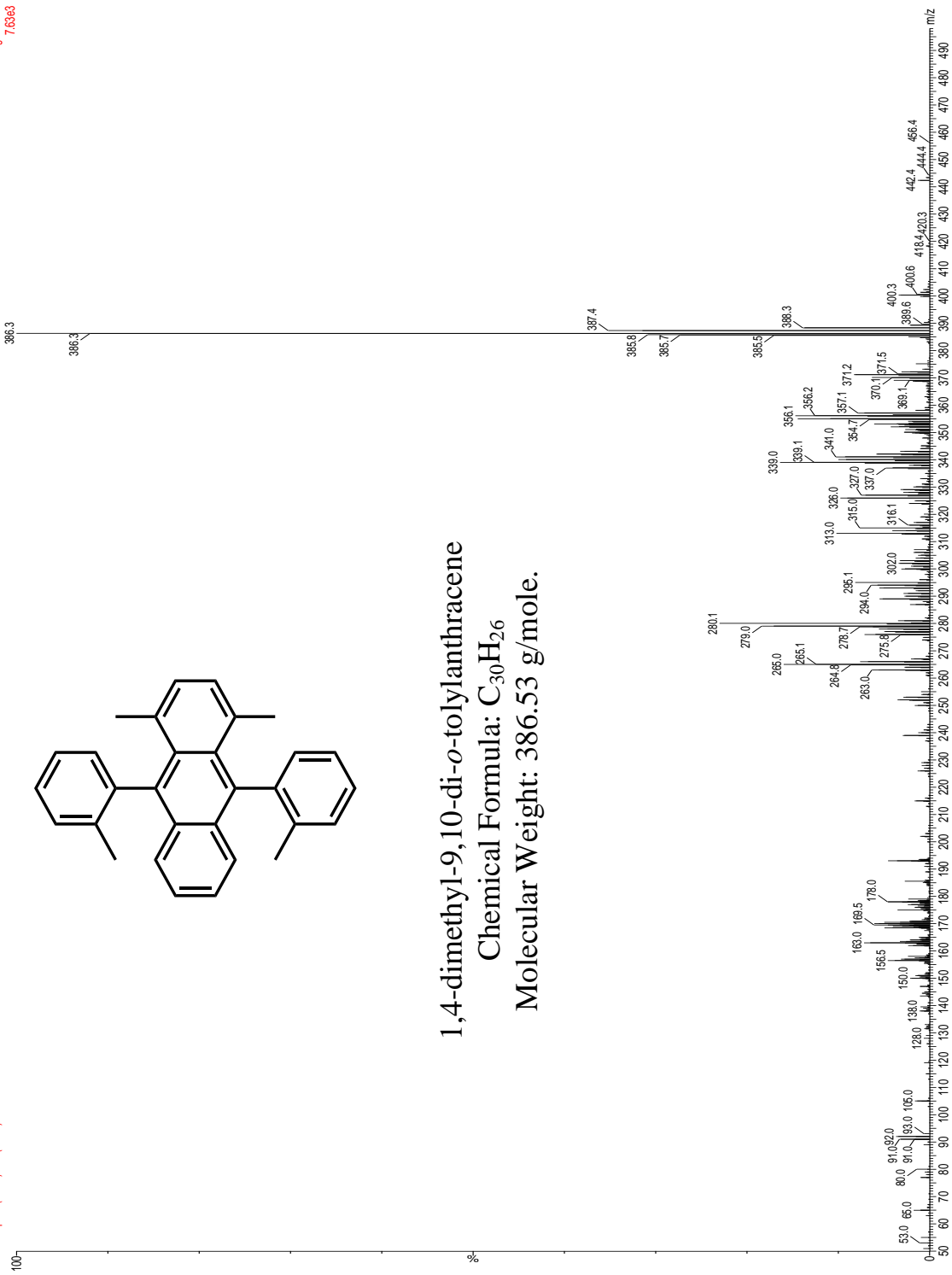
A.31 ^{13}C -NMR spectrum of 1,4-dimethyl-9,10-di-o-tolylanthracene (13).



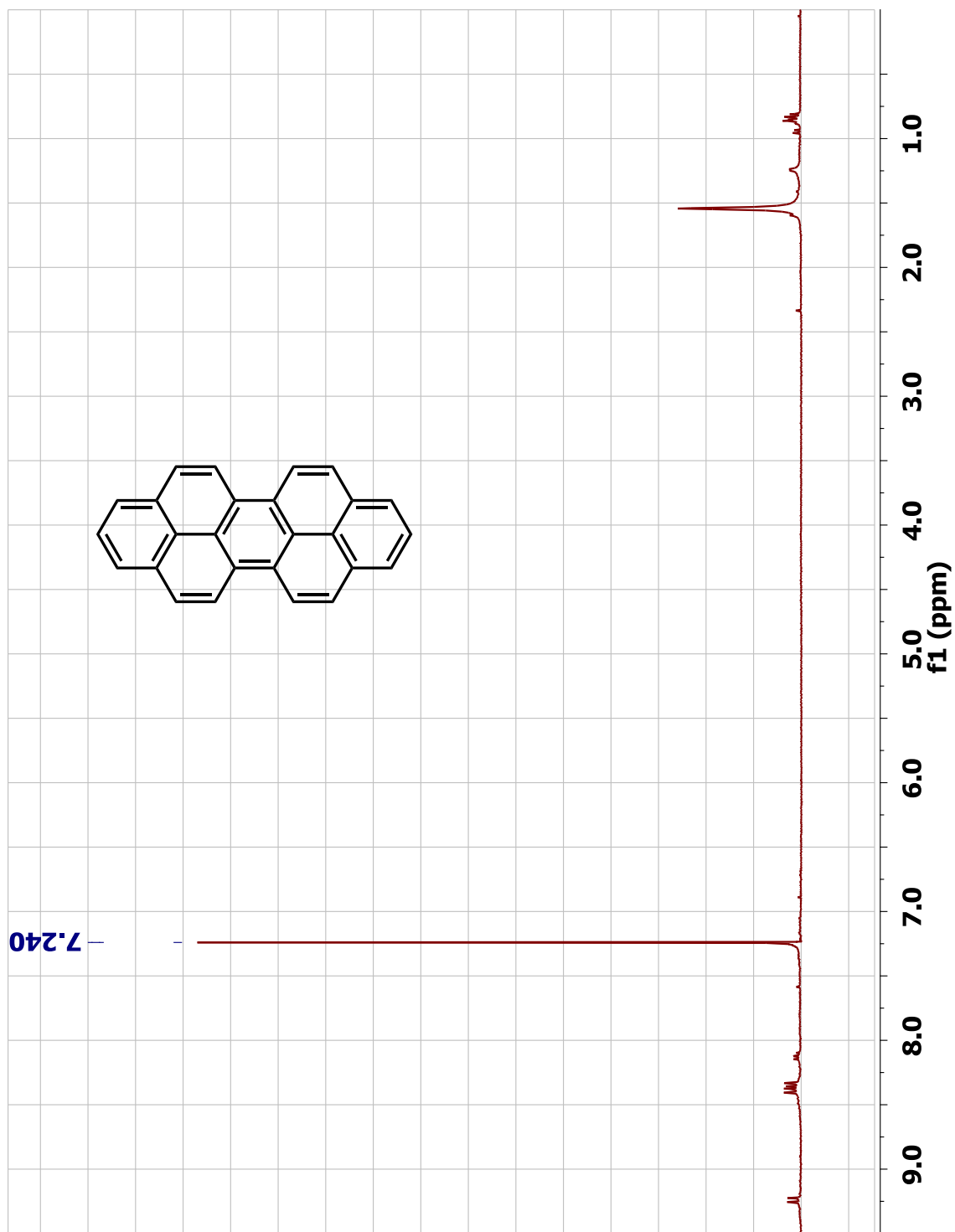
1,4-dimethyl-9,10-di-*o*-tolylanthracene

Chemical Formula: C₃₀H₂₆

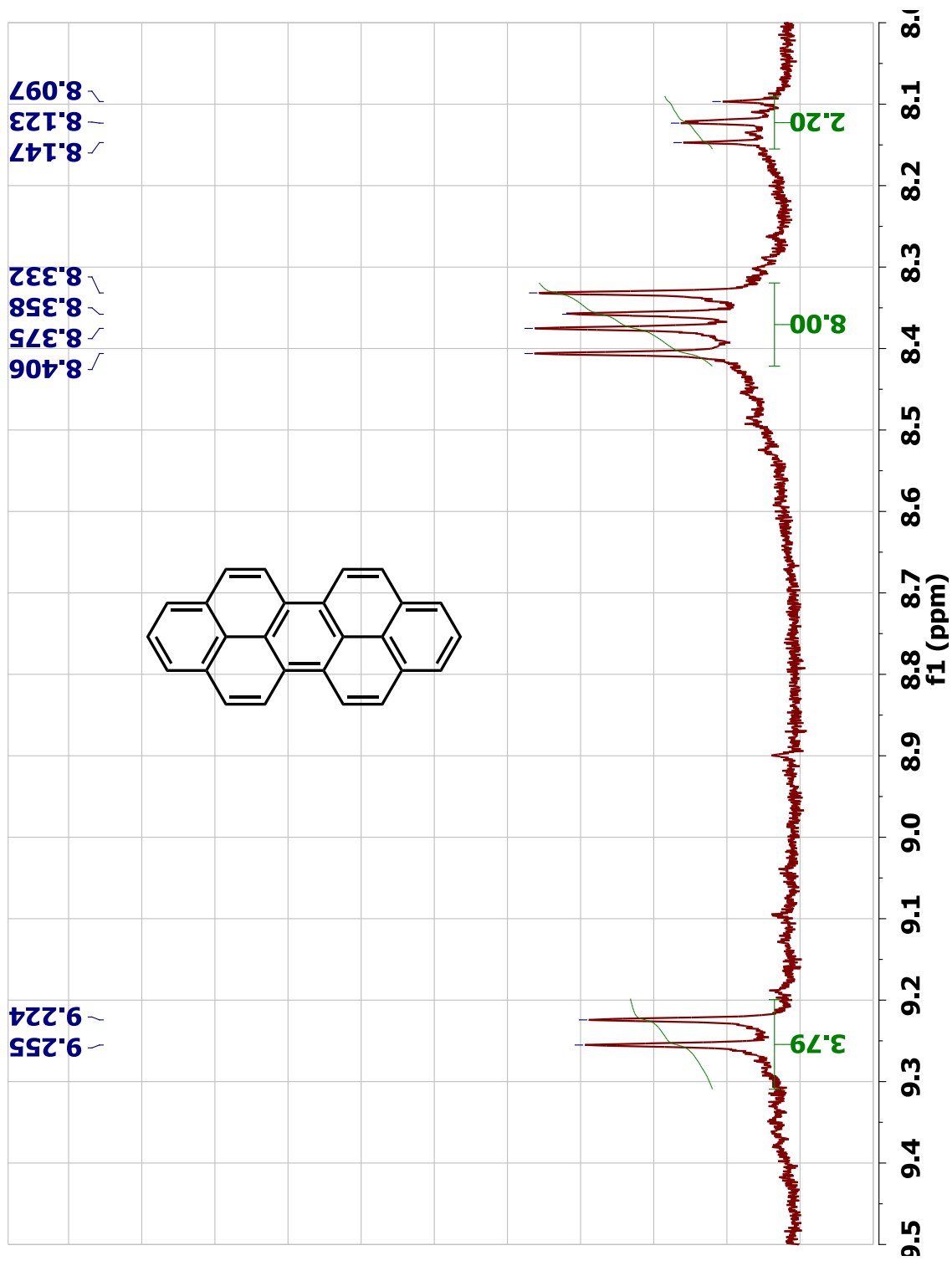
Molecular Weight: 386.53 g/mole.



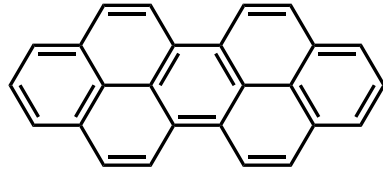
A.32 Mass spectrum of 1,4-dimethyl-9,10-di-*o*-tolylanthracene (13).



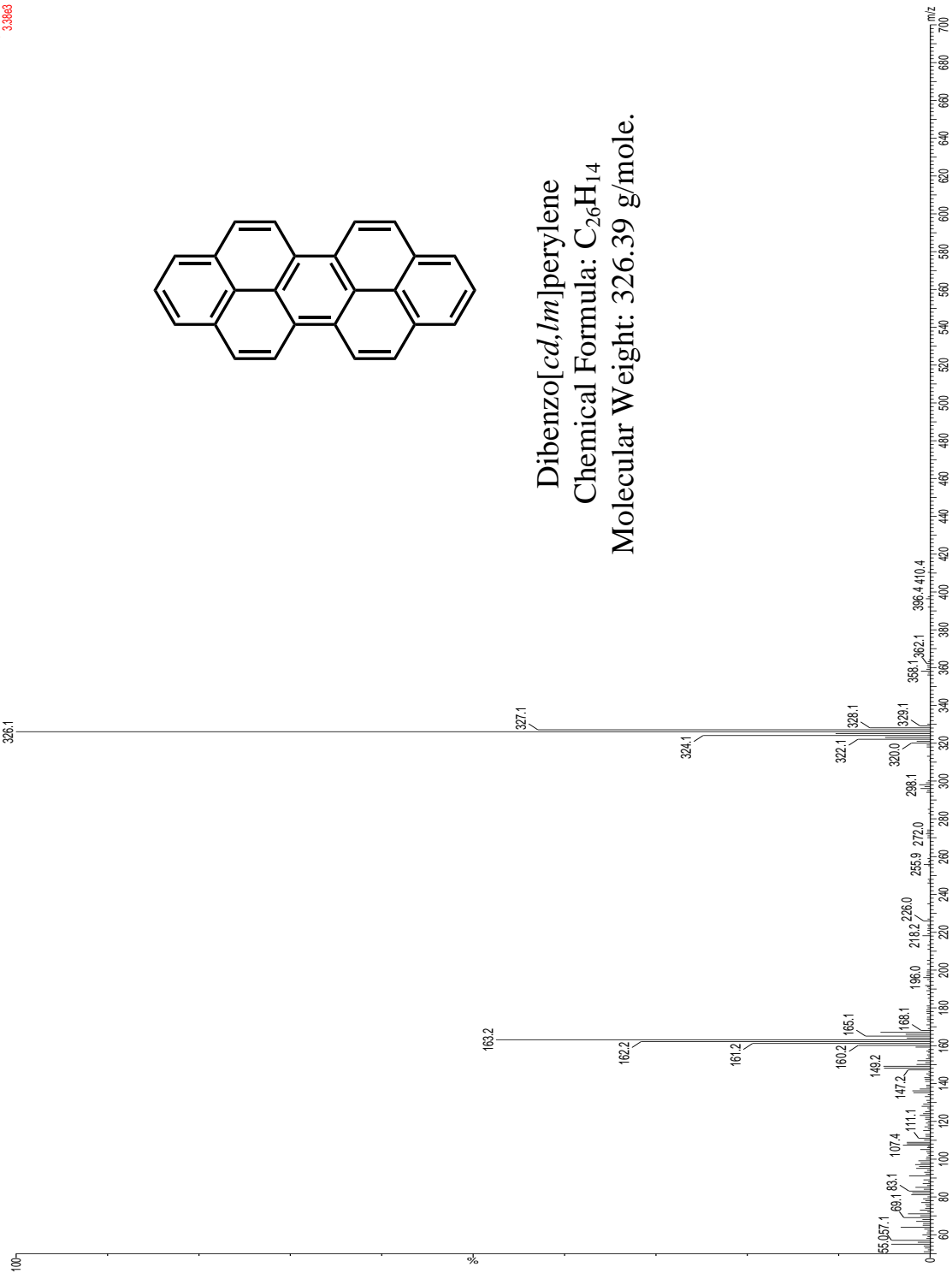
A.33 $^1\text{H-NMR}$ spectrum of dibenzo[*cd,lm*]perylene (18).



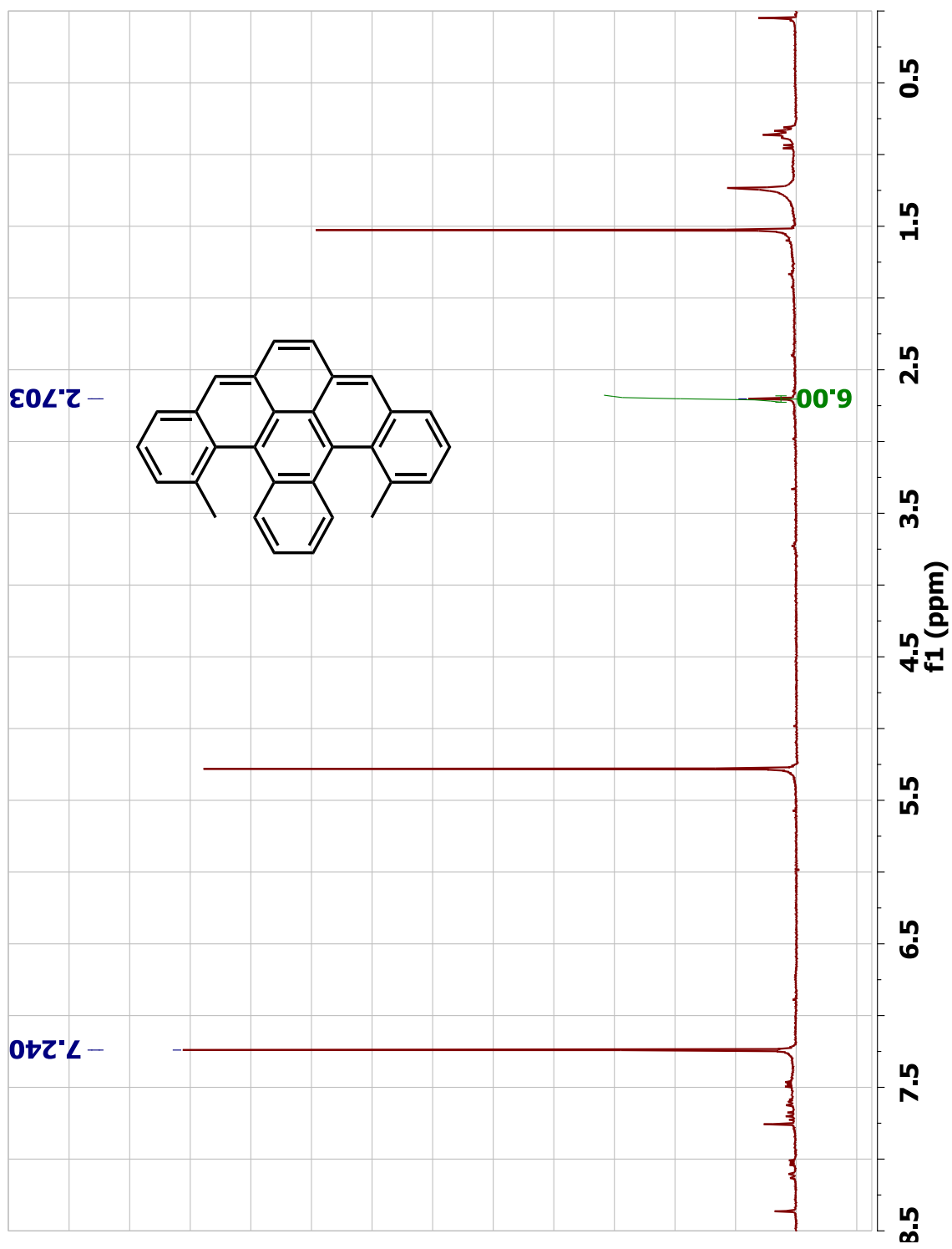
A.34 Expanded ¹H-NMR spectrum of dibenzo[cd,lm]perylene (18).



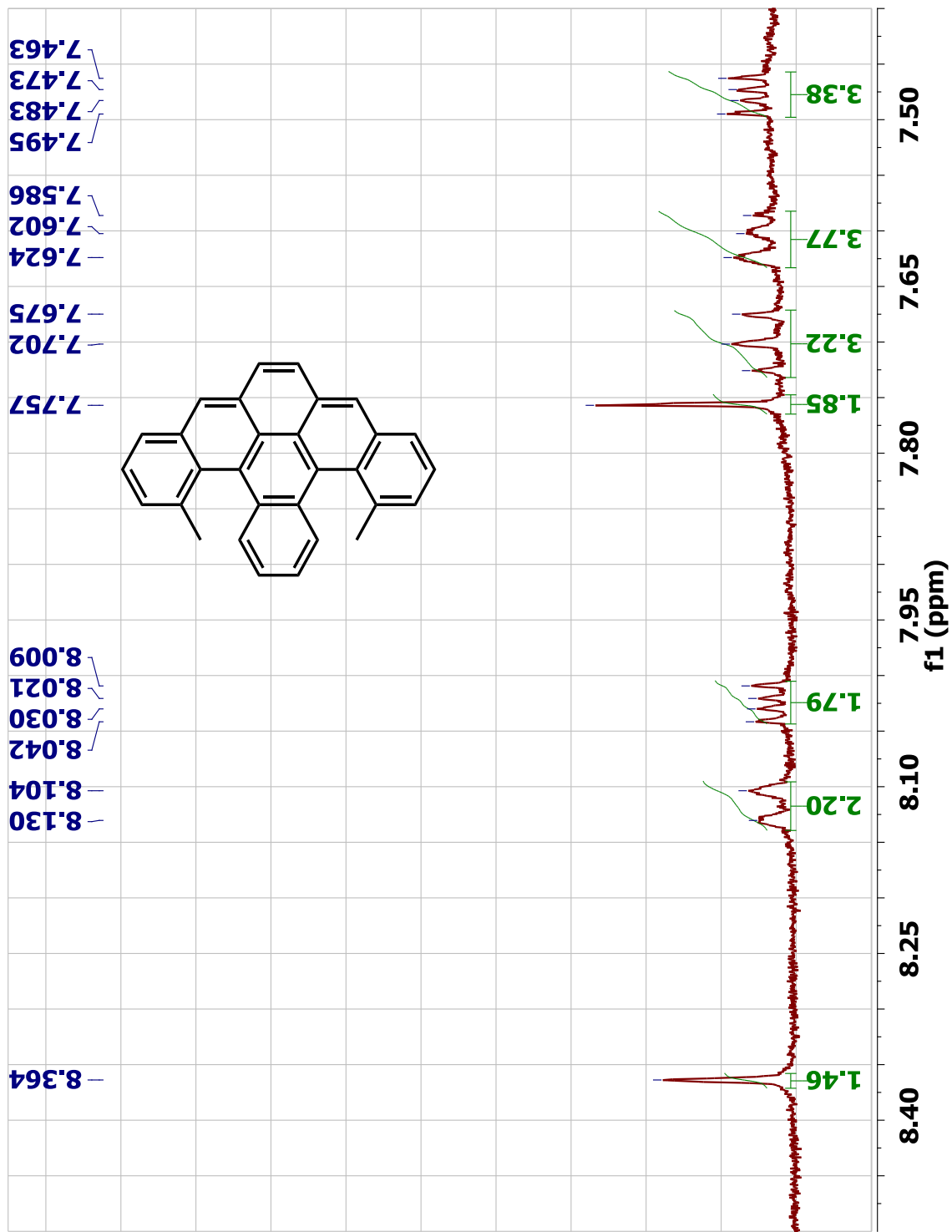
Dibenzo[*cd,lm*]perylene
Chemical Formula: $C_{26}H_{14}$
Molecular Weight: 326.39 g/mole.



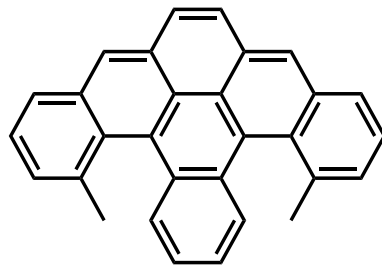
A.35 Mass spectrum of dibenzo[*cd,lm*]perylene (18).



A.36 $^1\text{H-NMR}$ spectrum of 1,12-dimethylnaphtho[1,2,3,4-*rst*]pentaphene (19).



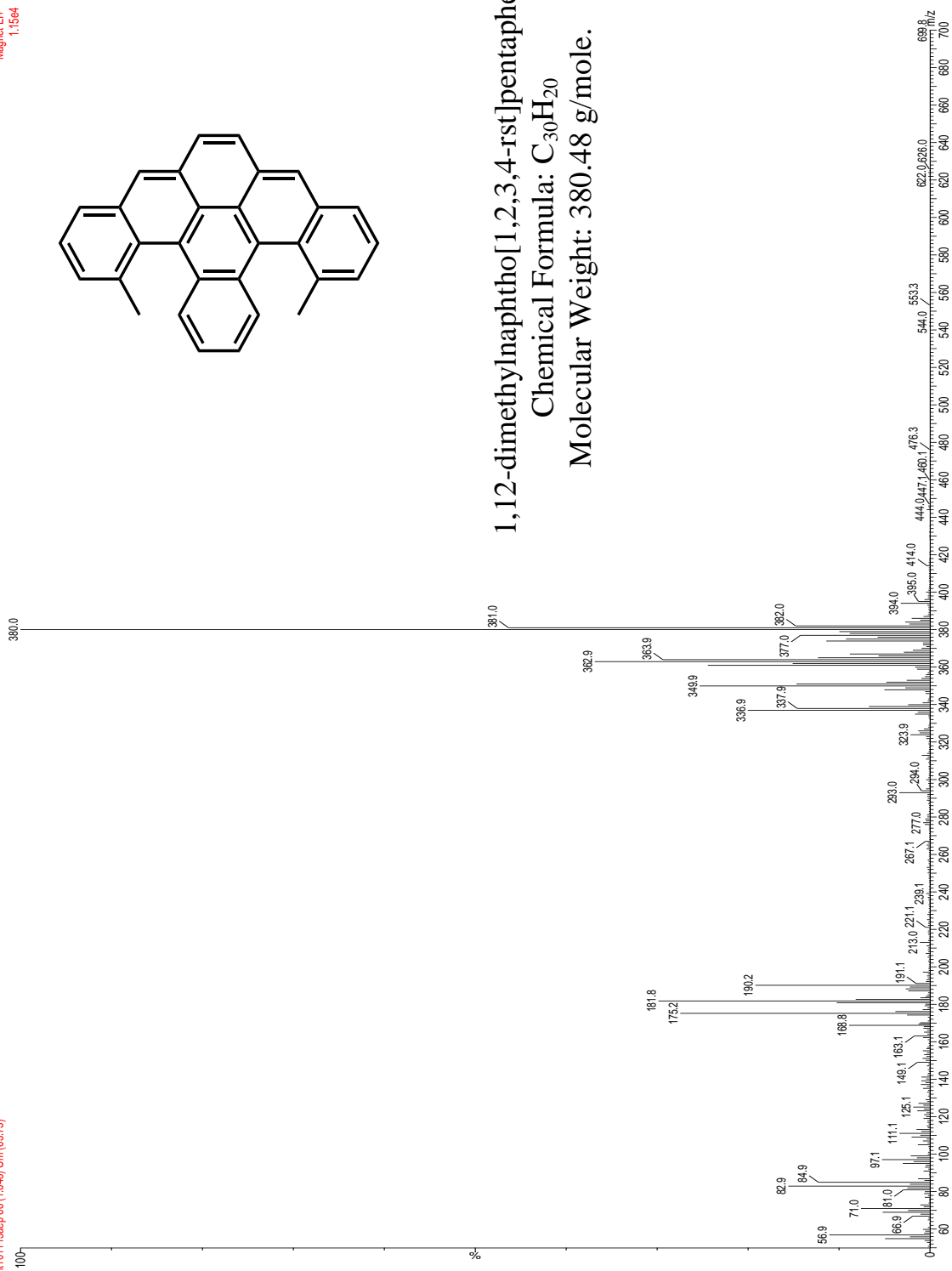
A.37 Expanded ¹H-NMR spectrum of 1,12-dimethylnaphtho[1,2,3,4-rst]pentaphene (19).



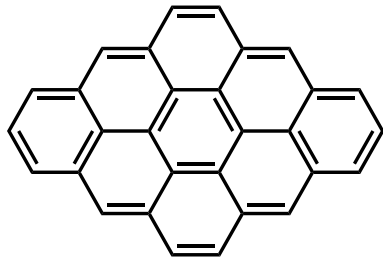
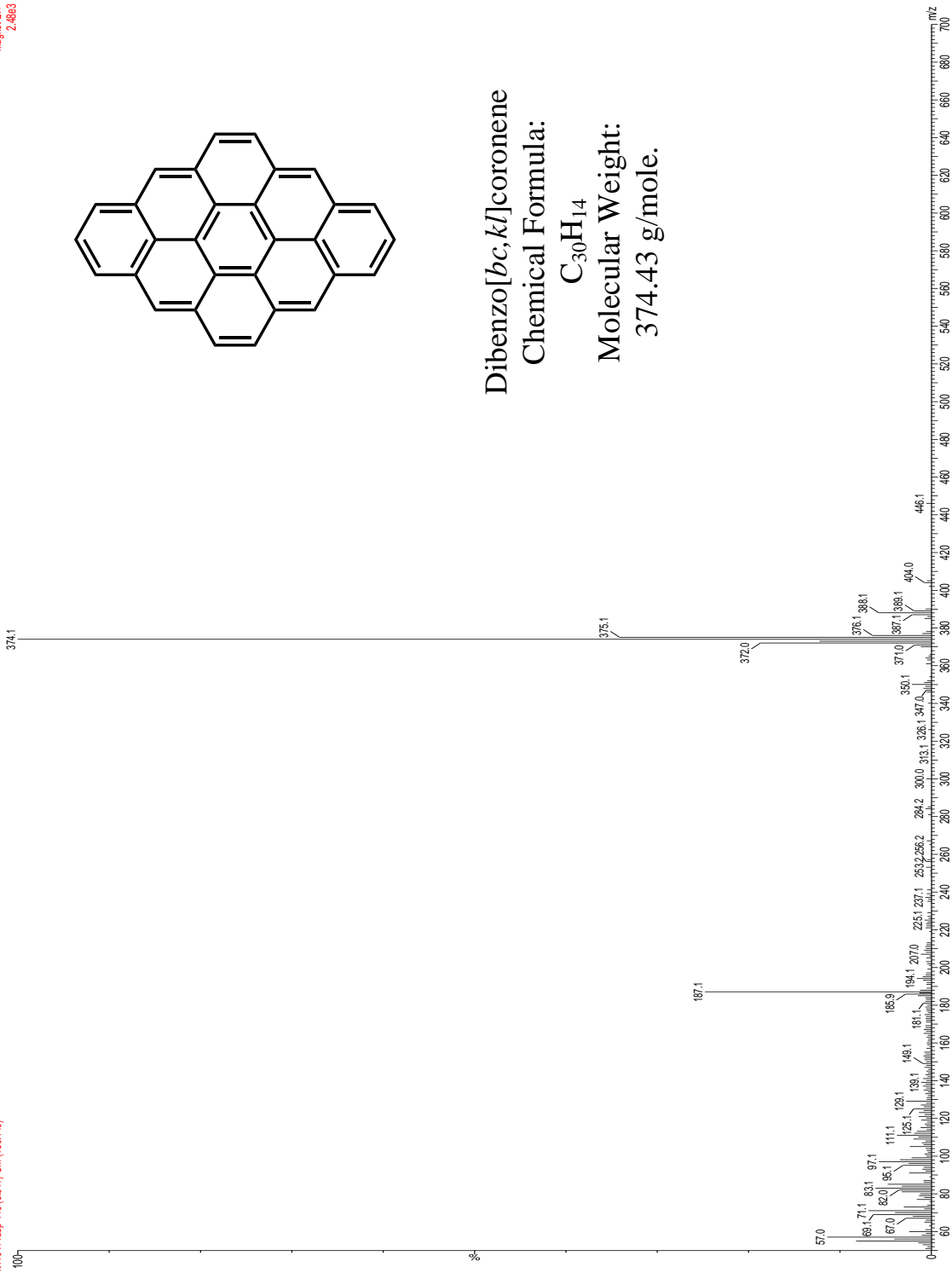
1,12-dimethylnaphtho[1,2,3,4-rst]pentaphene

Chemical Formula: C₃₀H₂₀

Molecular Weight: 380.48 g/mole.



A.38 Mass spectrum of 1,12-dimethylnaphtho[1,2,3,4-rst]pentaphene (19).



Dibenzo[bc,k]coronene

Chemical Formula:

$C_{30}H_{14}$

Molecular Weight:

374.43 g/mole.

A.39 Mass spectrum of dibenzo[bc,k]coronene (16).

VITA

JUAN MANUEL VARGAS MORALES

Vargas Morales was born in Mexico City. He attended public schools in Mexico City, Mexico. After moving to the United States, he received a B.S. in Chemistry from Edinboro University of Pennsylvania, Edinboro, Pennsylvania in 2004 before coming to Georgia Tech to pursue a doctorate in Chemistry.